Fundamental Efforts to Develop Novel Biotechnological Approaches in Pest Management Applications against Coleoptera:

Transcriptomic Exploration of the Chemical Defense Mechanism in the Red Flour Beetle, *Tribolium castaneum*

Dissertation

for the award of the degree

"Doctor rerum naturalium" (Dr.rer.nat.)

of the Georg-August-Universität Göttingen

within the doctoral program Biology

of the Georg-August University School of Science (GAUSS)

submitted by

Jianwei Li

from Gansu, P.R. China

Göttingen, 2013

Thesis Committee

Prof. Dr. Ernst A. Wimmer (Supervisor, Dept. of Developmental Biology, Johann-Friedrich-Blumenbach-Institute of Zoology and Anthropology)

Prof. Dr. Gregor Bucher (Co-supervisor, Dept. of Developmental Biology, Johann-Friedrich-Blumenbach-Institute of Zoology and Anthropology)

Members of the Examination Board

Reviewer: Prof. Dr. Ernst A. Wimmer (Dept. of Developmental Biology, Johann-Friedrich-Blumenbach-Institute of Zoology and Anthropology)

Second Reviewer: Prof. Dr. Gregor Bucher (Dept. of Developmental Biology, Johann-Friedrich-Blumenbach-Institute of Zoology and Anthropology)

Further members of the Examination Board:

Prof. Dr. Reinhard Schuh (Dept. of Molecular Developmental Biology, Max Planck Institute for Biophysical Chemistry)

Prof. Dr. Andreas Stumpner (Dept. Cellular Neurobiology, Johann-Friedrich-Blumenbach-Institute of Zoology and Anthropology, Schwann-Schleiden Research Centre)

Prof. Dr. Ralf Heinrich (Dept. Cellular Neurobiology, Johann-Friedrich-Blumenbach-Institute of Zoology and Anthropology, Schwann-Schleiden Research Centre)

Dr. Roland Dosch (Dept. of Developmental Biochemistry, Göttingen University Medical School)

Date of the oral examination: 24.01.2013

Declaration

I declare that this doctoral thesis titled “Fundamental Efforts to Develop Novel Biotechnological Approaches in Pest Management Applications against Coleoptera: Transcriptomic Exploration of the Chemical Defense Mechanism in the Red Flour Beetle, *Tribolium castaneum*” was a product of my experimental research work carried out in the Department of Developmental Biology, Georg-August University Göttingen, and that it has not been submitted elsewhere for the award of any degree. Works of other people cited herein have been indicated specifically, or acknowledged by means of completed references.

Dedication

To all who cared, gave me support, understanding and encouragement

Acknowledgement

I would like to thank my family and relatives for all their understanding, support, concern and encouragement that keep me going during the whole study in Germany.

My sincere gratitude goes to my supervisor, Prof. Dr. Ernst A. Wimmer, for giving me the great opportunity to study in this university at the beginning, and then guiding me with his extraordinary intelligence and remarkable professional experience. I thank Prof. Dr. Gregor Bucher for being the co-supervisor of this work and for all the advice, support and encouragement which helped me to finish.

Many thanks to our collaborative partners, Prof. Dr. Stefan Schütz and Dr. Berhard Weißbecker of the Department of Forest Zoology and Forest Conservation, Buesgen-Institute, Georg-August-University Göttingen for their generosity and help with Gas Chromatography–Mass Spectrometry (GC-MS) system and related analyses, as well as Dr. Gerrit Joop (Previously: Department of Evolutionary Ecology and Genetics, Zoological Institute, Christian-Albrechts-Universität zu Kiel; now: Institute for Phytopathology and Applied Zoology, University of Giessen) for her help on building up the ecological testing systems and teaching us the related techniques. My gratitude also go to Prof. Dr. Ivo Feussner, Dr. Ellen Hornung and Dr. Florian Brodhun (Department of Pant Biochemistry, GZMB, Georg-August-University of Göttingen) for offering the professional suggestions and related analyzing systems on biochemistry related research.

Special thanks go to Sabrina Lehmann for her wonderful help and inputs into my work. To the past and present colleagues /friends, Christian Ogaugwu, Irene Ojeda Naharros, Bernhard Schmid, Stefan Dippel, Kefei Yang, Nikolaus Koniszewski, Sebastian Kittelmann and Georg Oberhofer, I am very grateful for all the help, suggestions and discussions. All

members in Department of Developmental Biology are very much appreciated for their help and assistance, especially Beate Preitz, Birgit Rossi, Elke Küster, Helma Gries, Angelika Löffers, Inga Schild and Selen Pfändner. I am obliged to Prof. Dr. Jörg Großhans for help on using Laser Scanning Microscopy, Yujun Zhang for discussions on improving *in situ* hybridization, Tselmeg Uriankhai and Nico Posnien for the help on statistical methods, Tobias Klös for assistance on cloning work, and Andreas Mitschke for providing the stock culture of *Aspergillus niger.* And thanks to the late lunch group (Christian Ogaugwu, Kefei Yang, Stefan Dippel, Martin Ehrle, Alice Metzger and Ingrid Curril) for all the nice company.

I thank Macrogen Inc. (Seoul, South Korea) and Transcriptome Analysis Labor (TAL, University of Göttingen), especially Dr. Gabriela Salinas-Riester, Claudia Pommerenke and Lennart Opitz for providing great transcriptomic data.

So much appreciated are Dr. Christian Ogaugwu, Dr. Ellen Hornung and Dr. Florian Brodhun for correcting this thesis.

Lots of thanks to my friends Xiaole Wang, Christian Ogaugwu, Kefei Yang, Jianfeng Wang, Ingrid Curril, Bernhard Schmid, Weronika Sura, Van Ahn Dao, Bing Zhang, Narisu Tao, Tselmeg Uriankhai, Yukey Kim, Rongtao Guo, Konglin Zhu, Yushuang Lin, Shuhong Huang, Fei Ren, Yang Liu, Rongrong Yu, Yuyun Xing, Yonggang Hu, Qiang Wu, Yuyin Cai, Sheng Zhao, Qin Zhang, Xinxin Cai, Rui Deng and Na Lin for their support and making my stay in Göttingen more exciting.

Last but not least, I am truly appreciated to the German Academic Exchange Service (DAAD), the China Scholarship Council (CSC) and the home institute for providing me a PhD scholarship, so that I do not need to worry about anything financially during my study. I will be always grateful for this generosity.

Table of Contents

Abbreviations

15ene: 1-pentadecene; 17ene: 1-heptadecene; 17diene: 1,8-heptadecadiene, or heptadecadiene with the double bonds' positions uncertain; abd: abdominal glands; al: alkene-less; EBQ: ethyl-1,4-benzoquinone; EHQ: ethyl quinol, or ethyl-1,4-hydroquinone; EGFP: enhanced green fluorescent protein; FA: fatty acid; FC: fold change; GC-MS: Gas chromatography and mass spectrometry; GT: gland transcriptome; GO: gene ontology; GWMFISH: gland whole mount fluorescent *in situ* hybridization; MBQ: methyl-1,4-benzoquinone; MHQ: 2-methylhydroquinone; NGS: next generation sequencing; OGS: official gene set; PO: phenol oxidase; ql: quinone-less; thr: prothoracic glands; wt: wild-type.

List of Figures and Tables

Supplementary Data Sets

All Data Sets are presented on the attached CD disk.

Dataset 1 Library subtraction procedures and results, including list of genes for GO. (The gland transcriptome library is presented in Dataset 8)

Dataset 2 77 candidate genes, including primers and Tm for PCR to clone dsRNA fragments and RACE PCR, as well as their RNAi-induced phenotypes.

Dataset 3 *Tribolium* homologs of *quinone-less* genes and their gland transcriptomic expression levels. For abbreviations see Table 1.

Dataset 4 Sequences for phylogenetic analyses. **4A**: GT39 (Tcas-ql VTGl) homologs; **4B**: GT62 (Tcas-ql ARSB) homologs; **4C**: GT63 (Tcas-ql MRP) homologs.

Dataset 5 All primers and their annealing temperatures in Part 2.21 and 2.22.

Dataset 6 The novel alkene-less gene homologs for phylogenetic analysis.

Dataset 7 The genes from the analyses of the enhancer trap lines and their relative transcriptomic expression levels.

Dataset 8 Gland transcriptome library. s1: sample1, anterior abdomen; s2: sample2, prothoracic glands from *tar* mutant; s3: sample 3, male prothoracic glands; s4: sample 4, female prothoracic glands; s5: sample 5, male abdominal glands; s6: sample 6, female abdominal glands (Except s2, all the other tissues were from wild-type). Fold change (FC) is calculated as log2[reads in one sample / reads in another sample]. For abbreviations see Table 1.

Dataset 9 Gene ontology results in details.

Dataset 10 Annotations and gland transcriptomic expression levels of quinone synthesis-related genes, such as glucosidases (Glu), phenol oxidases (PO) and peroxidases (Per). For abbreviations see Table 1.

Dataset 11 Quantification of main gland volatiles, including standard series, and statistical analyses of sex and group comparisons for wild-type, EGFP-injection control, and the three *quinone-less* gene knock-downs.

Dataset 12 The detailed data in FA metabolism related gene annotation and the whole integrated transcriptome library.

Dataset 13 The whole sequences of the five candidate genes in Part 3.14 and 3.15.

Dataset 14 *Tribolium* homologs of the alkene-less gene and their gland transcriptomic expression levels.

Abstract

Chemical defense is one of the most important traits, which endow insects with the ability to conquer diverse ecological environments. Chemical secretions are used for defense against anything from vertebrate or invertebrate predators to prokaryotic or eukaryotic parasites or food competitors. Tenebrionid beetles are especially prolific in this category, producing several varieties of substituted benzoquinone compounds. Better understanding of the genetic and molecular basis of defensive systems will not only answer fundamental biological questions, but also inspire the development of novel methods for pest control.

To do so, I performed RNA sequencing in a newly emerging insect model, the red flour beetle *Tribolium castaneum* (Coleoptera: Tenebrionidae). The odoriferous gland tissues that secret defensive chemical compounds were compared to a control tissue, the anterior abdomen, to detect genes that are highly and specifically expressed in the different glands. A total of 511 genes were identified in different subtraction groups. Of these, 77 genes were functionally analyzed by RNA interference (RNAi) to recognize induced gland alterations morphologically or changes in gland volatiles by gas chromatography-mass spectrometry. 29 genes (38%) presented strong visible phenotypes, while 67 genes (87%) showed alterations of at least one gland content. Three of these genes showing quinone-less (ql) phenotypes – *Tcas-ql VTGl*; *Tcas-ql ARSB*; *Tcas-ql MRP* – were isolated, molecularly characterized, their expression identified in both types of the secretory glandular cells, and their function determined by

quantification of all main volatile components after RNAi. In addition, microbe inhibition assays revealed that a quinone-free status is unable to impede bacterial or fungal growth. Phylogenetic analyses of these three genes indicate that they have evolved independently and specifically for chemical defense in beetles.

Another major content of the glands is represented by alkenes. In order to identify the alkene biosynthetic mechanisms, the fatty acid profile was explored in glands and different developmental stages of *Tribolium castaneum* with the fatty acid metabolism related genes being annotated, and their relative transcriptomic expression levels being investigated. Further characterization of three candidate genes isolated two desaturases with *in vivo* tested activities and one novel gene (*Tcas-al P450*) with alkene-less RNAi phenotype, which are very rare in nature and have the potential to be applied to produce both fuels and chemicals in industry. The alkene-less gene function was confirmed by the quantification of the main volatiles in the glands, its specific and independent evolution by phylogenetic analysis, and its particular expression in only one type of secretory glandular cells by fluorescent *in situ* hybridization. Additionally, the phenoloxidase activity tests of the *quinone-less* and *alkene-less* genes suggested that the chemical defense system might be linked with innate immunity in *Tribolium castaneum.*

All the data obtained in this thesis bring the chemical defensive secretion in *Tribolium castaneum* to a molecular level for the first time, which opens a new biological research field and sheds light on many future studies.

1. Introduction

1.1 The importance of chemical defense

Insects are among the most diverse group of animals on the planet and amazingly include more than a million described species, which is more than half of all known living organisms (Chapman, 2009; Wilson, 2006). Moreover, they have conquered almost every environment on earth. From a series of distinctive attributes that orchestrate together to endow them with the ability to live in a wide range of ecological environments, chemical defense is one of the most important traits (Eisner, 1970). Many chemical secretions have repellent or irritant properties (Eisner, 1966; Blum, 1981, 183–205). Tenebrionid beetles are especially prolific by producing several various substituted benzoquinone compounds (Eisner and Meinwald, 1966; Weatherston, 1967; Blum, 1981; Unruh et al., 1998; Villaverde et al., 2007). *Tribolium* beetles (Coleoptera: Tenebrionidae) have dragged attentions of researchers to their particular secretions, since it was noted that their flour medium turns pink over time due to the secretion of a gaseous substance from adults (Chittenden, 1896), which also deleteriously affects the viscous and elastic properties of dough made from such infested flour (Payne, 1925).

1.2 Chemical defense in the red flour beetle

Tribolium beetles possess for the purpose of chemical defense two pairs of specialized secretory organs – one in the prothorax and one in the posterior abdomen – termed odoriferous or stink glands (Roth, 1943; see **Figure 1**). The glands located in the prothorax are called prothoracic, thoracic, or anterior glands, while the other pair in the abdomen is referred to as abdominal, posterior, or pygidial glands. The fine structure of these glands revealed two types of secretory units composed of two slightly different types of cells with particular vesicular organelles (cell type 1 and cell type 2), tubules, reservoir, ducts and muscles (Roth, 1943; Eisner et al., 1964; Happ, 1968; see **Figure 2 and 3**). At least four members of the genus *Tribolium (T. anaphe, T. castaneum, T. confusum,* and *T. destructor)* use the glands to produce the quinone derivatives 2-methoxybenzoquinone, ethyl-1,4-benzoquinone (EBQ), and methyl-1,4-benzoquinone (MBQ) (Alexander and Barton, 1943; Roth, 1943; Loconti and Roth, 1953; Happ, 1968; Villaverde et al., 2007). However, only the latter two substances were detected in *T. confusum* (Weatherston, 1967; Blum, 1981; Markarian et al., 1978). Besides benzoquinone derivatives, hydrocarbons were also reported as major secretion components. *T. confusum* secrets 1-pentadecene (Von Endt and Wheeler, 1971), 1,6-pentadecadiene and smaller amounts of 1-hexadecene, 1,6-hexadecadiene, hexadecatriene, 1-heptadecene, 1,8-heptadecadiene and heptadecatriene (Suzuki et al., 1975; Görgen et al., 1990). In *T. castaneum*, 1-pentadecene and 1,6-pentadecadiene were identified, with the former as the main component (Markarian et al., 1978;

Villaverde et al., 2007), plus two still unidentified hydrocarbons were found (Markarian et al., 1978).

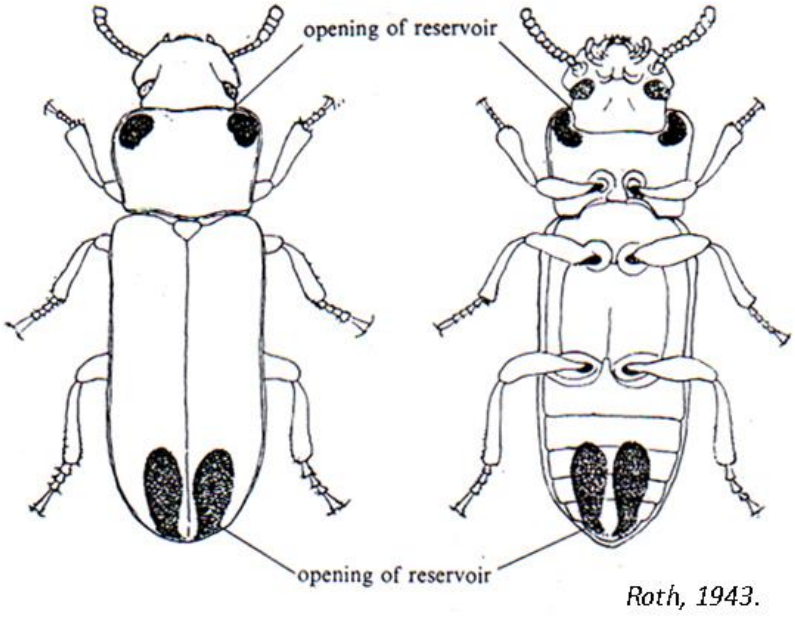

Figure 1 Drawings of adult *Tribolium* showing two pairs of odoriferous glands. The prothoracic and abdominal glands are indicated with stippled areas in thorax and abdomen, viewing from back (to the left) and abdomen (to the right) (Roth, 1943).

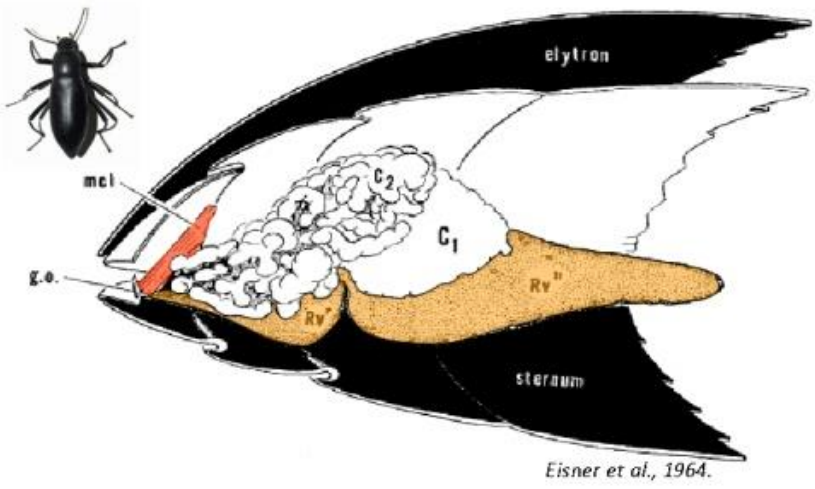

Figure 2 Left half of abdominal tip of another Tenebrionid beetle, *Eleodes longgicollis*, with similar quinone-producing defensive gland in place. Note: mcl, the single muscle that serves to dilate the gland opening (g.o.); C1, patch of cell 1; C2, tissue of cell 2a and 2b; Rv', basal lobe of reservoir; Rv", distal lobe of reservoir. (Eisner *et al.*, 1964)

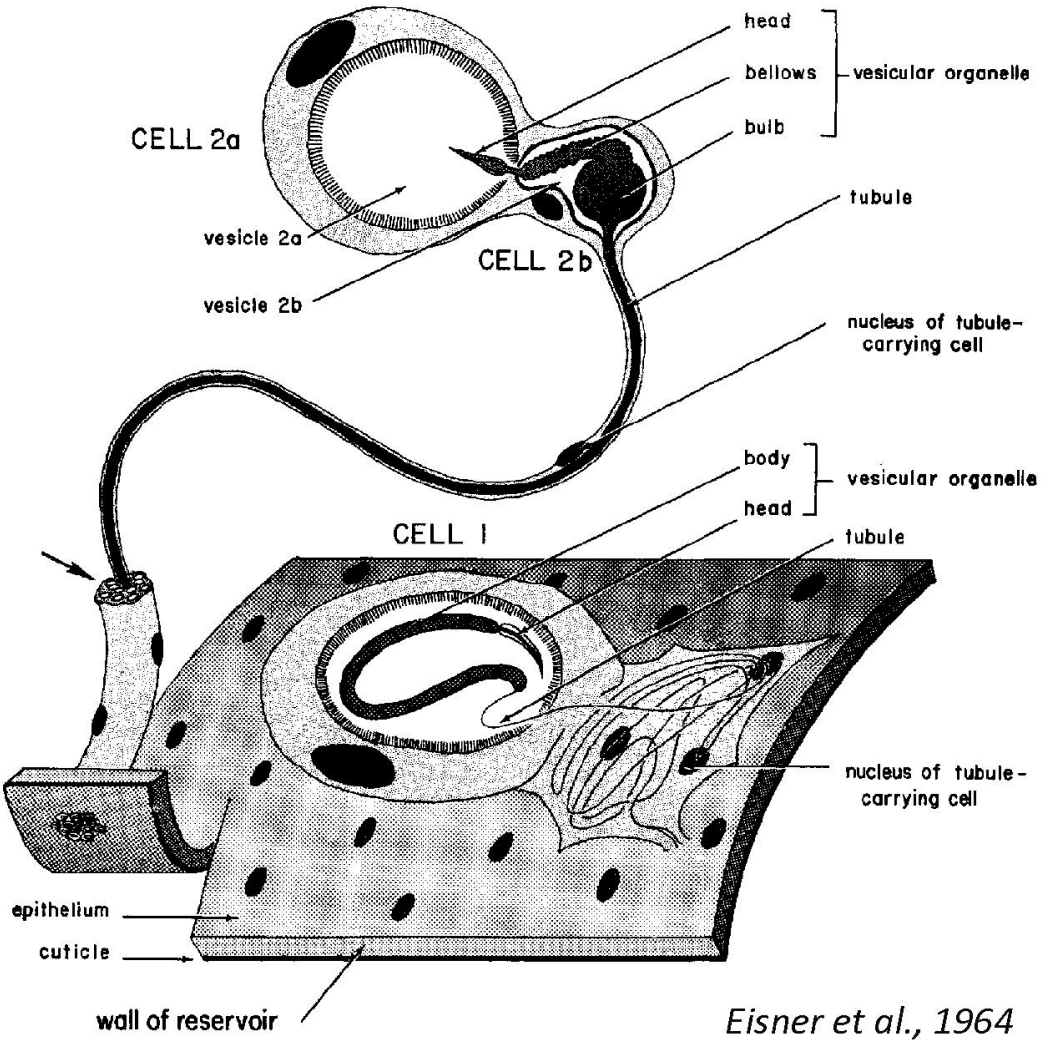

Figure 3 Diagram of the fine structure of the quinone-producing gland in *Eleodes longgicollis*. Based on the data from electronmicroscopy, the secretory cells of type 1 and types 2a + b, and their associated tubule-carrying cells, are shown in relation to the reservoir wall. The tubule that drains cells 2a + b ordinarily joins others of its kind to form a bundle of tubules. The accompanying tubules are here shown cut (arrow) near the wall of the reservoir. (Eisner *et al.*, 1964)

1.3 The feasibility and significance of the study in *Tribolium*

The red flour beetle, *T. castaneum* has been developed into a highly sophisticated genetic model organism (Wang et al., 2007) with plenty of genetic and genomic tools: reverse genetics based on systemic RNA interference (Bucher et al., 2002; Tomoyasu et al., 2008), forward genetics based on insertional mutagenesis (Lorenzen et al., 2005; Trauner et al., 2009), transgene-based mis-expression systems (Schinko et al., 2010, 2012), as well as a fully annotated genome sequence (Tribolium Genome Sequencing Consortium et al., 2008). Moreover, several mutants with odoriferous gland phenotypes, such as *melanotic stink glands* (*msg*, with both pairs of glands melanized) (Engelhardt et al., 1965), *tar* (only prothoracic glands are darkly pigmented), and *box* (A^{box}, similar to *tar,* but only the abdominal glands are affected) (Beeman et al., 1992). For the defense mechanism in *Tribolium*, only two publications have addressed how the quinones and alkenes are produced (Happ, 1968; Görgen et al., 1990), but no data are available on the genes involved in these processes. Moreover, understanding of the mechanisms involved in the autodetoxication of the defensive compounds might provide inspirations to manage this cosmopolitan pest and potentially other coleopteran pests. Benzoquinones are highly reactive, unstable and also toxic. Obviously, tenebrionids are protected from their own toxic secretions by cuticular linings both internally and externally (Blum, 1981). *Tribolium* beetles have the ability to partition the secretion away from the somatic cells, firstly by producing the secretions in the cuticle-lined organelles (Happ, 1968) and then keeping them in storage sacs (reservoirs) that are formed from invaginations of the cuticle (Roth, 1943). The newly

emerged *Tribolium* adults lack the defensive secretions, implying the need for building up an adequate self-protective barrier (Unruh et al., 1998). Consequently, if this self-protection system could be broken, the pests will harm themselves.

1.4 Fatty acids

Fatty acids (FA) are aliphatic monocarboxylic acids with hydrocarbon chains ranging from 4 to 36 carbons long (C_4 to C_{36}) (Lehninger et al., 2005), which are derived from or contained in esterified form in an animal or vegetable fat, oil or wax. Most naturally occurring fatty acids have a chain of an even number of carbon atoms, from 4 to 28 (usually unbranched), which may be saturated or unsaturated. By extension, the term is sometimes used to embrace all acyclic aliphatic carboxylic acids (IUPAC, 1997).

Fatty acids are usually derived from triglycerides or phospholipids. When they are not attached to other molecules, they are known as "free" fatty acids. Fatty acids are important sources of fuel because they yield large quantities of ATP after being metabolized. For this purpose, either fatty acids or glucose can be used in many cell types. In particular, heart and skeletal muscle prefer fatty acids. The brain cannot use fatty acids as a source of fuel; it relies on glucose or ketone bodies (Campbell and Farrell, 2006).

1.5 Fatty acids and the fat body in insects

In insects, fatty acid metabolism takes place in a special organ called fat body (Arrese and Soulages, 2010). Unlike many other insect tissues, the fat body does not have clear vertebrate analogs. Being unique to insects, fat body plays an essential role in energy storage and utilization. It is the central storage depot for excess nutrients. In addition, it is an organ of great biosynthetic and metabolic activity (Law and Wells, 1989). Most of the insect's intermediary metabolism takes place in this organ, including lipid and carbohydrate metabolism, protein synthesis, and amino acid and nitrogen metabolism (Arrese and Soulages, 2010).

Unlike the solid structure of the liver, the fat body is a loose tissue, but a relatively large organ distributed throughout the insect body, preferentially underneath the integument and surrounding the gut and reproductive organ (Dean et al., 1985). The fat body is disposed in thin layers with one or two cells of thickness. It can also appear as small suspended strings in the hemocele, filling the cavities of the head, the thorax and the abdomen, functioning as connective tissue between the organs (Chapman, 1998; Roma et al., 2010). Generally, the organ is arranged in thin lobes that are bathed by the hemolymph. This type of organization provides maximal exposure to the hemolymph, which is vital for the organism to adjust appropriately to the changes in the concentration of energy precursors in circulation (Arrese and Soulages, 2010). This fulfills all the energy needs efficiently in the whole insect body.

1.6 Fatty acids and alkenes in defensive glands of *T. castaneum*

Insect fatty acids were suggested as precursors to produce hydrocarbons (Happ, 1968), which include aromatic hydrocarbons (arenes), alkanes, alkenes, cycloalkanes and alkyne-based compounds. Alkenes are unsaturated hydrocarbons with one or more double bonds.

In chemical defensive secretions of the red flour beetle, several alkenes were reported. *Tribolium confusum* secrets 1-pentadecene (Von Endt and Wheeler, 1971), 1,6-pentadecadiene and smaller amounts of 1-hexadecene, 1,6-hexadecadiene, hexadecatriene, 1-heptadecene, 1,8-heptadecadiene and heptadecatriene (Suzuki, Huynh, & Muto, 1975; Görgen, Frößl, Boland, & Dettner, 1990). In *T. castaneum*, 1-pentadecene and 1,6-pentadecadiene were identified, with the former as the main component (Markarian et al., 1978; Villaverde et al., 2007), plus two still unidentified hydrocarbons found (Markarian et al., 1978). My data in this thesis (see Part 3.7) have shown that 1-pentadecene is the main alkene in *T. castaneum*, possessing 60-88% (in molar) of all detectable hydrocarbons.

1-pentadecene belongs to terminal olefins (1-alkenes), which represent extremely versatile chemical intermediates and thus serve as important products with direct application in the production of biofuels or other industrial chemicals such as plasticizers or biodegradable surfactants (Lappin and Sauer, 1989). Despite their importance only a very limited set of production pathways are known. So far only two natural pathways that convert fatty acid derivatives into terminal olefins have been

described. One has been identified in a cyanobacterium involving a sulphonation-assisted decarboxylase reaction mediated by a polyketide synthesis (Mendez-Perez et al., 2011), and a second one in marine staphylococcaceaen bacteria by a P450 cytochrome that catalyzes a decarboxylative oxidation reaction (Rude et al., 2011). Only few eukaryotes have been described to produce terminal olefins: microalgae (Templiera et al., 1991a, 1991b), plants such as safflower (Ney and Boland, 1987), and beetles of the genus *Tribolium* (Von Endt and Wheeler, 1971; Suzuki et al., 1975; Görgen et al., 1990; Villaverde et al., 2007). However, enzymes and encoding genes of eukaryotes that catalyze terminal olefin synthesis have so far not been described. Therefore, *T. castaneum* provides a unique animal model system to potentially identify novel genes involved in terminal olefin synthesis, then elucidation of the related metabolism may provide solutions to the key steps of developing bio-renewable fuels.

2. Materials and Methods

2.1 Beetles

Experiments were performed with the wild-type *Tribolium castaneum* strain San Bernardino. Animals were kept at 25°C, 40-60% relative humidity. After dsRNA injection, they were maintained at 32.5°C until phenotypic analysis.

2.2 Phenotype clarification of several enhancer trap or mutant lines and inverse PCR

The insertional enhancer trap lines (Trauner et al., 2009) were screened by our technician Elke Küster for fluorescent (or visible under cold light) signals in the odoriferous glands at either pupa or adult stage. The lines possessing positive signals were analyzed further to confirm the phenotype morphologically and locate the genomic insertion sites by inverse PCR. For phenotype confirmation, glands were dissected out of pupa or adult, directly embedded in PBS and immediately observed under Zeiss Axio Observer Z1 inverted fluorescent microscope (Carl Zeiss, Oberkochen, Germany). Inverse PCR was performed following the protocol from Sambrook & Russell (2006). The obtained fragments were blasted in Beetlebase (Wang et al., 2007; Kim et al., 2010) to get their locations in the genome.

2.3 Gland cytology

Odoriferous glands were dissected out of adult beetles (during this process the gland secretions in the reservoir are lost) and washed 3 times (5min each) with PBS in a 24-well cell culture plate, then incubated in DAPI solution (SIGMA-ALDRICH® Chemie GmbH, Munich, Germany, Cat. No. D9542, final concentration 0.1ug/mL in PBS) for 20min. After incubation, glands were washed 3 times (10min each) with PBS again, and embedded in 80% glycerol for observation and photo imaging under Zeiss Axio Observer Z1 inverted fluorescent microscope (Carl Zeiss, Oberkochen, Germany).

2.4 Transcriptome sequencing

Prothoracic and abdominal odoriferous glands were dissected separately from A10-A30 (reared at 32.5°C, 10 - 30 days after eclosion) adult beetles and stored in RNA*later*® solution (Ambion®, Life Technologies GmbH, Darmstadt, Germany, Cat. No. AM7020) on ice. Males and females were separately prepared except for the prothoracic glands from *tar* mutants. About 500 beetles were used for each gland sample, while the anterior abdomen, where no glands are located, was taken as a control tissue. Then total RNA was extracted using RNAqueous®-Micro Kit (Ambion®, Life Technologies GmbH, Darmstadt, Germany, Cat. No. AM1931) and treated by DNase I. Transcriptome sequencing (mRNA-seq) was performed by Macrogen Inc. (Seoul, South Korea), on a

next generation sequencing (NGS) platform (Illumina/Solexa Genome Analyzer IIx). After sequencing, reads (38bp each) were mapped to the mRNAs of the official gene set (OGS) from Beetlebase 3.0 (Wang et al., 2007; Kim et al., 2010) by Maq tool (http://maq.sourceforge.net/). The samples (s) were, s1: anterior abdomen; s2: prothoracic glands from *tar* mutant; s3: male prothoracic glands; s4: female prothoracic glands; s5: male abdominal glands; s6: female abdominal glands. Except of s2, all other tissues were wild-type. Coverage (depth) is calculated as reads times 38 divided by specific length of gene transcript.

2.5 Gene ontology annotation and mRNA-seq library subtractions

The genes, which had coverage over 50 (about 2 times of the whole sequencing coverage), were regarded as abundant or richly expressed in either all wild-type gland samples or control. Their functionalities were explored by gene ontology (GO) annotation (The Gene Ontology Consortium et al., 2000) using Blast2go (Conesa et al., 2005; Götz et al., 2008). In order to screen gland specific genes, statistical subtractions were carried out among different samples for various comparisons. In general, the cutoff for logarithm of fold change, with 2 as the base, was 6, which meant 64 times more reads in one sample than the other. The detailed subtraction conditions are presented in **Dataset 1.**

2.6 Transcriptomic exploration of candidate genes for quinone synthesis

Tribolium glucosidase, phenol oxidase and peroxidase were searched initially in protein database at the National Center for Biotechnology Information (NCBI) (http://www.ncbi.nlm.nih.gov/protein/). The obtained proteins were characterized based on conserved domains (CDD of NCBI, http://www.ncbi.nlm.nih.gov/Structure/cdd/cdd.shtml) and probed back to the publicly accessible *Tribolium* genome at Beetlebase with blastp algorithm in order to be linked with OGS, avoid redundancies, and identify the homologs which were not covered by the previous searches. The newly identified proteins were then analyzed in CDD for confirmation.

2.7 RNA extraction and cDNA library construction

Adult total RNA was extracted by using TRIzol® reagent (Invitrogen™, Life Technologies GmbH, Darmstadt, Germany, Cat. No. 15596-018) following manufacturer's instructions from a mixture of different adult stages (A0-A30), pre-adult and late pupal stages were also included in order to cover all the potential adult developmental genes. Then poly(A) was purified with the MicroPoly(A)Purist™ Kit (Ambion®, Life Technologies GmbH, Darmstadt, Germany, Cat. No. AM1919). Gland total RNA was prepared as preparing the mRNA-seq materials from same stages. The concentrations were measured on NanoDrop® spectrometer, and the qualities were checked on agarose gels. Double stranded cDNA libraries were constructed with SMART™ PCR cDNA Synthesis Kit

(Clontech, Saint-Germain-en-Laye, France, Cat. No. 634902) according to the user manual.

2.8 Cloning of 77 candidate genes

The chosen 77 candidate genes are listed in **Dataset 2**, as well as their primers and annealing temperatures for amplification using either Phusion® High-Fidelity DNA Polymerase (Finnzymes, Thermo Fisher Scientific, Inc., Waltham, USA, Cat. No. F-530) or Advantage® 2 PCR Enzyme System (Clontech, Saint-Germain-en-Laye, France, Cat. No.PT3281-1) from the adult cDNA library. Amplified fragments were ligated to PCR vectors with CloneJET™ PCR Cloning Kit (Fermentas, Thermo Fisher Scientific, Inc., Waltham, USA, Cat. No. K1231) or TA Cloning® Kit Dual Promoter (pCR®II) (Invitrogen™, Life Technologies GmbH, Darmstadt, Germany, Cat. No. K2070).

2.9 Functional analysis of the most highly and gland-specifically expressed genes

To evaluate the subtraction results, 77 candidate genes were chosen from the gland transcriptome screening and functional analysis was performed by using RNA interference (RNAi) (Hannon, 2002; Posnien et al., 2009). An online tool, E-RNAi (Horn and Boutros, 2010) was used to design fragments for double stranded RNA (dsRNA) synthesis with no or lowest off-target effects. Primers were designed by Primer Premier 5 (Lalitha, 2000) and listed in **Dataset 2.** Animals were injected with dsRNAs at mid

pupal (Posnien et al., 2009) or larval L5-L6 stage (Tomoyasu and Denell, 2004), and were checked at A10 and A24 (32.5°C) for morphological phenotypes on prothoracic and abdominal glands. Furthermore, both pairs of glands were dissected carefully and intact from one male and one female beetle and smashed in 100 µl methanol (Merck Millipore SupraSolv®, Merck KGaA, Darmstadt, Germany, Cat. No. 106011). Then the samples were stored at -20°C and measured within 24 hours. One microliter was loaded by a split injector into an Agilent gas chromatograph coupled with a mass spectrometer (GC-MS) (Detailed parameters are described in Part 2.11). The areas of the signals in chromatograms were calculated using the software MSD ChemStation D.02.00.275 (Agilent Technologies, Santa Clara, USA) under auto-integration mode. Then the data were compared between each candidate gene knock-down and the control. The phenotypes were grouped according to strengths of the alterations of the major components. For the three genes with quinone-less phenotypes, second independent dsRNA fragments, which had no overlaps with the first fragments, were designed with the same tools and used to confirm the phenotypes.

2.10 Photo imaging and processing

During dissection after RNAi, the abnormal glands were recorded using a CCD camera linked with a stereomicroscope Leica MZ16FA (Leica Microsystems GmbH, Wetzlar, Germany). Then the photos were processed with Adobe Photoshop CS2.

2.11 Gas chromatography and mass spectrometry (GC-MS)

The GC-MS system consisted of a 6980N gas chromatograph and a 5973N mass spectrometer from Agilent Technologies (Santa Clara, USA) together with an MPS autosampler from Gerstel (Mülheim, Germany). The samples were measured as soon as possible after preparations. During the analysis, the samples were kept in a cooled autosampler rack at ~10°C. One microliter of each sample was injected to the system. A capillary column HP-5ms (Agilent Technologies) was used (length 30 m, I.D. 0.25 mm, film thickness 0.25 µm). The split/splitless injector was operated at 250°C in the splitless mode. The carrier gas used was helium with a constant flow of 1.0 ml/min, which is equivalent to 36 cm/sec. The following temperature program was used: initial temperature 50°C, hold for 1.5 min, then with a rate of 7.5°C/min to 200°C, which was maintained for 5 min. Total run time was 26.5 min. The mass spectrometer was used in the scan mode (mass range 20–345 u). The data were analysed with the software MSD ChemStation D.02.00.275 (Agilent Technoligies, Santa Clara, USA). Substance identification was performed with the NIST 2008 and Wiley 9th edition databases (National Institute for Standards and Technology, Gaithersburg, USA / Wiley, Hoboken, USA). When available, the identification was verified with authentic standards.

2.12 Quantification of volatile gland contents

In order to quantify different volatile components in the secretion, the following chemicals were obtained from commercial sources: methyl-1,4-benzoquinone (MBQ)

(abcr GmbH & Co. KG, Karlsruhe, Germany, Cat. No. AB208176), 2-methylhydroquinone (MHQ) (abcr GmbH & Co. KG, Karlsruhe, Germany, Cat. No. AB132029), ethyl quinol (EHQ) (abcr GmbH & Co. KG, Karlsruhe, Germany, Cat. No. AB148997), 1-pentadecene (Fluka®, SIGMA-ALDRICH® Chemie GmbH, Munich, Germany, Cat. No. 76560) and 1-heptadecene (Fluka®, SIGMA-ALDRICH® Chemie GmbH, Munich, Germany, Cat. No. 51665). Then authentic standard solution series were made and a five-point calibration was performed by GC-MS. Based on the standard curves, the areas of the abundances from GC-MS were transformed to masses. Ethyl-1,4-benzoquinone (EBQ) and heptadecadiene, which were commercially unavailable, were calculated as equivalents based on the standard curve of EHQ and 1-heptadecene respectively. Quantification was carried out in wild-type, buffer injected, a dsRNA-EGFP injected control, and three *quinone-less* knock-downs. After pupal RNAi, glands were prepared from A10 beetles (15-30 animals each sex). It was proposed that more than 80% of the glandular quinones are benzoquinones (Unruh et al., 1998). Because the small amounts of hydroquinones detected are precursors of benzoquinones [24, 64], the quantities of hydroquinones and benzoquinones were summed up and treated as secreted quinones. After quantification, statistical analyses were performed with software JMP® 9.0.2 (SAS Institute, 2010) using student t-test for sex comparisons and a nonparametric method (Mann–Whitney–Wilcoxon) for group comparisons.

2.13 RACE PCR

RACE cDNA template was prepared from adult poly(A) RNA with SMART^{TM} RACE cDNA Amplification Kit (Clontech, Saint-Germain-en-Laye, France, Cat. No. 634914) according to the user manual. The specific primers were designed based on the amplified fragments and known sequences using Primer Premier 5.0 (Lalitha, 2000) according to the specifications in the manual of the kit and are listed in **Dataset 2**.

2.14 Phylogeny of the three novel *quinone-less* genes

Full length cDNAs obtained from RACE reactions were analyzed by the online tool ORF Finder (Open Reading Frame finder, http://www.ncbi.nlm.nih.gov/gorf/orfig.cgi) and translated to proteins. The amino acid sequences were submitted to NCBI to find the homologs through blastp search in Reference Proteins Database and the first fifty sequences were chosen, in which the *Tribolium* homologs were blasted again in Beetlebase (http://beetlebase.org/) to check redundancies and find the corresponding OGS numbers (listed in **Dataset 3**) in order to analyze their expressions at the glandular transcriptome level. Then all proteins (listed in **Dataset 4**) were aligned by using MAFFT (Katoh et al., 2005) and analyzed with FastTree (Price et al., 2010) using maximum likelihood methods to construct dendrograms, which were displayed, marked and computed based on the branching frequencies (cutoff was 60%) using MEGA5 (Tamura et al., 2011).

2.15 Gland whole mount fluorescent *in situ* hybridization

The protocol for gland whole mount fluorescent *in situ* hybridization (GWMFISH) was based on previous methods (Friedrich and Benzer, 2000; Osborne and Dearden, 2005; Schinko et al., 2009; Suzuki et al., 2009; Asp et al., 2006) with a few modifications. Details are described below.

Probe preparation. Sense and anti-sense Digoxigenin (DIG) labeled probes were synthesized from gel extraction purified PCR products, which were amplified with T7 and T3-pJET-R primers, by using DIG RNA Labeling Mix (Roche, Cat. No. 11277073910), T3 RNA Polymerase (Roche Applied Science, Roche Diagnostics Deutschland GmbH, Mannheim, Germany, Cat. No. 11031163001) or T7 RNA Polymerase (Roche Applied Science, Roche Diagnostics Deutschland GmbH, Mannheim, Germany, Cat. No. 10881767001) as instructed by the user manuals. Then alkaline hydrolysis was used to hydrolyze the probes. Equal volume of carbonate buffer (120 mM Na_2CO_3, 80 mM $NaHCO_3$, pH 10.2) was added to the probe and incubated at 60°C for 30 min. Six volumes of hybridization buffer [hyb-buffer: 50% formamide, 5 x SSC (pH 5.5), 100 µg/mL salmon sperm DNA, 100 µg/mL heparin, 0.1% Tween-20] were then added to halt the reaction (Osborne and Dearden, 2005). Probes were stored at -20°C until use (-80 °C is suggested for long time storage).

GWMFISH. Glands were dissected in chilled phosphate-buffered saline [PBS: 145 mM NaCl, 1.4 Mm KH_2PO_4, 8 Mm Na_2HPO_4 (pH 7.4)] on ice and placed in 4% PFA

(paraformaldehyde, in PBS) in a 24-well culture plate. When enough glands were collected, they were fixed for 30-40 min at RT or overnight at 4°C, washed twice in PBS, 15min each, then once in 50% PBS-methanol, twice in 100% methanol, and twice in ethanol for dehydration. Fixed glands were stored at -20°C for months or used right away. Glands were rehydrated through washing in 50% ethanol/PBT (PBS with 0.1% Tween-20) twice and then three times in PBT. A 6 min proteinase K (5 µg/mL in PBT) digest was followed by washes in PBT with 2 mg/mL glycine. After two washes in PBT, the tissues were post-fixed in 4% PFA for 40-60 min without agitation. The tissues were then washed three to four times in PBT and subsequently transferred to pre-warmed (66°C) W1 buffer [50% formamide, 5 x SSC (pH5.5), 1% SDS] for 5 min, then to the pre-warmed hyb-buffer. After at least 1 h of incubation in hyb-buffer at 66°C, the probe was mixed with hyb-buffer at a concentration of 2-10 ng/µl and heated to 95°C for 2 min, then placed on ice 5 min, and pre-warmed to 66°C.

After incubation with the probe for 14–48 h, the probe was removed, and the glands were washed three times 30 min each (rinse once before the first wash) in pre-warmed W1 buffer at 66°C, then overnight. The next day, the glands were washed twice with W2 Buffer (50% formamide, 2 x SSC, 1% SDS) at 66°C, once at RT, rinsed with W3 Buffer (2 x SSC, 0.1% Tween-20), and washed twice 10 min each. Optionally an RNAse treatment (0.02 mg/mL in W3 buffer, 37°C 20 min, then two times washes with W3) was performed. After an additional rinse in W4 Buffer (0.2 x SSC, 0.1% Tween-20), the tissues were washed in MABT buffer (100 mM maleic acid, 150 mM NaCl, 0.1% Tween-20, pH 7.5, fresh made) two times and blocked for 1 h at room temperature in

blocking solution (2 mg/mL BSA and 10% sheep serum in MABT, fresh made). Glands were incubated overnight at 4 °C with anti-DIG-alkaline phosphatase (AP) Fab fragments (Roche Applied Science, Roche Diagnostics Deutschland GmbH, Mannheim, Germany, Cat. No. 11093274910) at a concentration of 1:3000. After washing with MABT buffer several times and then with detection buffer (100mM Tris-HCl, 100 mM NaCl, 10mM $MgCl_2$, pH8.0), the color reaction was performed using HNPP Fluorescent Detection Set (Roche Applied Science, Roche Diagnostics Deutschland GmbH, Mannheim, Germany, Cat. No. 11758888001). Glands were rinsed in PBS to stop the color reaction and counterstained with Hoechst 33342 (SIGMA-ALDRICH® Chemie GmbH, Munich, Germany, Cat. No. B2261) prior to mounting and embedding in Aqua-Poly/Mount (Polyscience, Niles, Illinois, USA, Cat. No. 18606). The stainings were observed and captured with a confocal laser scanning microscope Zeiss LSM780. 3D (3-dimensional) construction was performed using software ZEN2011 (Carl Zeiss MicroImaging GmbH, Oberkochen, Germany). Contrast and brightness were adjusted using Adobe Photoshop CS2. All washes were carried out with gentle agitations for 15min unless otherwise described.

2.16 Microbe inhibition assays

A fungus, *Aspergillus niger*, and a gram positive bacterium, *Arthrobacter globiformis* (Conn and Dimmick, 1947), were used to test the strength of the chemical defense. The *A. niger* strain was an isolate from old beetle cultures (GJ, unpublished), which was

determined by the German collection of microorganisms and cell cultures (DSMZ) as *Aspergillus niger*, a common soil fungus also growing e.g. on bread and other food, known as 'Black mold'. *A. globiformis* (from DSMZ, Braunschweig, Germany, strain DSM20124) was another basic soil microbe and believed to have no contacts with *Tribolium* in nature.

A. niger was maintained at 25°C on plates of Potato Extract Glucose Broth (Carl-Roth GmbH & Co. KG, Karlsruhe, Germany, Cat. No. CP74.1) with 15g/L Agar Bacteriological Oxoid No.1 (Oxoid^{TM}, Thermo Fisher Scientific, Inc., Waltham, USA, Code LP0011). After sporulation of the fungi, spores were scraped off in Ringer's solution (128mM NaCl, 18mM $CaCl_2$, 1.3mM KCl, 2.3mM $NaHCO_3$) using a pipette tip (3mL each plate). The spore suspension was diluted 10 times with Ringer's and used for inoculation (1mL dilution for 10 mL medium). Reduced agar concentration was used for the assay plates (6g/L, 6mL per Ø9cm plate).

A. globiformis was activated from lyophilization and cultured at 28°C overnight in CASO broth (Carl-Roth GmbH & Co. KG, Karlsruhe, Germany, Cat. No. X938.1). OD value was measured using UV spectrometer. According to the OD, culture was diluted to a final OD of 0.6. Then 1mL dilution was added to 250mL CASO (10g/L agar) to make assay plates (also 6mL per Ø9cm plate).

Microbe lawns were made in the petri dishes using the method of (Faye and Wyatt, 1980; Prendeville and Stevens, 2002), by the modification that I put dissected abdominal glands to the holes on the lawn poked by a sterile glass pipet (one pair of glands per

hole and breaking of the reservoirs in the holes) instead of freezing beetles on the plates. The plates were incubated at 25°C for 72h (*A. niger*) or 28°C for 48h (*A. globiformis*) respectively, and then the inhibition zones were photographed with a digital camera. The areas of the inhibition zones were measured with freeware ImageJ 1.44p.

2.17 Phenol oxidase activity assays

After RNAi, A10 beetles were harvested and frozen individually at -80°C in 150 µl Bis-Tris buffer (0.1 M, pH 7.5, sterile filtered. Bis-Tris: Fluka®, SIGMA-ALDRICH® Chemie GmbH, Munich, Germany, Cat. No. 14880) for at least 24 hours. To the frozen samples, a sterile steel ball (Ø 3mm) was added each, and samples were homogenized using a GenoGrinder® tissue homogenizer for 30 seconds at a speed of 1000 strokes per minute. After grinding, samples were placed on ice immediately before centrifuging three times at 6200 rpm 4°C (Eppendorf centrifuge 5810R) for five minutes to remove beetle debris. After each centrifugation step the supernatant was transferred to a new tube on ice before being centrifuged again. For measuring actual PO activity, a flat bottom 96well plate was prepared on ice with 50 µl sterile deionized water and 50 µl Bis-Tris buffer. In each well 20 µl of an individual sample extract was pipetted, or 20 µl Bis-Tris buffer when the well was serving as a blank. As PO activates the transfer of DOPA to Dopamine in insects (Cerenius et al., 2008), we added 50 µl L-DOPA (3,4-Dihydroxy-L-phenylalanine, SIGMA-ALDRICH® Chemie GmbH, Munich, Germany,

Cat. No. D9628; 4mg/ml in Bis-Tris buffer, sterile filtered) into each well on ice. As the addition of substrate starts the reaction, plates needed to go to the Eon™ Microplate Spectrophotometer (Biotek Instruments, Inc., Bad Friedrichshall, Germany) immediately. Plates were read at 490nm and 37°C with readings every two minutes for 90 minutes. After correcting the self-darkening of the substrate by subtracting the blanks, PO activity was estimated as Vmax of the linear phase of the reaction on every individual sample well [also compare with previous data (Roth et al., 2010)].

2.18 Fatty acid profiling

Samples were collected from different immature stages of *T. castaneum* or adult tissues: eggs (0-12h), larvae (L7 stage), male pupae, female pupae, A0 male adults, A0 female adults, A10 males, A10 females, male glands at A10 stage and female glands at A10 stage. The beetle rearing flour was used as a control. Then all the samples were lyophylized (about 10 mg material each), transferred to Kimble glass tubes, and weighed. To each tube, 1 ml FAME-Solution (2.5 % H_2SO_4, 2 % Dimethoxipropan in Methanol), 20µl 5 mg/ml triheptadecanoate Standard and Argon gas (prevent the oxidation of fatty acids) were added before incubation for 1h in 80°C water bath. Fatty acid methyl esters were extracted by adding 200 µl saturated aqueous NaCl and 2 ml hexane, 10 min of centrifugation at 1500 rpm, and transferring the upper phase to a new tube. The lower phase was re-extracted with 2 ml hexane. Then 4 ml H_2O and Argon gas were added before centrifugation at 1500 rpm for 10 min. In order to remove residual water, the

upper phase was filtered through cotton wool overlaid with $NaSO_4$, got dried under streaming Nitrogen, and resuspended in 20-50 µl Acetonitrile (hypergrade for LC-MS LiChrosolv®, Merck Millipore, Merck KGaA, Darmstadt, Germany. Cat. No. 100029). Of these, 1µl was used for GC-FID [Gas Chromatograph(y) with Flame Ionization Detector]. Moreover, an aliquot can be used for DMOX (4,4-dimethy-loxazoline) derivatization followed by GC-MS; to localize double bonds.

2.19 Trancriptomic library construction of different developmental stages and gland samples

RNA was extracted as described in Part 2.4 from different tissues: larvae (L5 to L7 stage), male pupae (a mixture of early-, mid- and late-pupa), female pupae (also a mixture), A0 male adults, A0 female adults, A10 males and A10 females. After DNase I treatment, RNA-seq was performed in NGS platform with read length of 100 nt (nucleotide) by Transcriptome Analysis Lab (TAL, Department of Developmental Biochemistry, University of Göttingen). Their bioinformaticians mapped the raw data to *Tribolium* OGS by using bowtie (version 0.12.7. URL: http://bowtie-bio.sourceforge.net/index.shtml). For embryonic stage, the data from another project were used for analyses.

Following mapping and library construction, this library was integrated together with the gland transcriptomic library and normalized, in order to compare expressions in different samples. Two indices were introduced for each gene during normalization, relative reads index (RRI) and relative depth index (RDI).

RRI = log2[reads in one sample / total mapped reads in that sample]

RDI = log2[depth in one sample / total mapped reads in that sample]

2.20 Annotation of fatty acid metabolism related genes and exploration of their transcriptomic expression levels

Tribolium fatty acid metabolism related genes were annotated based on the related information on KEGG (Kyoto Encyclopedia of Genes and Genomes) pathway database (http://www.genome.jp/kegg/pathway.html). The referred entries were tca00071 and tca00061. Additional searches were performed in protein database at the National Center for Biotechnology Information (NCBI) (http://www.ncbi.nlm.nih.gov/protein/). All the obtained proteins were characterized based on conserved domains (CDD of NCBI, http://www.ncbi.nlm.nih.gov/Structure/cdd/cdd.shtml) and probed back to the publicly accessible *Tribolium* genome at Beetlebase (Wang et al., 2007; Kim et al., 2010) with blastp algorithm in order to be linked with OGS, avoid redundancies, and identify the homologs which were not covered by the previous searches. The newly identified proteins were then analyzed in CDD for confirmation.

Subcellular localization of putative proteins was predicted using TargetP 1.1 (http://www.cbs.dtu.dk/services/TargetP/), WoLF PSORT (http://wolfpsort.seq.cbrc.jp/) predotar server (http://urgi.versailles.inra.fr/predotar/predotar.html), MitoProt server

(http://ihg.gsf.de/ihg/mitoprot.html) and PSORT II (http://psort.hgc.jp/form2.html) prediction algorithms.

2.21 Characterization of desaturase candidates

Based on the conserved domains and gland transcriptomic expression levels, four desaturases were characterized further by RNAi analyses and *in vivo* activity tests. RACE was performed to amplify the whole open reading frame (ORF).The detailed description on RNAi and RACE can be found above. The primers are listed in **Dataset 5**. For *in vivo* expression, two types of different vectors were used to link with the ORFs. The vector pYES2 (Invitrogen^{TM}, Life Technologies GmbH, Darmstadt, Germany, Cat. No.: V825-20) was used for single expression. And for coexpression, vector pESC-LEU (Agilent Technologies, California, United States, Cat. No.: 217452) and pESC-HIS (Agilent Technologies, California, United States, Cat. No.: 217451) were used.

Then the yeast strains InvSc1 (Life Technologies GmbH, Darmstadt, Germany, Cat. No.: 500053) and InvSc2-Ole1-KO (in which the yeast Ole1 gene, i.e. Delta9 fatty acid desaturase gene, was disabled by targeted knockout) were used for transformation and expression induction. After the expression, the cells and culture medium were prepared for fatty acid profiling (see section 2.18).

2.22 Characterization of an *alkene-less* gene

Possessing an alkene-less phenotype in functional analysis in Part 2.9 of this thesis, one *P450* gene (GT12) was analyzed further.

2.22.1 Cloning, RNAi and quantification of the glandular volatiles in knockdowns

The primers for cloning and the second dsRNA are listed in **Dataset 5**. And the other methods are described in details in Part 2.8, 2.9 and 2.12 of this thesis.

2.22.2 Phylogeny, gland whole mount fluorescent *in situ* hybridization and phenoloxidase activity test

Please refer to Part 2.14, 2.15 and 2.17. And the sequences used for phylogenetic analysis are presented in **Dataset 6**.

2.22.3 *In vivo* activity test

Prokaryotic expression system: *Escherichia coli* strain BL21 Star™ (DE3) (Invitrogen™, Life Technologies GmbH, Darmstadt, Germany, Cat. No. C6010-03). Vector: pET28a (Novagen®, Merck Millipore, Merck Chemicals Ltd., Nottingham, UK, Cat. No. 69864). Culture conditions: 28°C/20h, protein expression was induced with 0.1mM IPTG (Isopropylthio-β-galactoside, Invitrogen™, Life Technologies GmbH, Darmstadt, Germany, Cat. No. 15529-019)

Eukaryotic expression system: yeast strains InvSc1 (Life Technologies GmbH, Darmstadt, Germany, Cat. No.: 500053) and InvSc2-Ole1-KO (in which the yeast Ole1 gene, i.e.

Delta9 fatty acid desaturase gene, was disabled by targeted knockout). Vectors: pYES2 (Invitrogen™, Life Technologies GmbH, Darmstadt, Germany, Cat. No.: V825-20), pESC-LEU (Agilent Technologies, California, United States, Cat. No.: 217452) and pESC-HIS (Agilent Technologies, California, United States, Cat. No.: 217451).

After the protein expression, fatty acid profiling was performed with both cell lysate and culture medium. The primers for vector construction are listed in **Dataset 5**.

3. Results

3.1 Phenotype clarification of several enhancer trap or mutant lines related to odoriferous glands.

3.1.1 Characterization of three insertional enhancer trap lines

Three insertional enhancer trap lines, G02218, KTR1728, and KS264 (Trauner et al., 2009), were characterized further based on fluorescence in the odoriferous glands. G02218: mid-pupa showed EGFP expressions in prothoracic stink glands (**Figure 4A, B**), which is localized at the wall of the reservoir after dissection (**Figure 4C**). KTR1728: EGFP is expressed from pupa to A3/A4 stage in both prothoracic and abdominal stink glands (**Figure 5A, B**). After dissection, only the secretory cells showed the fluorescent signals (**Figure 5C, D**). KS264: EGFP started to be expressed at early pupal stage, and was visible at all pupal stages in prothoracic glands, while it was weaker in abdominal glands (**Figure 6**). Similar to G02218, the expression was only localized at the reservoir wall (not shown here). However, at a very early pupal stage (**Figure 6B, C**), all the differentiating cells were fluorescent. So the affected gene(s) probably play an important role in gland development rather than in gland physiology.

In order to locate the genomic insertion site of these three lines, inverse PCR was performed. For line KTR1728, the insertion site was in a region with no gene annotated. The insertion site in G02218 was mapped in an intron of the XM_001810848.1 gene, so was the insertion site in line KS264. But this gene was based on GNOMON, an

automated computational prediction method. Several trials on cloning did not yield any positive fragments. Then eight genes close to the insertion site were chosen (**Dataset 7**) for *in situ* hybridization, but none of them showed positive expression. Based on the putative functions, two of them (SG5 and SG8, similar to dimethylaniline monooxygenase) were chosen to perform RNAi, which did not cause any visible phenotype.

Therefore, the modern RNA sequencing-based transcriptome method was applied to answer our scientific question of which gene close to the insertion is expressed in the glands. Later on, when the odoriferous gland transcriptome library was constructed, several genes related to the enhancer trap lines were analyzed to explore their relative expression levels (**Dataset 7**).

Starting from the insertion site of KTR1728 line, 120 genes were picked upstream and downstream (60 genes each side) to check the relative expression levels in different gland tissues comparing to the control tissue. And one gene had more than 32 times increased reads in the glands compared to the control, this gene XM_967531.1 represents the best candidate for this insertions site, which is annotated as PREDICTED: *Tribolium castaneum* similar to pheromone-degrading enzyme (LOC661371), and belongs to cytochrome P450 superfamiliy. The proteins from this family are involved in the oxidative degradation of various compounds and are particularly well known for their role in the degradation of environmental toxins and mutagens. This gene is suggested to be followed and analyzed further.

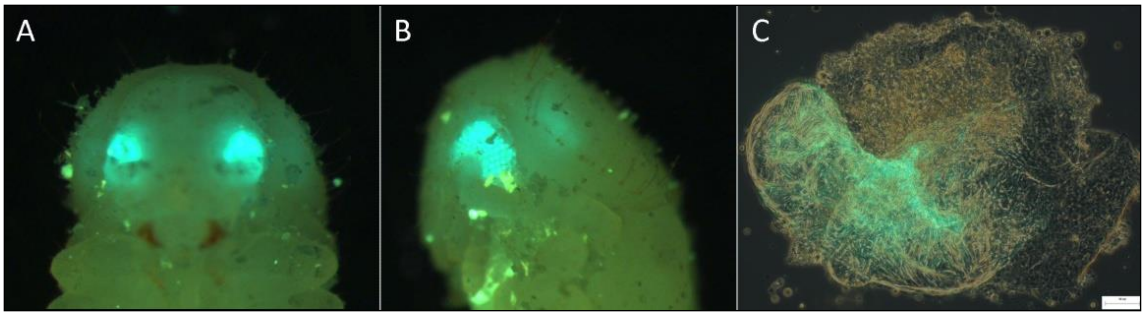

Figure 4 EGFP expressions in prothoracic odoriferous glands of the insertional enhancer trap line G02218. A, front view; B, lateral view; C, the dissected gland showed a fluorescent signal at the wall of reservoir. PS: the fluorescent eyes in pupa are screen markers. Scale bar in C: 50μm.

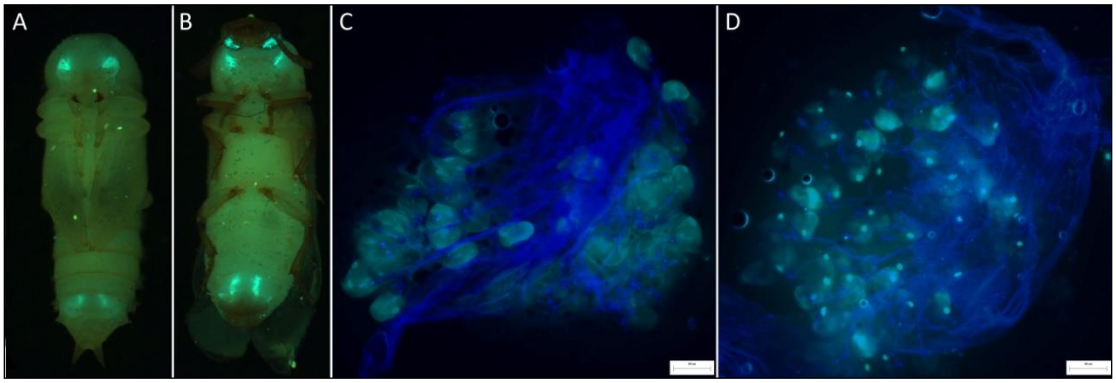

Figure 5 EGFP expressions in both pairs of odoriferous glands of the insertional enhancer trap line KTR1728. A, pupa; B, newly emerged adult; C, the dissected prothoracic gland; D, the dissected abdominal gland, the secretory cells showed the fluorescent signals (green), while the blue indicated the autofluorescent tubules and vesicular organelles. PS: the fluorescent eyes in pupa are screen markers. Scale bars in C and D: 50μm.

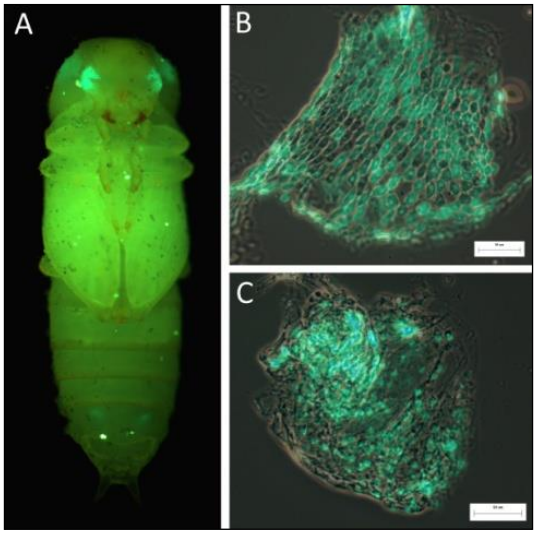

Figure 6 EGFP expressions in both pairs of odoriferous glands of the insertional enhancer trap line KS264. A, early pupa; B and C were the dissected prothoracic gland from very early stage (B) and early pupa stage (C). Scale bars in B and C: 50μm.

3.1.2 Characterization of two mutant lines with GC-MS

The gland volatiles were analyzed by GC-MS in two mutant lines: *melanotic stink glands* (*msg*, with both pairs of glands melanized, **Figure 7A-D**) (Engelhardt et al., 1965) and *tar* (more darkly pigmented prothoracic glands but unaffected abdominal glands, **Figure 7E-H**) (Beeman et al., 1992). It was shown that almost no alkenes were detected in the prothoracic glands of *tar* mutants while the abdominal glands had similar volatile pattern with wild-type (**Figure 8**). However, the *msg* mutant presented only small alterations on the volatiles (data not shown). (The GC-MS measurements were performed by Irene Ojeda Naharros, a bachelor student under my supervision)

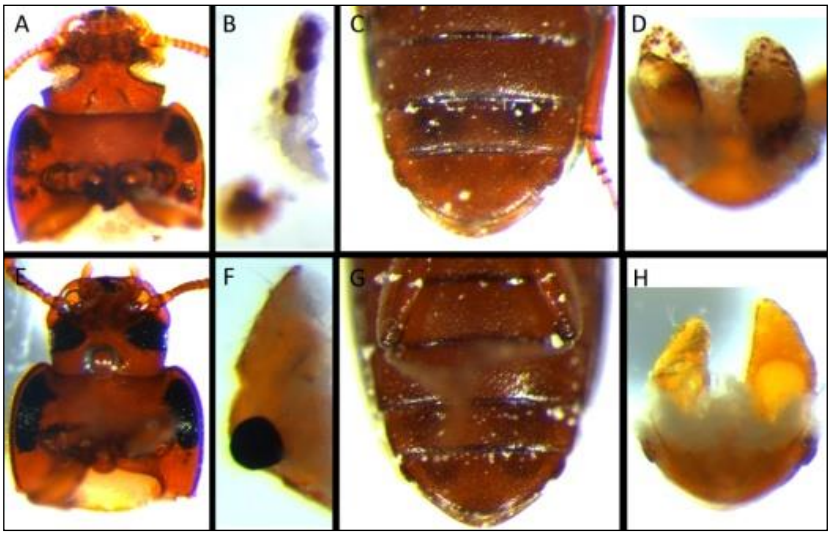

Figure 7 Abnormal glands in *msg* and *tar* mutant lines. A-D, *msg* mutant; E-H, *tar* mutant; A, E, adult thorax; B, F, dissected thoracic glands; C, G, abdomen in ventral view; D, H, dissected abdominal glands. In wild type, all the secretions are yellowish and in oil form as in H.

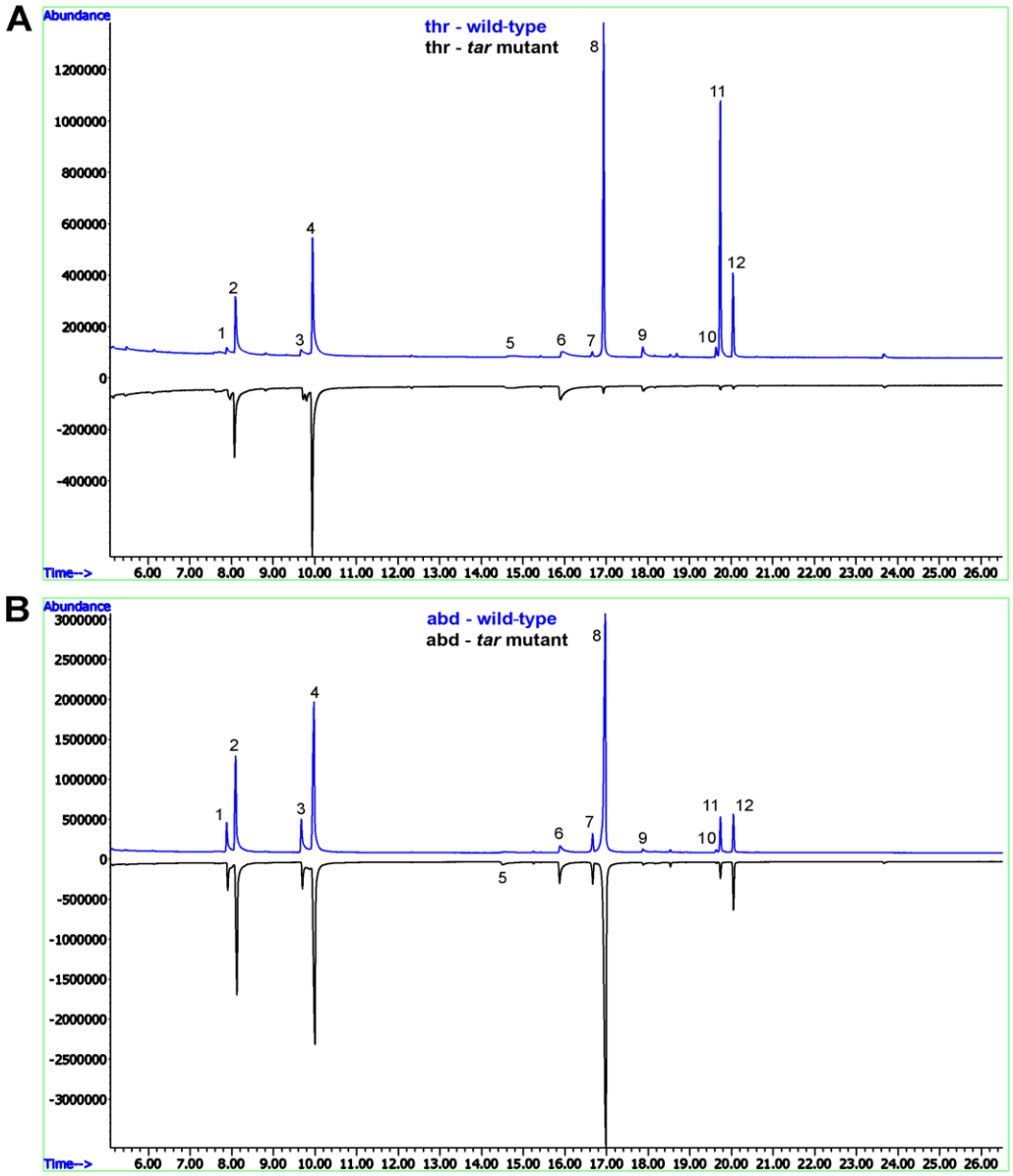

Figure 8 GC-MS Chromatograms of wild-type and *tar* mutant odoriferous glands. A, prothoracic glands, B, abdominal glands. Chromatograms show volatile detection from wild-type (upper blue) and *tar* mutants (lower black). The prothoracic glands of *tar* mutants presented very low levels of alkenes, while the abdominal glands showed no significant difference to wild-type beetles. The peaks are: 1 and 2: methyl-1,4-benzoquinone; 3 and 4: ethyl-1,4-benzoquinone; 5: methyl-1,4-hydroquinone; 6: ethyl-1,4-hydroquinone; 7: 1,6-pentadecadiene; 8: 1-pentadecene; 9: 1,2-dimethoxy-4-n-propylbenzene; 10: 1-Hexadecene; 11: 1,8-heptadecadiene; 12: 1-Heptadecene. Double bond positions in 1,6-pentadecadiene and 1,8-heptadecadiene have not been confirmed, since these chemicals were not identified in the NIST database, but only assigned to similar peaks based on previous data (Görgen et al., 1990; Suzuki et al., 1975). (These GC-MS chromatograms were done mainly by a bachelor student, Irene Ojeda Naharros, under my supervision.)

3.2 Stink gland transcriptome sequencing

The odoriferous defensive stink glands were dissected and identified by their special morphological structures, the vesicular organelles (Eisner et al., 1964; Happ, 1968) (**Figure 9**). mRNA sequencing was performed in six stink gland samples and one control sample (anterior abdomen, where no odoriferous gland located) on a next generation sequencing (NGS) platform. The abbreviations for the samples were, s1: sample 1, anterior abdomen from wild-type; s2: prothoracic glands from *tar* mutant; s3: wild-type male prothoracic glands; s4: wild-type female prothoracic glands; s5: wild-type male abdominal glands; s6: wild-type female abdominal glands. After sequencing, 27.8 to 29.7 million reads were obtained from each sample. About 50% of them were successfully mapped to the reference database, i.e. mRNAs of the *Tribolium* OGS in Beetlebase (Wang et al., 2007; Kim et al., 2010). And the average depths/coverages were in the range of 23.5 to 27.8. Moreover, ratios of covered region in reference varied from 52.5% to 68.0%. Detailed statistics are presented in **Table 1**.

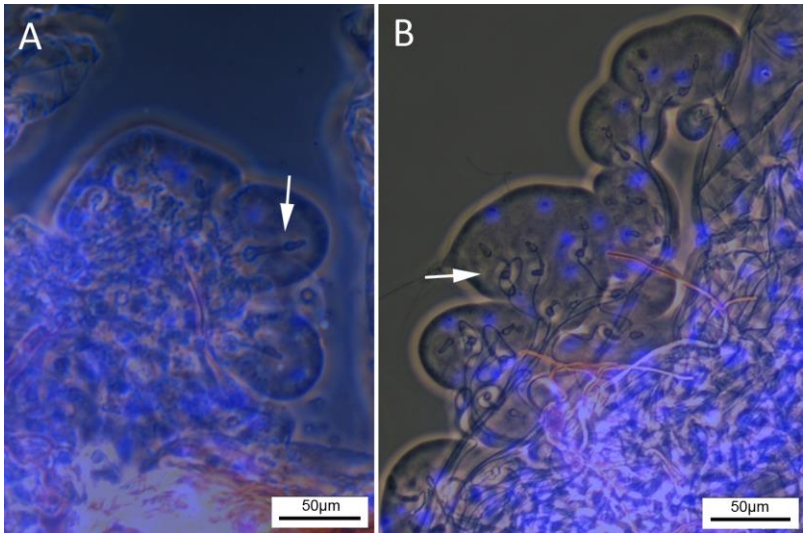

Figure 9 Secretory cell morphology of odoriferous glands. Dissected DAPI-stained odoriferous glands. A, prothoracic glands. B, abdominal glands. The arrows indicate the vesicular organelles of cell type 2 that have been described previously in *Tribolium castaneum* (Happ, 1968) and another tenebrionid beetle, *Eleodes longicollis*, (Eisner et al., 1964; Happ, 1968). Scale bars: 50µm.

Table 1 Statistics of transcriptome sequencing.

Sample name	s1_ctl	s2_tthr	s3_mthr	s4_fthr	s5_mabd	s6_fabd
Total reads	29,527,715	29,690,989	28,544,764	29,350,110	27,929,437	27,786,784
Mapped reads	14,727,172	15,773,797	14,605,945	15,590,528	14,327,863	16,955,288
Ratio of Mapping	49.88%	53.13%	51.17%	53.12%	51.30%	61.02%
Total mapped bases	559,632,536	599,404,286	555,025,910	592,440,064	544,458,794	644,300,944
Reference total base	23,149,063	23,149,063	23,149,063	23,149,063	23,149,063	23,149,063
Covered total base	15,746,380	13,768,019	13,279,109	12,151,610	13,943,411	13,272,086
Ratio of Covered region	68.02%	59.48%	57.36%	52.49%	60.23%	57.33%
Average Depth(Coverage)	24.18	25.89	23.98	25.59	23.52	27.83
Relative total reads	1.00000	1.00553	0.96671	0.99399	0.94587	0.94104

s1_ctl: sample 1, anterior abdomen control; s2_tthr: sample 2, *tar* prothoracic glands; s3_mthr: sample 3, male prothoracic glands; s4_fthr: sample 4, female prothoracic glands; s5_mabd: sample 5, male abdominal glands; s6_fabd: sample 6, female abdominal glands.

3.3 mRNA-seq library subtractions

The constructed mRNA-seq libraries are presented in **Dataset 8**, which shows the reads and coverage (depth) of each gene in all the samples, respectively. **Table 1** indicates that the relative total reads of all samples were quite close to each other. Therefore, the read number represented actual expression levels of all the *Tribolium* genes in various samples. In order to screen out the differentially or specifically expressed genes in odoriferous glands, ten different groups of subtractions were performed and in total 511 genes were identified (**Figure 10**; for detailed list and the subtractive conditions, see **Dataset 1**)**.** There were 62 genes in Group 1, standing for the gland specific genes, which were highly expressed in all wild-type gland samples (s3, s4, s5, s6) but not in the anterior abdomen control (s1). Group 2 presented 23 thoracic glands specific genes, which had higher reads in wild-type thoracic glands (s3 and s4) than in wild-type abdominal glands (s5 and s6) (and s1 control). Group 3 had 40 abdominal gland specific genes [s5 and s6 against s3, s4 (and s1)]. For sex related subtractions, Group 4 offered zero male stink glands specific gene [s3 and s5 against s4, s6 (and s1)], but Group 5 had four female stink glands specific genes (s4 and s6 against s3 and s5). There were zero male thoracic glands specific gene in Group 6 (s3 against s4 and s1), yet 299 male abdominal glands specific genes in Group 7 (s5 against s6 and s1). Meanwhile, there were also zero female thoracic glands specific gene in Group 8 (s4 against s3 and s1), but 39 female abdominal glands specific genes in Group 9 (s6 against s5 and s1). And Group 10 presented 44 genes which were either up or down regulated in prothoracic glands of *tar* mutants. The high number of genes identified in Group 7 is probably due to the

contamination of the abdominal gland sample by male accessary glands, which are hard to separate from the abdominal glands.

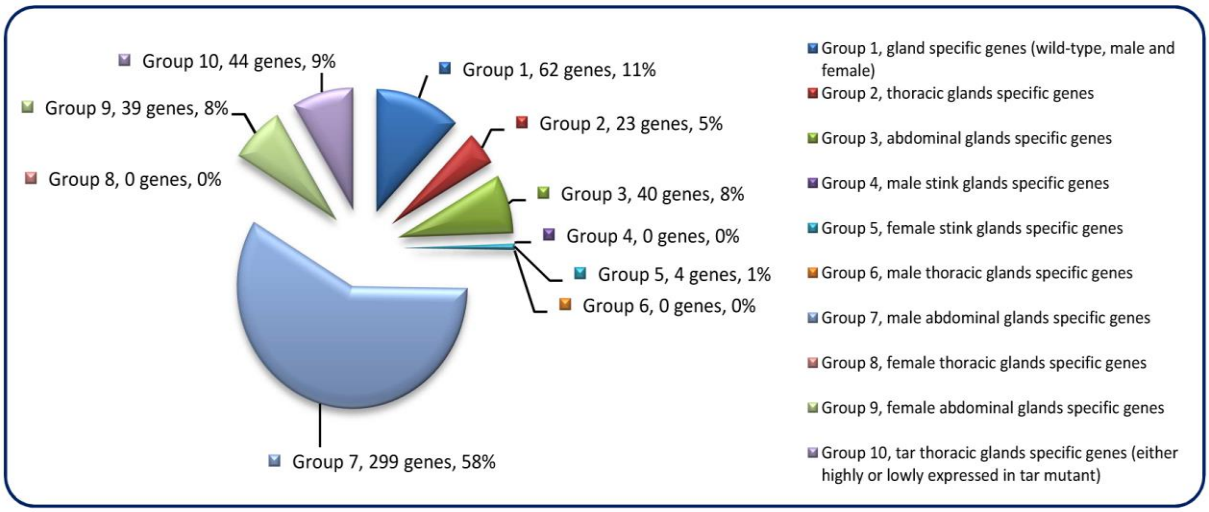

Figure 10 Odoriferous gland transcriptome screening result. Each pie slice is indicated with the group name, the number of genes classified, and their percentage. Each group is signified as a specific non-overlapping subtraction group with each gene belonging to only one group. E.g. Group 1 consists of genes that are highly expressed in all glands but not specifically in one gland type or only in one sex.

3.4 Gene ontology annotation

Gene ontology (GO) annotation allows meta-analyses of gene populations and associates the targeted genes to specific terms with hierarchical vocabularies describing three independent ontologies: biological process, molecular function, and cellular component (The Gene Ontology Consortium et al., 2000). Analyses were performed with 1451 genes abundant in the control, 1206 genes abundant in wild-type glands, and

the 511 genes from subtraction Group 1 to Group 10 (The genes are listed in **Dataset 1**). Results (**Figure 11A**) showed that many genes were classified to metabolic and cellular processes in the GO term of biological process, and to catalytic activity and binding in molecular function. For the cellular component, most genes belonged to cell, macromolecular complex and organelle. These implied the existence of strong metabolisms in both glands and anterior abdomen. Moreover, similar trends were observed in separated analyses in the different subtraction groups (**Figure 11B**). Detailed GO results are presented in **Dataset 9**.

See next page for **Figure 11**.

Figure 11 GO annotation of odoriferous glands transcriptome data. A, analyses of the genes abundant in control (Ctl; 1451 genes abundant in anterior abdomen transcriptome), wild-type glands (Glands; 1206 genes), and the genes identified in all ten subtraction groups (Figure 10) together (G1-G10; 511 genes). B, analyses of individual Group 1 to Group 10, respectively and the control (Ctl; 290 genes possessing at least 64 times higher reads in anterior abdomen than the wild-type gland samples). X-axis: different GO terms (level 2); Y-axis: percentage of the genes classified in each group.

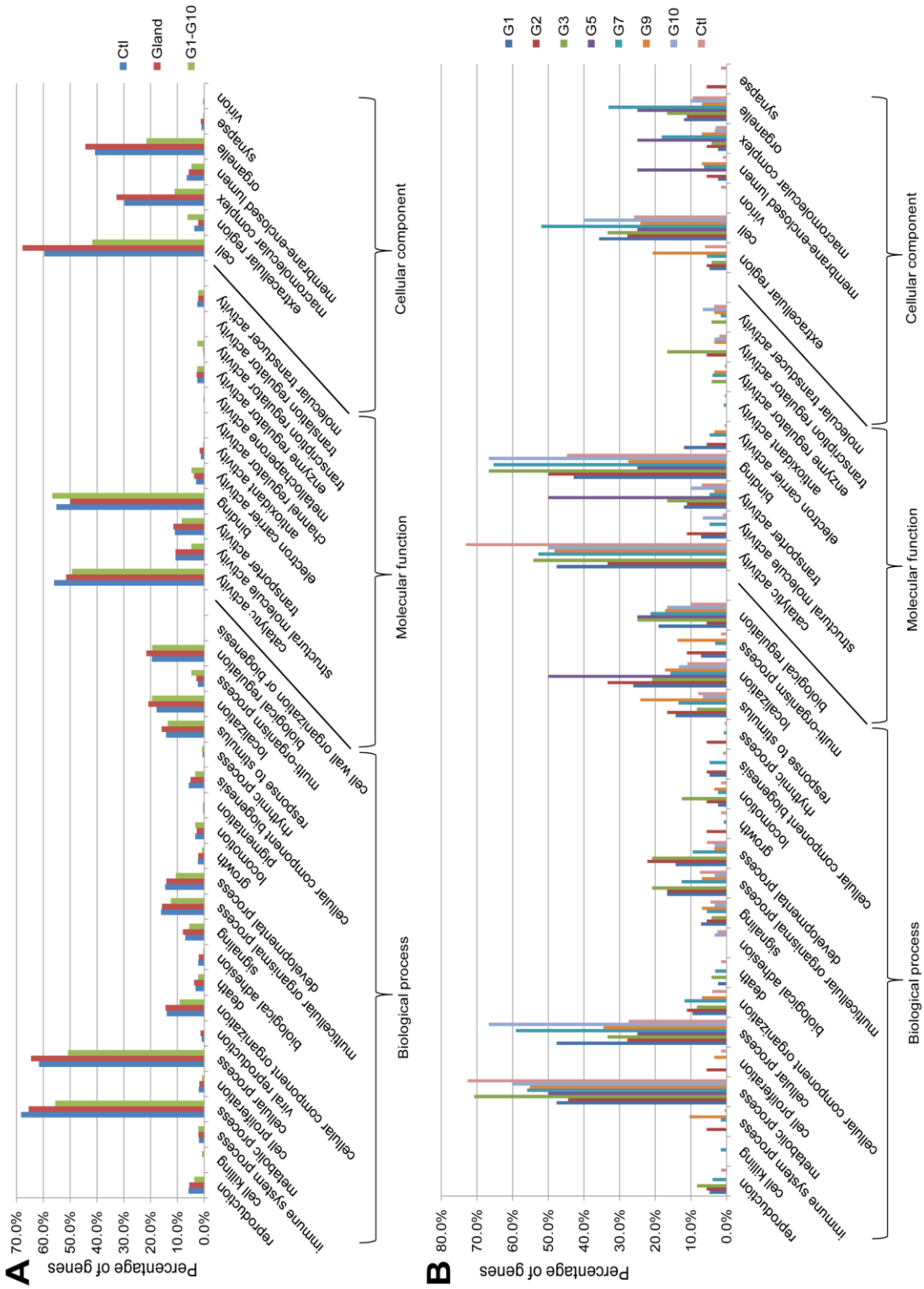

Figure 11 GO annotation of odoriferous glands transcriptome data.

3.5 Transcriptomic exploration of candidate genes for quinone synthesis

Glucosidases, phenol oxidases, and peroxidases have been considered to be involved in the production of quinones in the odoriferous glands (Happ, 1968) and were annotated in the *Tribolium* genome (Tribolium Genome Sequencing Consortium et al., 2008). In the stink gland transcriptome analysis, I have now explored these candidate genes for expression at the gland transcriptome level (**Figure 12**, details in **Dataset 10**). In total, 19 glucosidase, 14 phenol oxidase, and 18 peroxidase encoding genes were identified through blast searches and conserved domain confirmation. Transcriptomic explorations revealed that at least four glucosidase (*TC000223*, *TC000537*, *TC002741*, and *TC011354*), five phenol oxidase (*TC000821*, *TC005376*, *TC006769*, *TC010489*, and *TC10490*) and four peroxidase (*TC010355*, *TC010362*, *TC012328* and *TC014929*) genes have increased reads in the gland samples, which confirms the importance of these three types of enzymes in defensive secretions and verifies the reliability of our transcriptome data.

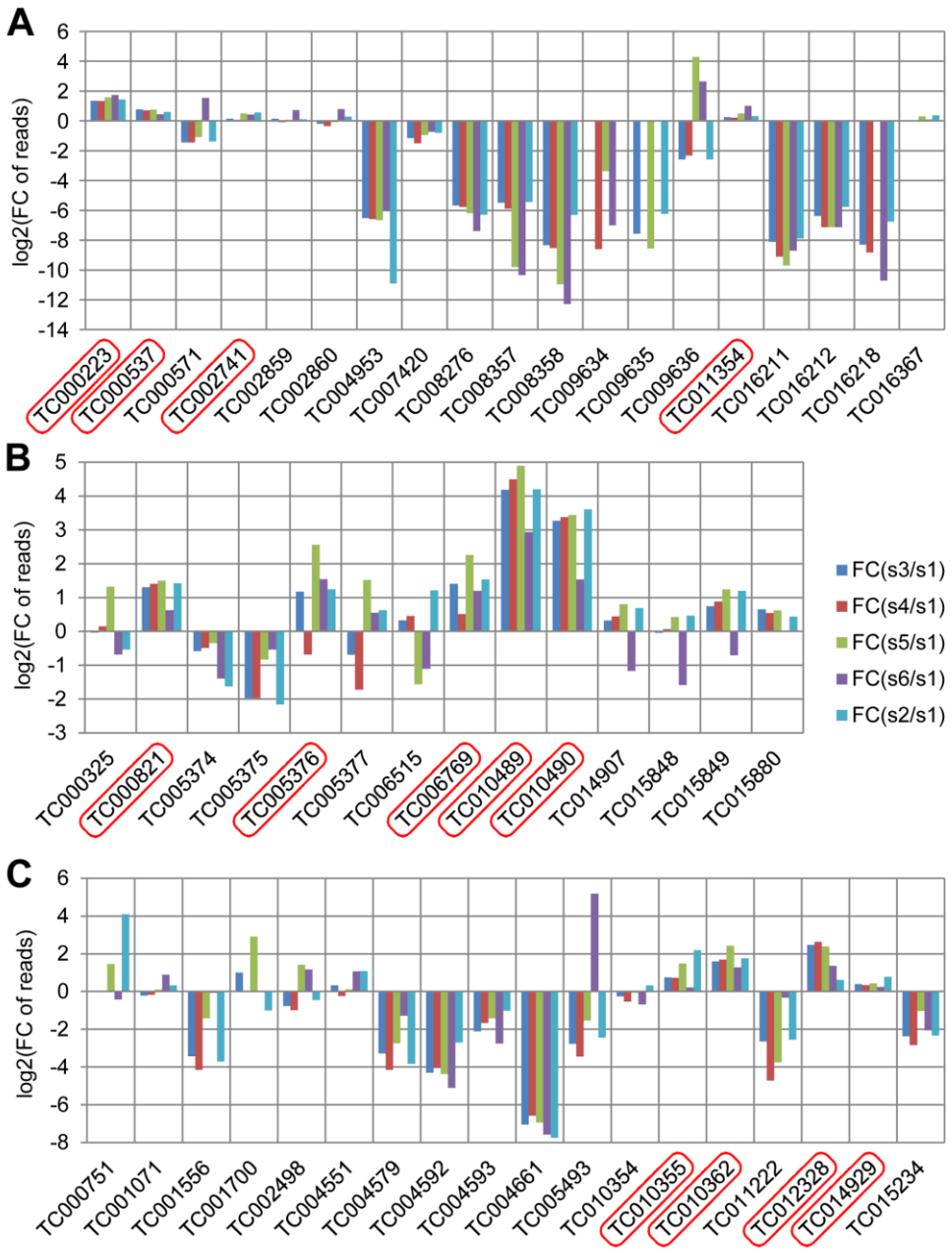

Figure 12 Annotated quinone synthesis-related genes and their relative gland transcriptome expression levels. A, glucosidases, 19 genes; B, phenol oxidases, 14 genes; C, peroxidases, 18 genes were annotated. In all charts, along the X-axes the different genes are presented, while the Y-axes present log2[fold change of reads in glands against control]. Abbreviations: FC: fold change; s1: sample 1, anterior abdomen as a control; s3: sample 3, male prothoracic glands; s4: sample 4, female prothoracic glands; s5: sample 5, male abdominal glands; s6: sample 6, female abdominal glands; s2: sample 2, *tar* prothoracic glands. The genes with higher reads in gland samples are marked with red squares.

3.6 Functional analysis of the most highly and gland-specifically expressed genes

In order to find novel gene functions involved in quinone synthesis, we functionally analyzed 77 genes from transcriptomic subtraction groups 1, 2, and 10 that were at least 64x higher expressed in the glands compared to the control tissue. RNAi of these genes resulted in various abnormal visible phenotypes (**Figure 13**). Additionally, GC-MS measurements revealed the alterations of different chemical components in both pairs of glands (an example of the chromatogram is depicted in **Figure 8**). The main components identified are listed in **Table 2**. Based on the extents of alterations of the chemicals, phenotypes were classified into six strengths (**Figure 14A**). 29 genes (38%, strength 1-3) showed strong changes, i.e. more than 75% reduction of at least one component, which were mostly accompanied with visible phenotypes (**Figure 14B**). In total, 67 of 77 genes (87%) showed alterations of at least one secreted chemical. Detailed descriptions on the phenotypic changes of all the 77 genes can be found in **Dataset 2.** In addition, gland cellular morphology was explored in all the 29 genes with strong phenotypes, but no visible abnormalities were observed in the secretory cells (data not shown).

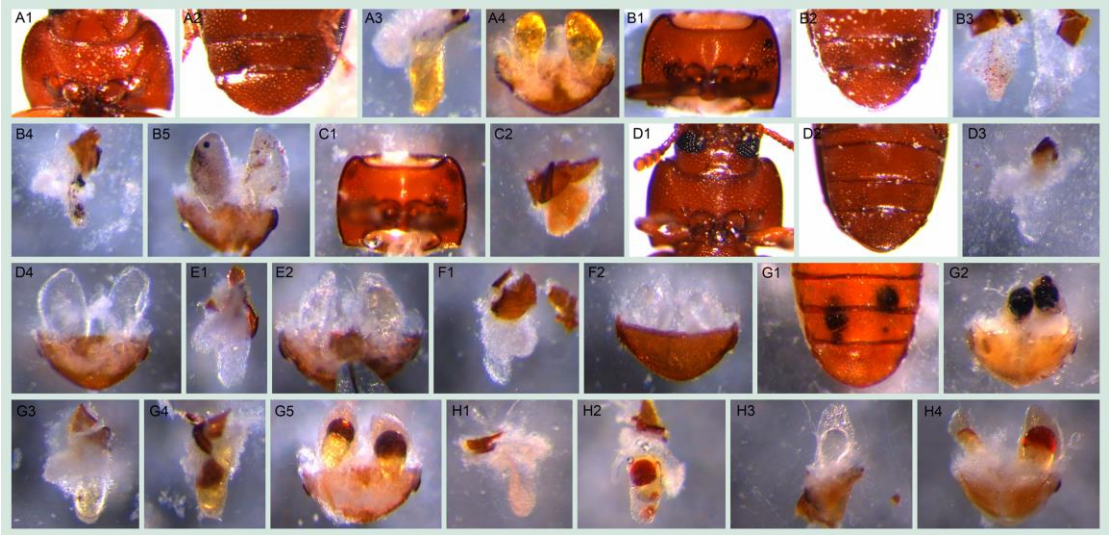

Figure 13 Visible morphological gland phenotypes after RNAi. A1-A4, wild-type; B1-B5, *GT20* knock-down, localized brown or melanized dots; C1-C2, *GT47* knock-down, condensed secretions; D1-D4, *GT62* knock-down, colorless secretions or empty-looking; E1-E2, *GT39* knock-down, colorless secretions; F1-F2, *GT63* knock-down, colorless secretions; G1-G5, *GT02* knock-down, localized brown or melanized dots; H1-H4, *GT25* knock-down, localized secretions or colorless. Prothoracic glands: A1, A3, B1, B3, B4, C1, C2, D1, D3, E1, F1, G3, G4, H1 and H2; abdominal glands: A2, A4, B2, B5, D2, D4, E2, F2, G1, G2, H3 and H4. G3-G5 were from stage A24, all the others were at stage A10. The statistics of the visible phenotypes are in Figure 14B.

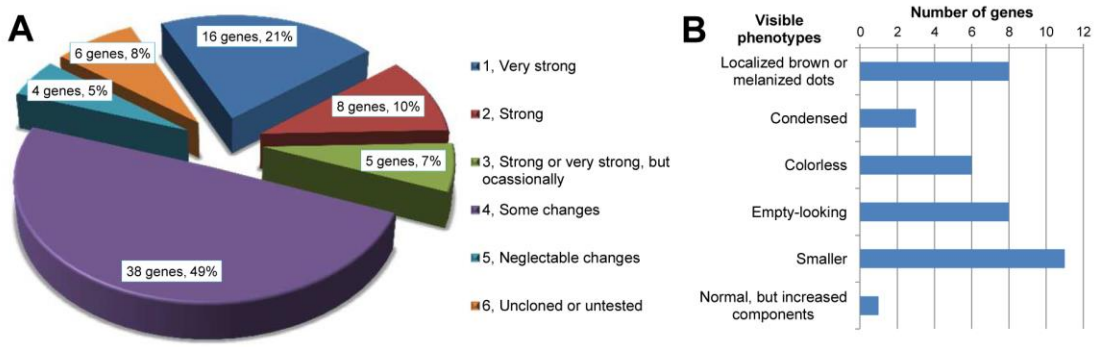

Figure 14 Phenotype classifications of 77 highly gland-specifically expressed genes by RNAi. A, Description of phenotype strengths: 1, Very strong: at least one type of chemical was undetectable or less than 5% left in thoracic or/ and abdominal glands; 2, Strong: at least one type of chemical was 75%-95% reduced or increased by more than 75% in thoracic or/and abdominal glands; 3, Strong or very strong but occasionally: phenotype was similar to 1 or 2 but not observed in all the injected beetles; 4, Some changes: at least one type of chemical was 25%-75% reduced or increased in thoracic or/and abdominal glands; 5, Neglectable changes: less than 25% reduction or increase in any type of chemical; 6, uncloned or untested. B, Strong and very strong gland phenotypes (strengths 1-3 in panel A) in details, some genes had more than one phenotype. Except for the last two classifications, examples are provided in Figure 13: localized brown or melanized dots (13B1-B5 and G2-G5); condensed (13C1-C2); colorless (13E1-F2); empty-looking (13D3).

Table 2 Main gland volatiles identified by GC-MS.

Retention indices	Compound name	CAS-Number	MW	Comment
1011/1018	methyl-1,4-benzoquinone	000553-97-9	122.04	
1098/1109	ethyl-1,4-benzoquinone	004754-26-1	136.05	
1350/1367	methyl-1,4-hydroquinone	000095-71-6	124.05	
1432	ethyl-1,4-hydroquinone	2349-70-4	138.07	
1477	1,6-pentadecadiene	58045-15-1	208.38	*, low peak
1492	1-pentadecene	013360-61-7	210.24	
1552	1,2-dimethoxy-4-n-propylbenzene	005888-52-8	180.12	low peak
1593	1-hexadecene	000629-73-2	224.25	low peak
1663/1672	1,8-heptadecadiene	Not available	236.25	*
1693	1-heptadecene	006765-39-5	238.27	

*: based on previous data (Görgen et al., 1990), the positions of the double bonds (especially the second one) need to be confirmed.

3.7 Quantification of volatile gland contents

Previous research has revealed the amount of different glandular components only on the whole beetle level (Loconti and Roth, 1953; Ladish et al., 1967; Markarian et al., 1978; Wirtz et al., 1978; Pappas and Wardrop, 1996; Unruh et al., 1998; Yezerski et al., 2004; Villaverde et al., 2007). In order to elucidate the chemical compositions of the volatiles in the different pairs of glands and the extent of reduction after gene knock-downs, three genes with strong quinone-less phenotypes were chosen from the 77 tested genes to quantify different glandular components. Wild-type and EGFP dsRNA-injected beetles were used as controls. **Figure 15** shows the complete losses of all quinones in both pairs of glands in both females and males from the knock-down beetles of these three *quinone-less* genes (except for one *GT39* dsRNA injected male out of sixteen injected males). In comparison, the alkenes were reduced to different extents. Statistical analyses revealed significant differences between wild-type and the knock-downs (**Dataset 11**), EGFP dsRNA injection surprisingly caused a few significant differences in alkenes compared to wild-type but not in quinones. Interestingly, all the alkenes in prothoracic glands of *GT63* knock-downs were not statistically different from the wild-type, while only heptadecadiene and heptadecene in the abdominal glands showed the same trend. Sex differences were also analyzed (**Dataset 11**), which showed that most chemicals had no significant differences between males and females, except for all the alkenes in abdominal glands of *GT39* knock-downs and in thoracic glands of *GT62*. In wild-type, only heptadecadiene showed a significant difference between different sexes while the other chemicals did not.

Additionally, the amount of all the main components in wild-type A10 beetles is presented in **Table 3** (details in **Dataset 11**). The prothoracic glands possess about 40% of either quinones or alkenes of all the stored secretions in the whole beetle, while abdominal glands have about 60%. But the molar ratios of quinones to alkenes are almost the same in both pairs of glands (thr, 2.60; abd, 2.70-2.74). And the molar ratios of MBQ to EBQ vary from 0.77 to 0.88 in different gland and sex levels. The only major dissimilarity between those two glands is the composition of distinct alkenes. The prothoracic glands have higher portions of heptadecadiene and heptadecene, especially the former, but a lower portion of pentadecene (15ene: 17diene: 17ene = ~60%: 28%: 12% in thr, ~88%: 4%: 8% in abd).

Full length cDNAs of the three *quinone-less* genes were cloned and the sequences submitted to GenBank with accession numbers of JX569829, JX569830 and JX569831. Based on the phenotypes and their homology (see **Dataset 4** for respective protein sequences), *GT39* has been designated as *Tcas-quinone-less vitellogenin-like* (*Tcas-ql VTGl*), *GT62* as *Tcas-quinone-less arylsulfatase b* (*Tcas-ql ARSB*) and *GT63* as *Tcas-quinone-less multi-drug resistance protein* (*Tcas-ql MRP*).

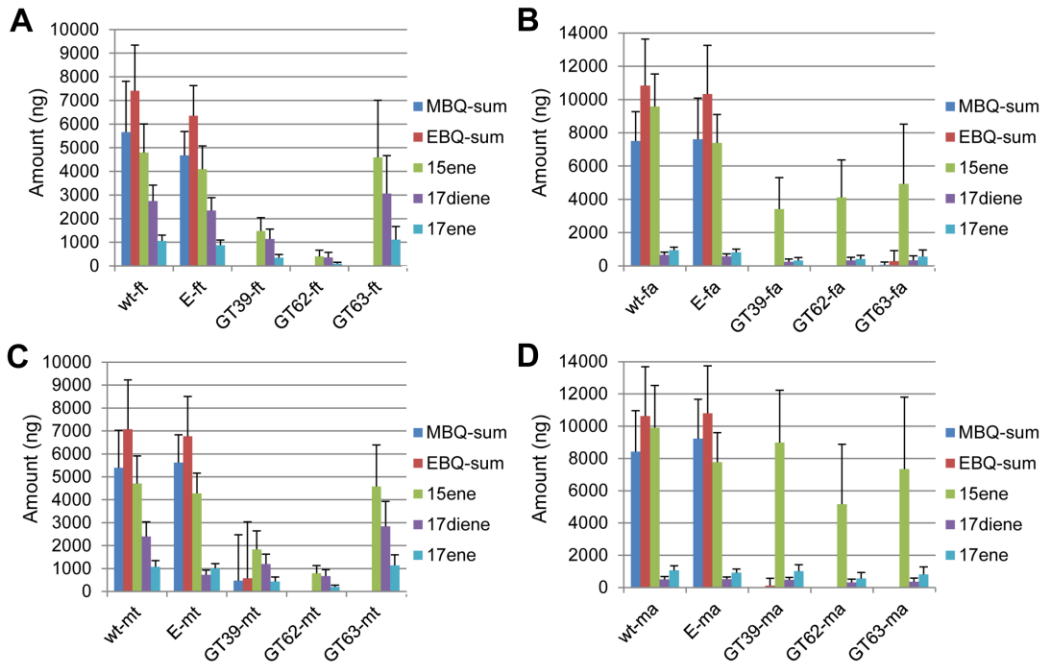

Figure 15 Quantification of main volatile glandular chemicals by GC-MS in wild-type and novel *quinone-less* gene RNAi-knock-downs. Comparisons in female thoracic glands (ft) (A), female abdominal glands (fa) (B), male thoracic glands (mt) (C), and male abdominal glands (ma) (D). Y-axis: amount in nanogram; X-axis: wild-type and different RNAi-knock-downs. Abbreviations: E: dsEGFP-injected control; GT39: *Tcas-ql VTGl*; GT62: *Tcas-ql ARSB*; GT63: *Tcas-ql MRP*; MBQ-sum: methyl-1,4-benzoquinone; EBQ-sum: ethyl-1,4-benzoquinone; 15ene: 1-pentadecene; 17diene: 1,8-heptadecadiene; 17ene: 1-heptadecene. The error bars indicate standard deviations at N=15-30.

Table 3 Quantification of the main volatiles in wild-type odoriferous stink glands.

Sex & gland types	MBQ (µg)	EBQ (µg)	15ene (µg)	17diene (µg)	17ene (µg)	Quinones (nmol)	Alkenes (nmol)
male thx	5.39 ±1.63	7.08 ±2.15	4.71 ±1.2	2.39 ±0.64	1.08 ±0.27	96.21 ±28.97	37.06 ±9.44
fem. thx	5.66 ±2.15	7.41 ±1.93	4.8 ±1.21	2.74 ±0.68	1.06 ±0.25	100.81 ±29.82	38.84 ±9.54
male abd	8.43 ±2.53	10.63 ±3.05	9.91 ±2.61	0.51 ±0.17	1.06 ±0.28	147.18 ±42.85	53.74 ±14.1
fem. abd	7.51 ±1.75	10.84 ±2.79	9.58 ±1.95	0.66 ±0.16	0.94 ±0.18	141.24 ±33.39	52.32 ±10.32
male thx+abd	13.82 ±3.61	17.71 ±4.6	14.62 ±3.17	2.9 ±0.71	2.14 ±0.46	243.39 ±62.9	90.8 ±19.16
fem. thx+abd	13.2 ±3.18	18.25 ±4.17	14.31 ±2.65	3.36 ±0.73	1.97 ±0.34	242.34 ±54.2	90.58 ±16.24

The amounts are indicated as mean ±standard deviation. N=15-30. Abbreviations: fem.: female; thx: thoracic glands; abd: abdominal glands.

3.8 Phylogeny of the three newly identified *quinone-less* genes

After quantification of the gland volatiles in these three gene knock-downs, their phylogeny was explored. In the phylogenetic tree (**Figure 16A**), Tcas-ql VTGl (GT39) was classified together with eight other *Tribolium* homologs, and 11 homologs were grouped in a branch close by, including proteins from *Strongylocentrotus purpuratus, Danio rerio, Gallus gallus, Homo sapiens, Mus musculus,* and *Nasonia vitripennis* (see **Dataset 4** for all the sequences). Tcas-ql ARSB (GT62) was grouped together with two other *Tribolium* homologs (**Figure 16B**), which were closest related to three *Nasonia* proteins, similarly to Tcas-ql MRP (GT63, **Figure 16C**). Since all three *quinone-less* genes had several *Tribolium* homologs, I checked their homologs expression levels in the gland transcriptome. The homologs were linked with corresponding GLEAN predictions and explored in the transcriptomic libraries (**Dataset 3**). It was shown (**Figure 17**) that no other gene was as highly expressed in the gland samples except for the three identified *quinone-less* genes, although some genes contained more than 16 times (2 to the power of 4, GI:91085475, **Figure 17C**) or 4 times (2 to the power of 2, GI:189236319, **Figure 17B**) higher reads in some cases. In conclusion, this indicates that all three quinone-less genes most probably have evolved independently and specifically for the quinone-based chemical defensive system in *Tribolium*.

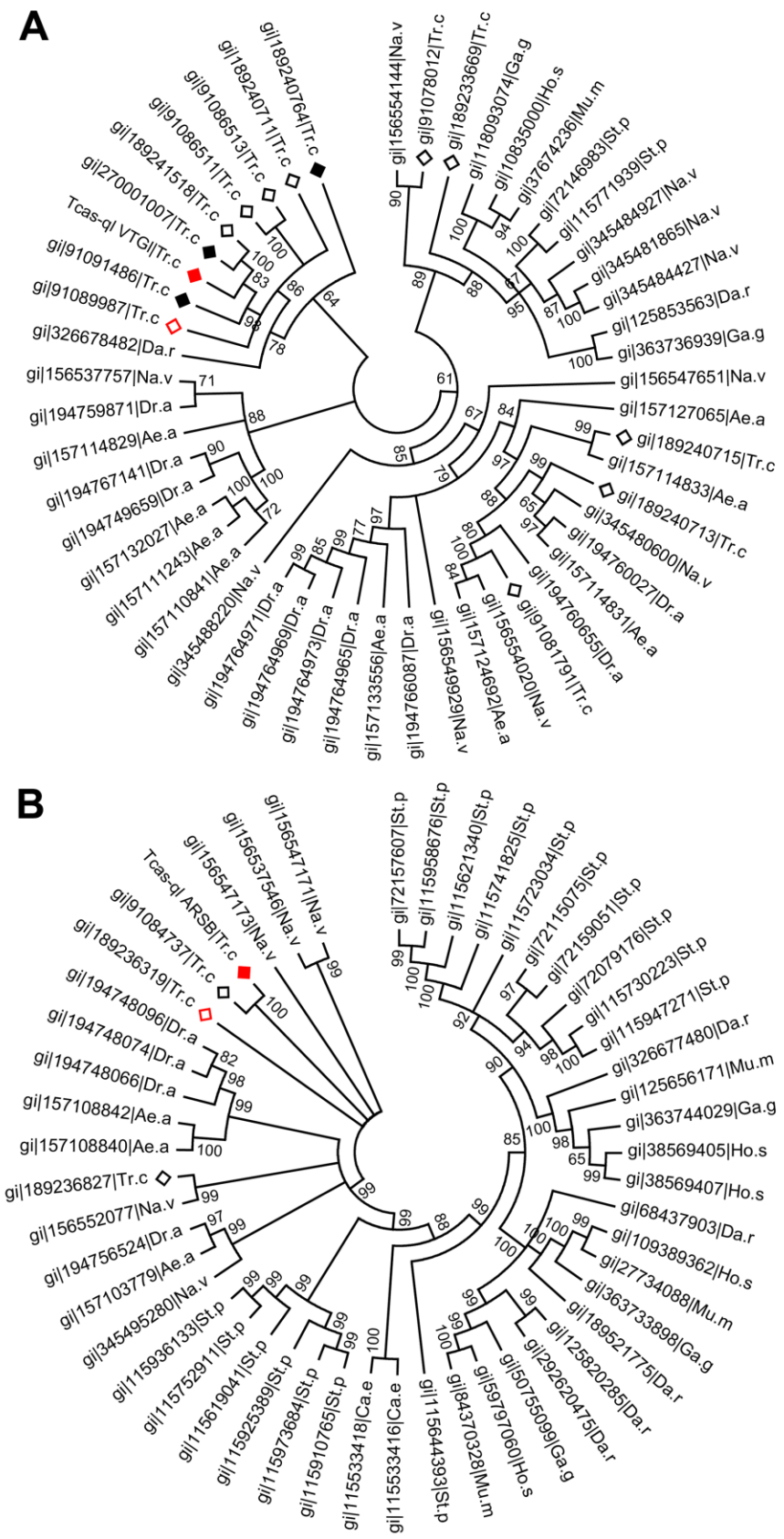

Figure 16 Phylogenetic trees of homologs of the three novel quinone-less genes.

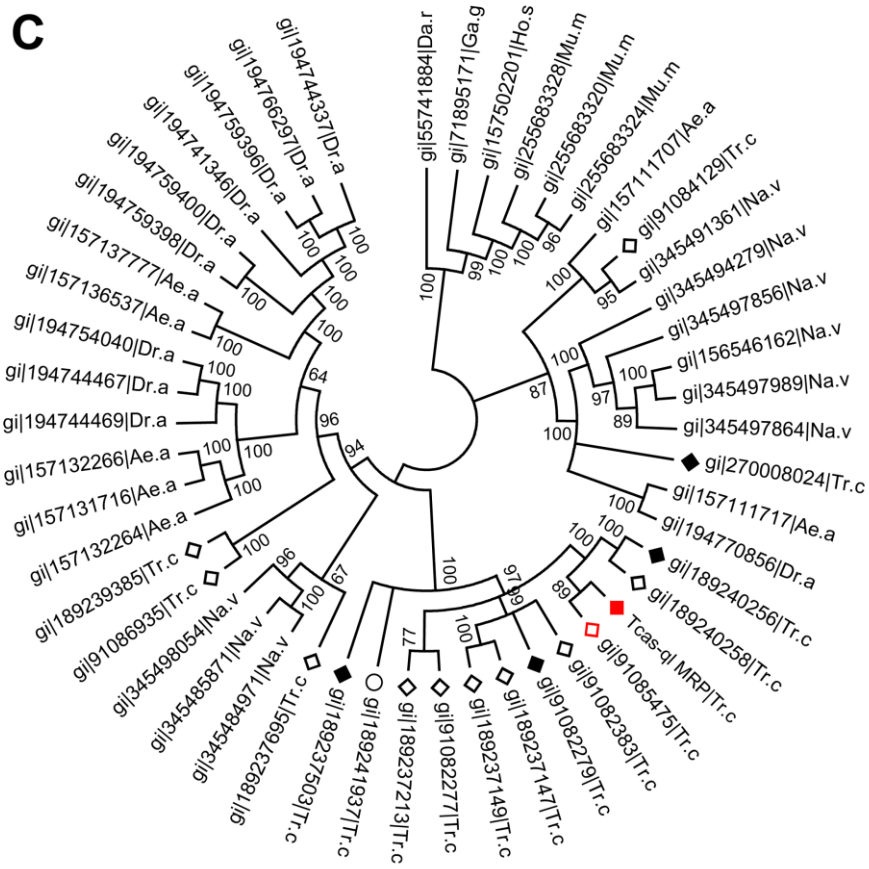

Figure 16 Phylogenetic trees of homologs of the three novel quinone-less genes. A, Tcas-ql VTGl (GT39); B, Tcas-ql ARSB (GT62); C, Tcas-ql MRP (GT63). All the *Tribolium* homologs were marked based on their relative gland expression levels (Figure 17), with the solid red squares indicating each of the three *quinone-less* genes, with open red squares genes relatively high expressed in gland samples, with solid black relatively high expressed in the control sample, with open black squares indicating the other *Tribolium* homologs, and with an open black circle indicating a *Tribolium* homolog without OGS annotation. The numbers on the branching points are the statistical frequencies. Abbreviations of species names are: Ae.a, *Aedes aegypti*; Ca.e, *Caenorhabditis elegans*; Da.r, *Danio rerio*; Dr.a, *Drosophila ananassae*; Ga.g, *Gallus gallus*; Ho.s, *Homo sapiens*; Mu.m, *Mus musculus*; Na.v, *Nasonia vitripennis*; St.p, *Strongylocentrotus purpuratus*; Tr.c, *Tribolium castaneum*.

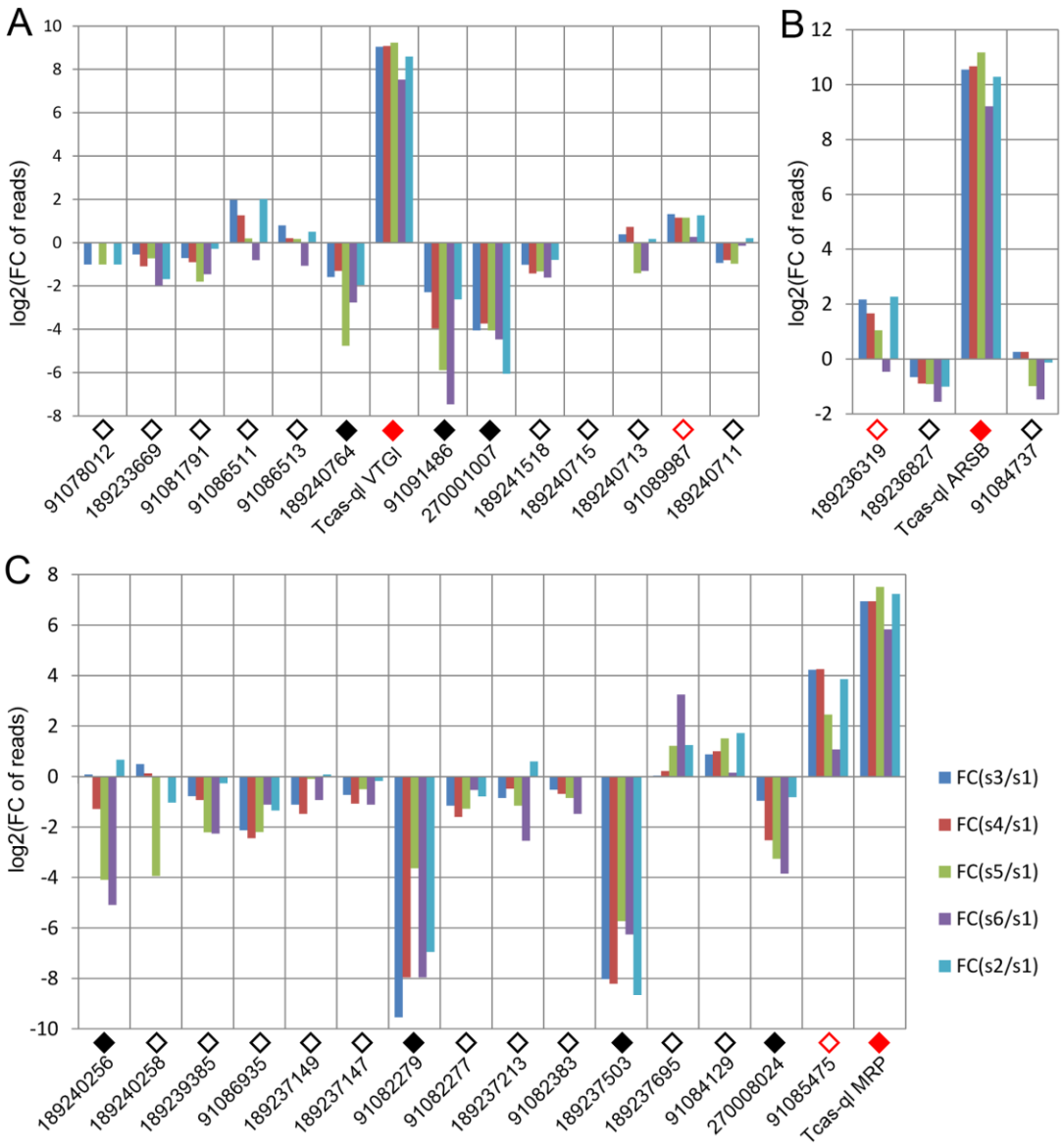

Figure 17 Relative transcriptomic gland expression levels of the *Tribolium* homologs of the three novel *quinone-less* genes. A, *Tcas-ql VTGl* (*GT39*) homologs. B, *Tcas-ql ARSB* (*GT62*) homologs. C, *Tcas-ql MRP* (*GT63*) homologs. In all charts, along the X-axes the different genes are presented (using the same GI numbers and expression level square codes as in Figure 16), while Y-axes present log2[fold change of reads in glands against control]. For abbreviations see Figure 12.

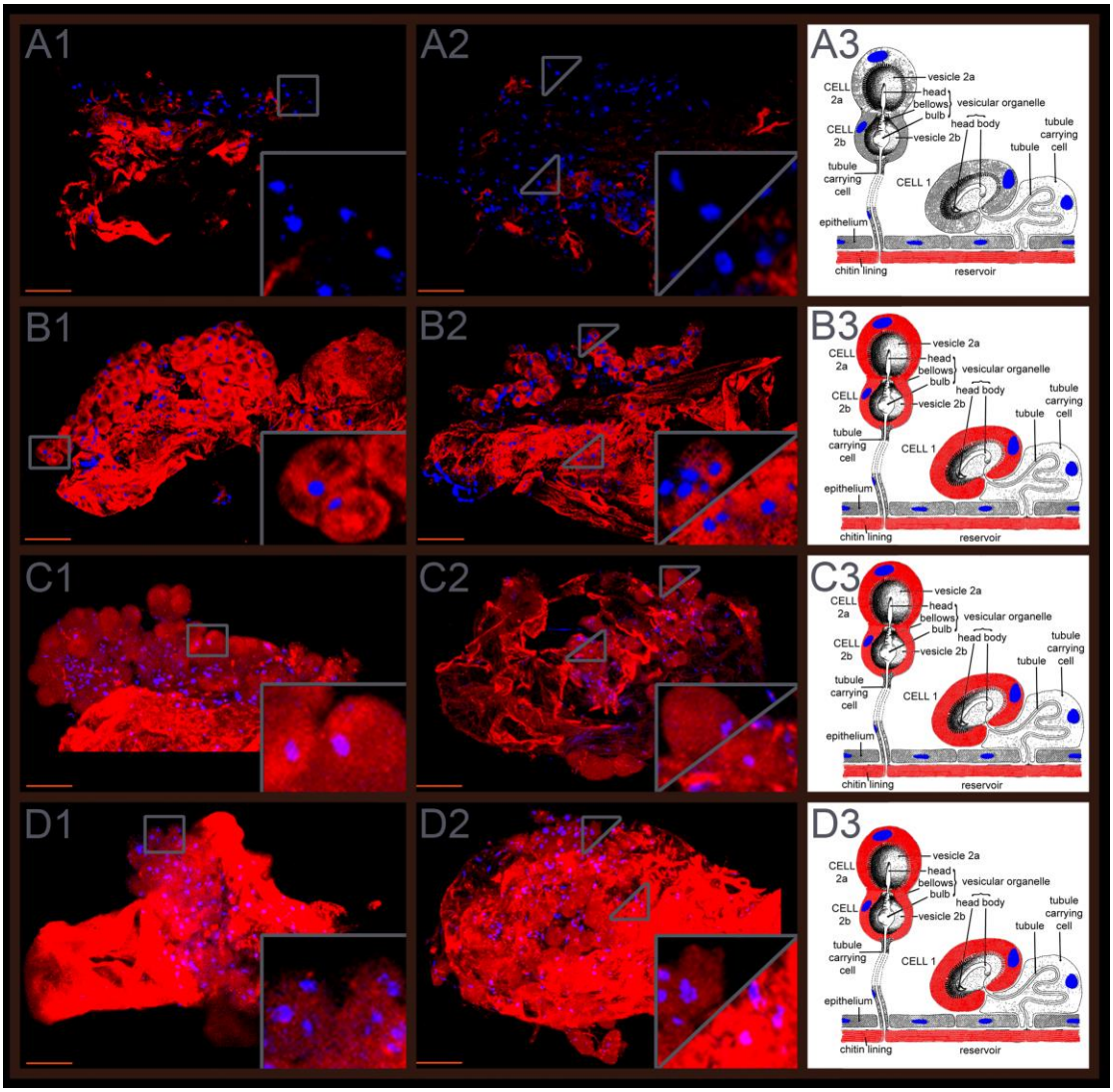

Figure 18 Expression patterns of the three *quinone-less* genes. The first column (A1, B1, C1, and D1) shows prothoracic glands, the second (A2, B2, C2, D2) abdominal glands, and the third (A3, B3, C3, D3) gland schemes modified after Happ (Happ, 1968). A1-A3, *Tcas-ql VTGl* (*GT39*) sense probes. B1-B3, *Tcas-ql VTGl* (*GT39*) antisense probes. C1-C3, *Tcas-ql ARSB* (*GT62*) antisense probes. D1-D3, *Tcas-ql MRP* (*GT63*) antisense probes. In the right lower corner of the panels in the first and second column, the expression was digitally magnified 4 times, with its original positions indicated by a square box or triangles within the same panel. Cell type 1 and cell type 2 were separately indicated in the abdominal glands, cell type 1 was zoomed in the lower triangle of the square, and cell type 2 in the left upper part of the square. Scale bars: 50 µm.

3.9 Expression patterns of the *quinone-less* genes in gland tissue

The expression patterns of *Tcas-ql VTGl* (*GT39*), *Tcas-ql ARSB* (*GT62*) and *Tcas-ql MRP* (*GT63*) were explored in dissected odoriferous glands. All three genes showed strong expressions in both gland cell type 1 and cell type 2 (Eisner et al., 1964; Happ, 1968) of both pairs of glands (**Figure 18**), which confirms their involvement in *Tribolium* defensive secretion.

3.10 Microbe inhibition assays

Microbe inhibition tests were carried out to identify the effect of losing quinones. It had been shown that beetle chemical secretions – especially the benzoquinones – can inhibit the growth of several microbes common to flour with artificial MBQ having the same effect (Prendeville and Stevens, 2002; Yezerski et al., 2007). In our experiments, a fungus, *Aspergillus niger*, and a gram positive bacterium, *Arthrobacter globiformis*, were used to test the strength of the chemical defense mediated by beetle glands. As a control, I used RNAi against *GT12*, representing a gene causing an alkene-less phenotype at knock-down (detailed analysis is presented in Part **3.15**). The results (**Figure 19**) showed that wild-type beetle secretions could inhibit microbe growth in a certain area, but loss of quinones led to undetectable inhibitions (*GT63*), while an alkene-less state had only reduced inhibition effects (*GT12*).

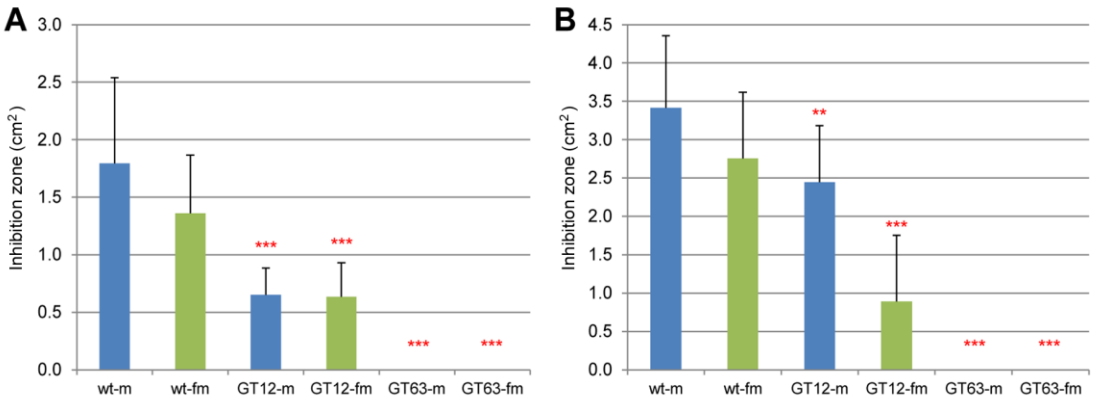

Figure 19 Microbe growth inhibition assays of wild-type and RNAi-knock-down glands. The fungus *A. niger* (A) and the bacterium *A. globiformis* (B) were analyzed for gland-mediated growth inhibition. Y-axes indicate the areas of respective inhibition zones (cm^2). X-axes: sex-specific wild-type (wt) and different RNAi-knock-downs (m: male; fm: female; GT12: gene causing alkene-less phenotype; GT63: *Tcas-ql MRP*). Non-parametric comparisons were made between wild-type and knock-downs using Wilcoxon method, ***, P<0.001; **, 0.001<p<0.01. The error bars indicate standard deviations at N=11-27.

3.11 Phenol oxidase activity assays

Since chemical defense systems are responsible for defending the host from infection, we wanted to test, whether also a part of the innate immune system is affected directly or indirectly by the quinone-less phenotype. Thus, after RNAi-mediated knock-down of the *quinone-less* genes, phenol oxidase (PO) activities were measured as a general index of the melanization innate immune responses in invertebrates (Armitage and Siva-Jothy, 2005). Compared to wild-type beetles, the three *quinone-less* knock-downs had significantly reduced levels of PO-activity both in females and males (**Figure 20**), while buffer or EGFP dsRNA injected animals did not show significant changes. These data indicate that the extra-corporal chemical defense may be linked with the function of a part of the innate immune system in *Tribolium*. (The PO tests were performed in

collaboration with Dr. Gerrit Joop from Department of Evolutionary Ecology and Genetics, Zoological Institute, Christian-Albrechts-University of Kiel)

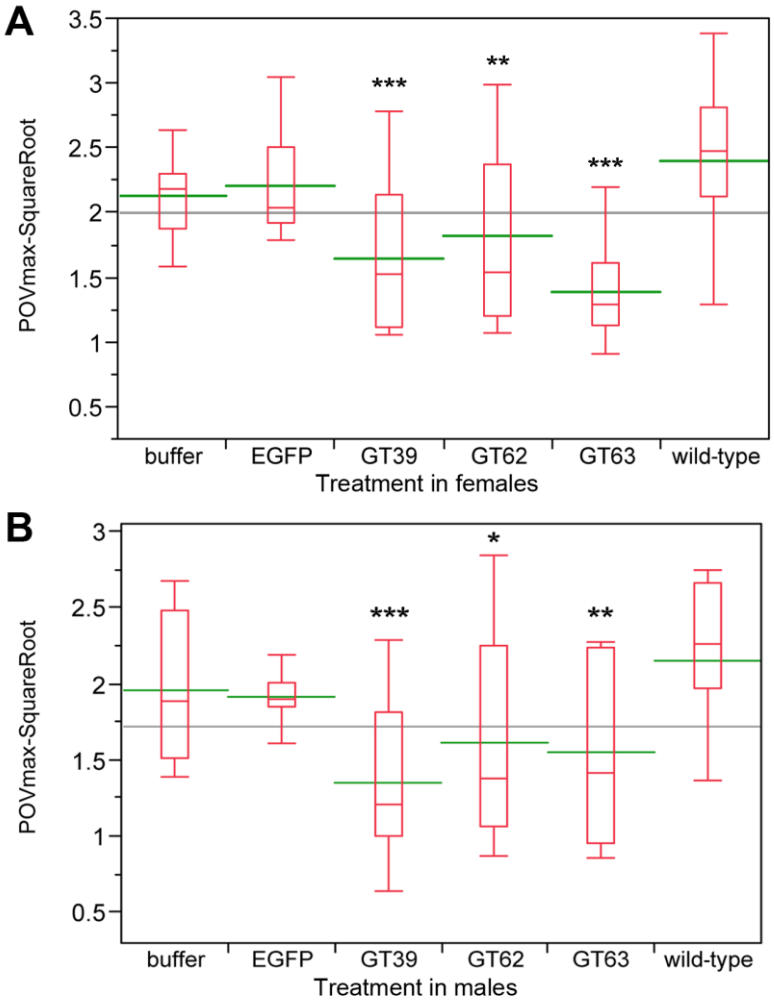

Figure 20 Phenol oxidase (PO) activity assays of wild-type and novel *quinone-less* gene RNAi knock-downs. The Y-axes indicate the square root of PO Vmax, red boxes are boxplots, green lines represent the mean value, the gray lines represent the grand mean, while the X-axes present wild-type, control injections, and different RNAi-knock-downs. A, in females (N=12-25); B, in males (N=12-15, but the buffer-injected control resulted in only 4 surviving beetles). Buffer: buffer-injection control; EGFP: dsEGFP-injection control; GT39: *Tcas-ql VTGl*; GT62: *Tcas-ql ARSB*; GT63: *Tcas-ql MRP*. The asterisks (*) mark the t-test results comparing to wild-type: ***: $p<0.001$; **: $0.001<p<0.01$; *, $0.01<p<0.05$. Buffer- and EGFP-injected controls were not significantly different from wild-type.

3.12 Fatty acid profiling

Fatty acids were profiled in different developmental stages and A10 odoriferous glands. Unsurprisingly, similar to most insect species (Fast, 1970; Thompson, 1973; Stanley-Samuelson et al., 1988), the main FAs in *Tribolium* were 16:0, 18:0, 18:1(9Z) and

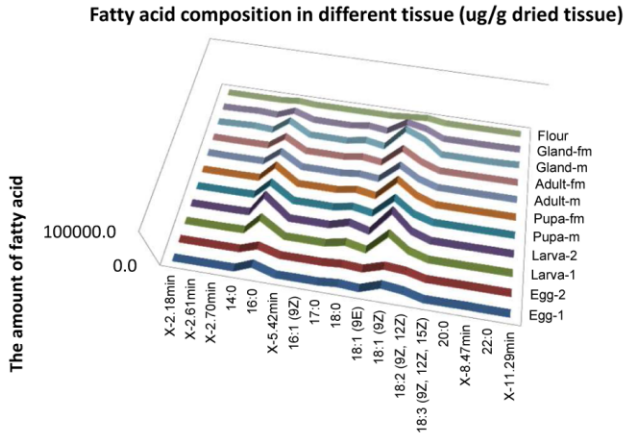

	X-2.18min	X-2.61min	X-2.70min	14:0	16:0	X-5.42min	16:1 (9Z)	17:0	18:0	18:1 (9E)	18:1 (9Z)	18:2 (9Z, 12Z)	18:3 (9Z, 12Z, 15Z)	20:0	X-8.47min	22:0	X-11.29 min
Egg-1	0.0	0.0	0.0	161.9	24015.	161.9	589.7	196.6	5815.9	1202.5	25656.	17887.	242.8	289.1	1387.5	219.7	0.0
Egg-2	0.0	0.0	0.0	108.9	19771.	127.1	544.7	172.5	4956.4	626.4	21232.	15940.	245.1	290.5	780.7	217.9	0.0
Larva-1	0.0	0.0	0.0	1188.4	46643.	905.4	1004.5	424.4	13164.	0.0	58774.	17825.	346.6	198.1	0.0	261.7	0.0
Larva-2	0.0	0.0	0.0	1432.9	56888.	921.1	824.8	439.5	16339.	0.0	68122.	19639.	427.5	234.8	0.0	228.8	0.0
Pupa-m	0.0	0.0	0.0	1115.4	42120.	812.2	1120.8	411.5	10206.	0.0	51639.	15978.	314.0	216.6	0.0	232.8	0.0
Pupa-fm	0.0	0.0	0.0	1000.7	41345.	765.3	936.5	406.7	9017.3	0.0	51818.	18179.	390.7	214.1	0.0	230.1	0.0
Adult-m	1359.5	260.9	480.6	830.8	33321.	844.5	1084.8	226.6	5334.9	0.0	43537.	15572.	212.8	137.3	0.0	185.4	0.0
Adult-fm	920.7	205.4	375.4	651.6	29702.	616.1	750.7	205.4	6692.6	0.0	42797.	16721.	240.8	170.0	0.0	205.4	0.0
Gland-m	1083.0	2299.2	3832.0	466.5	29606.	1582.8	1049.6	316.6	8463.7	0.0	49782.	31805.	0.0	399.9	0.0	816.4	2732.4
Gland-fm	890.0	1520.1	3197.7	275.7	16232.	1055.4	315.0	0.0	5844.0	0.0	27589.	18697.	189.0	283.5	0.0	519.8	1362.6
Flour	0.0	0.0	0.0	0.0	3699.5	0.0	415.7	0.0	457.2	0.0	3242.3	6817.1	415.7	0.0	0.0	0.0	0.0

Figure 21 Fatty acid composition in different developmental stages and glands. X axis stands for various fatty acids, Y axis different samples, and Z axis the amount of the fatty acid (μg) per gram dried tissues. At egg and larva stage, two samples were examined as replicates. The red boxes mark the fatty acids specifically presented in only one sample, and the blue highly presented in certain samples. In the fatty acid names, some remained to be identified, which were marked with X-retention time. Abbreviations: m: male; fm: female.

18:2(9Z,12Z) (**Figure 21**). However, a few FAs were specifically found in one or two sample(s) (marked with red boxes in **Figure 21**), or higher presented in certain samples (marked with blue boxes in **Figure 21**). (This section was in collaboration with Dr. Tim Iven from Department of Biochemistry, GZMB, Georg-August-University of Göttingen)

3.13 Annotation of fatty acid metabolism related genes and exploration of their transcriptomic expression levels

Combining the data from KEGG database and blast search, 74 fatty acid metabolism related genes were identified from the *Tribolium* genomic official gene set and listed in **Table 4.** There were 12 genes involved in fatty acid biosynthesis, 27 in FA metabolism, 19 desaturases and 16 elongases. Additionally, their transcriptomic expression levels were also explored in different developmental stages and various types of gland tissues (see **Table 5**). The higher the standard deviation of all RDIs (RDI-SD in **Table 5**) is, the more different the expressions in distinct samples are. The detailed data in annotation and the whole integrated transcriptome library are presented in **Dataset 12**.

Table 4 The annotated gene families of fatty acid metabolism in *Tribolium.*

Putative function	OGS No.	Protein GI number	Chromosomal localization	EST	RNA-seq	Subcellular localization
Fatty acid biosynthesis						
acetyl-CoA carboxylase / biotin carboxylase	TC015613	270008988, 189238375	LG6	y	y	N
[acyl-carrier-protein] S-malonyltransferase	TC003204	91078278, 270003914	LG3	y	y	C
fatty acid synthase, animal type	TC000238	91078002, 270001419	LG2	y	y	C
fatty acid synthase, animal type	TC015340	189238065	LG6	n	yp	C
fatty acid synthase, animal type	TC011521	270014916, 189233593	LG1=X	yp	y	N
fatty acid synthase, animal type	TC011522	270014917, 189233593	LG1=X	yp	y	C
fatty acid synthase, animal type	TC015339	189238067	LG6	n	y	PM
fatty acid synthase, animal type	TC015337	91084261, 270008753	LG6	y	y	C
fatty acid synthase, animal type	TC015399	91084277, 270008800	LG6	y	y	C
fatty acid synthase, animal type	TC015400	91084281, 270008801	LG6	y	y	PM
fatty acid synthase, animal type	TC007689	91080297	LG4	y	y	C
3-oxoacyl-[acyl-carrier-protein] synthase II	TC011607	91091392, 270013058	LG9	y	y	ER
Fatty acid metabolism						
long-chain-fatty-acid--CoA ligase ACSBG	TC004625	91076084, 270014586	LG1=X	y	y	C
long-chain acyl-CoA synthetase	TC006471	91088831, 270012333	LG8	y	y	C
long-chain acyl-CoA synthetase	TC014440	91083237	LG5	y	y	ER
carnitine O-palmitoyltransferase 1	TC002462	189235959	LG3	y	y	ER
carnitine O-palmitoyltransferase 2	TC004777	189233986	LG1=X	y	y	C

Putative function	OGS No.	Protein GI number	Chromosomal localization	EST	RNA-seq	Subcellular localization
acyl-CoA oxidase	TC010636	91093755, 270012977	LG9	y	y	M
acyl-CoA oxidase	TC011683	91091178, 270013121	LG9	y	y	C
acyl-CoA oxidase	TC014245	91082769, 270015082	LG1=X	n	y	C
acyl-CoA dehydrogenase	TC002547	91079744, 270003324	LG3	y	y	M
very long chain acyl-CoA dehydrogenase	TC004634	91076006, 270014595	LG1=X	y	y	M
enoyl-CoA hydratase	TC005928	91088159, 270011845, 227471671	LG8	y	y	M
enoyl-CoA hydratase / long-chain 3-hydroxyacyl-CoA dehydrogenase	TC014680	270007934, 91083819	LG5	y	y	C
enoyl-CoA hydratase	TC000708	91076844, 270001819	LG2	n	y	M
3-hydroxyacyl-CoA dehydrogenase	TC005769	91088569, 270011703	LG8	y	y	M
acetyl-CoA acyltransferase 2	TC008729	91087491, 270009465	LG7	y	y	M
acetyl-CoA acyltransferase	TC008872	91087131, 270009593	LG7	y	y	M
butyryl-CoA dehydrogenase	TC015428	91084343	LG6	y	y	CS
acetyl-CoA C-acetyltransferase	TC010774	91092744, 270014794	LG1=X	y	y	M
acetyl-CoA C-acetyltransferase	TC000365	189234785, 270001523	LG2	y	y	M
glutaryl-CoA dehydrogenase	TC001629	91094295, 270014404	LG1=X	y	y	M
peroxisomal 3,2-trans-enoyl-CoA isomerase	TC003466	91078892, 270004147, 227483017	LG3	n	y	C
S-(hydroxymethyl) glutathione dehydrogenase / alcohol dehydrogenase	TC004574	237681130	LG2	y	y	C

Putative function	OGS No.	Protein GI number	Chromosomal localization	EST	RNA-seq	Subcellular localization
aldehyde dehydrogenase (NAD+)	TC000960	189234454, 270002022	LG2	y	y	M
aldehyde dehydrogenase family 7 member A1	TC005191	91095113, 270015550	LGUn	y	n	C
aldehyde dehydrogenase (NAD+)	TC011192	91091542, 270000922	LG10	y	y	C
short/branched chain acyl-CoA dehydrogenase	TC005122	91093605, 270015758	LGUn	y	n	M
short/branched chain acyl-CoA dehydrogenase	TC005123	91093613	LGUn	y	n	CS
Desaturase						
delta-9 desaturase	TC000549	91077254, 270001678	LG2	y	y	PM
delta-9 desaturase	TC003656	219522038, 270004322, 163311890	LG3	n	y	M
cytochrome b5 protein	TC006231	270012128	LG8	n	y	PM
cytochrome b5 protein	TC006232	91088131, 270012129	LG8	y	y	PM
delta-11/9 desaturase	TC011471	305377095, 300432598, 270001155	LG10	n	y	PM
delta-11/9 desaturase	TC014819	91094409, 270016351	LGUn	y	y	PM
delta-11/9 desaturase	TC014820	270016352, 189242438	LGUn	n	n	PM
delta-11/9 desaturase	TC014821	270016353, 189242440	LGUn	n	n	PM
delta-11/9 desaturase	TC015108	189238343, 270008574	LG6	y	y	M
delta-9/11 desaturase	TC015338	91084259, 270008754	LG6	n	n	ER
delta-11/9 desaturase	TC015349	91084221, 270008761	LG6	n	y	ER
delta-11/9 desaturase	TC015382	91084223, 270008788	LG6	n	y	M
delta-11/9 desaturase	TC015383	91084225, 270008789	LG6	n	y	ER

Putative function	OGS No.	Protein GI number	Chromosomal localization	EST	RNA-seq	Subcellular localization
delta-11/9 desaturase	TC015395	270008797, 189238070	LG6	n	y	M
sphingolipid delta4 desaturase	TC015856	91085523, 270009198	LG6	n	y	PM
delta-11/9 desaturase	TC016399	270015949	LGUn	n	n	M
delta-11/9 desaturase	TC016409	189242065	LGUn	n	n	M
delta-11/9 desaturase	TC016414	270015964	LGUn	n	y	C
delta-11/9 desaturase	TC016415	302371202, 300432600, 270015965	LGUn	n	n	PM
Elongase						
elongation of very long chain fatty acids protein	no hit	91093074	LG9	n	y	ER
elongase	TC002898	270003635	LG3	yp	y	M
elongase	TC002899	270003636, 189235338	LG3	yp	y	M
elongase	TC008803	270009529	LG7	n	y	PM
elongation of very long chain fatty acids protein	TC010977	91093076, 270013035	LG9	y	y	PM
elongase	TC010980	189240748	LG9	n	y	E
elongation of very long chain fatty acids protein 4	TC010987	91093072, 270013045	LG9	y	y	C
elongase	TC010988	270013046	LG9	n	y	ER
elongation of very long chain fatty acids protein 4	TC011121	91091714, 270000864	LG10	n	y	PM
elongase	TC011937	91090562, 270013347	LG9	y	y	C
elongase	TC011938	91090560, 270013348	LG9	y	y	C
elongase	TC013861	91082031, 270007304	LG5	n	y	C
elongase	TC015657	189238440, 270009025	LG6	n	y	PM
elongase	TC015658	91085031, 270009026	LG6	y	y	PM
elongase	TC016278	270014193, 189241045	LG9	n	y	PM

Putative function	OGS No.	Protein GI number	Chromosomal localization	EST	RNA-seq	Subcellular localization
elongase	TC016279	189241043, 270014194	LG9	n	y	ER
elongase	TC016280	91093290, 270014195	LG9	n	y	PM

Abbreviations: For EST and RNA-seq: y, yes; n, no; yp, yes but partially, which results from different prediction results giving by different methods. For predicted subcellular localization: C, cytosol; CS, cytoskeleton; E, extracellular; ER, endoplasmatic reticulum; M, mitochondrion; N, nuclear; PM, plasma membrane; -, not predictable. P, peroxisome; PTS1/2, sequence contains peroxisomal target sequence 1/2.

Table 5 Transcriptomic expression level of the annotated fatty acid metabolism related genes

OGS No.	E	L	P_fm	P_m	A0_fm	A0_m	A10_fm	A10_m	s1-ctl	s2-tthr	s3-mthr	s4-fthr	s5-mabd	s6-fabd	RDI-SD
Fatty acid biosynthesis															
TC015613	-18.5	-17.9	-20.3	-19.9	-21.2	-21.1	-19.2	-19.3	-18.5	-17.8	-18.3	-18.6	-19.2	-20.0	1.1
TC003204	-17.6	-18.7	-19.3	-18.7	-18.8	-18.4	-17.4	-17.7	-20.0	-19.5	-19.6	-19.8	-19.8	-20.3	0.9
TC000238	-19.3	-18.4	-24.6	-26.1	-22.4	-24.5	-19.2	-19.8	-20.1	-29.0	-28.4	-29.0	-19.1	-20.1	4.0
TC015340	-25.4	-19.0	-26.4	-25.8	-23.1	-25.2	-20.8	-21.3	-23.8	-28.5	-28.4	-31.3	-23.1	-24.0	3.3
TC011521	-23.8	-25.2	-24.1	-25.5	-22.9	-25.4	-22.3	-24.0	-26.8	-26.4	-26.2	-28.9	-27.4	NA	1.9
TC011522	-19.7	-16.9	-23.8	-23.0	-23.4	-22.8	-17.7	-17.3	-17.9	-16.8	-16.9	-17.1	-17.6	-18.9	2.7
TC015339	-24.9	-17.7	-24.2	-22.2	-22.0	-21.8	-16.9	-17.9	-21.0	-27.9	-30.2	-29.0	-20.2	-20.9	4.2
TC015337	-23.8	-19.3	-23.2	-22.5	-21.3	-22.2	-17.7	-18.0	-20.9	-24.3	-31.2	-31.3	-20.1	-20.9	4.2
TC015399	-21.4	-19.9	-24.7	-24.6	-22.8	-24.1	-20.4	-20.4	-21.8	-27.5	-27.8	-27.6	-20.5	-22.2	2.8
TC015400	-18.2	-19.6	-24.8	-24.8	-21.2	-22.1	-20.3	-20.2	-20.7	-26.9	-24.6	-25.4	-19.8	-20.8	2.7
TC007689	-25.5	-21.1	-17.1	-19.2	-14.1	-14.3	-16.3	-15.6	-15.7	-25.7	-25.9	-26.5	-14.8	-16.9	4.8
TC011607	-21.2	-19.6	-20.5	-20.6	-20.2	-20.4	-19.8	-20.4	-21.2	-20.0	-20.9	-21.1	-20.9	-22.0	0.6
Fatty acid metabolism															
TC004625	-18.7	-17.1	-18.0	-17.9	-18.5	-18.7	-17.3	-17.2	-18.4	-17.3	-17.2	-17.6	-18.6	-18.1	0.6
TC006471	-18.0	-17.9	-16.8	-17.1	-16.8	-17.3	-18.2	-18.5	-16.7	-18.5	-16.3	-16.4	-17.7	-19.8	1.0
TC014440	-16.2	-16.2	-18.6	-18.3	-19.1	-18.5	-16.7	-17.5	-16.5	-17.4	-17.6	-17.7	-16.5	-17.7	0.9
TC002462	-16.4	-15.6	-16.1	-16.5	-14.5	-14.9	-16.2	-16.8	-17.7	-17.1	-16.9	-16.8	-16.5	-17.6	0.9
TC004777	-16.9	-17.1	-16.7	-17.0	-16.3	-17.1	-16.3	-17.7	-18.3	-18.2	-17.9	-18.0	-17.9	-18.5	0.7
TC010636	-19.3	-16.9	-18.1	-18.5	-17.0	-17.4	-17.6	-17.8	-18.7	-17.7	-15.9	-16.1	-15.2	-17.2	1.1
TC011683	-18.0	-18.5	-20.3	-20.4	-19.4	-19.3	-18.5	-19.2	-19.4	-17.3	-16.9	-16.9	-16.5	-17.7	1.3
TC014245	-17.7	-16.3	-17.3	-17.6	-16.8	-17.5	-15.8	-16.4	-17.6	-18.0	-18.3	-18.9	-18.6	-19.4	1.0
TC002547	-16.8	-15.8	-16.5	-16.7	-15.6	-16.1	-14.3	-14.8	-16.0	-15.9	-15.7	-16.1	-16.3	-17.5	0.8
TC004634	-16.5	-16.6	-16.6	-16.9	-16.6	-17.3	-16.1	-17.1	-16.5	-16.6	-16.4	-16.8	-17.0	-17.7	0.4

OGS No.	E	L	P_fm	P_m	A0_fm	A0_m	A10_fm	A10_m	s1-ctl	s2-tthr	s3-mthr	s4-fthr	s5-mabd	s6-fabd	RDI-SD
TC005928	-16.1	-14.1	-16.9	-17.2	-15.8	-16.3	-14.6	-14.8	-16.1	-15.1	-15.0	-15.5	-15.7	-17.0	0.9
TC014680	-15.9	-15.2	-15.6	-15.7	-15.4	-15.4	-15.5	-15.2	-16.0	-16.1	-15.6	-15.6	-15.7	-16.6	0.4
TC000708	-18.9	-18.2	-19.4	-19.6	-18.3	-18.8	-17.4	-18.3	-19.9	-19.3	-19.3	-19.8	-20.0	-20.7	0.9
TC005769	-17.5	-15.3	-15.7	-16.1	-15.8	-16.1	-14.7	-15.1	-16.2	-16.2	-15.6	-15.7	-15.6	-17.2	0.7
TC008729	-16.8	-14.9	-16.1	-16.5	-15.4	-15.9	-15.2	-15.5	-15.8	-15.8	-15.0	-15.2	-14.7	-16.2	0.6
TC008872	-16.0	-15.5	-16.1	-16.3	-15.9	-16.1	-13.8	-14.5	-16.2	-16.7	-16.3	-16.4	-16.7	-17.3	0.9
TC015428	-19.2	-17.5	-18.3	-19.0	-16.9	-17.3	-16.8	-17.1	-18.0	-17.7	-16.7	-16.9	-17.0	-18.4	0.8
TC010774	-17.9	-18.2	-17.7	-18.3	-18.6	-19.2	-17.6	-19.3	-20.1	-18.4	-19.2	-18.6	-19.2	-19.9	0.8
TC000365	-18.1	-16.3	-17.6	-18.0	-17.0	-17.5	-16.0	-16.8	-18.2	-17.0	-17.3	-17.6	-17.6	-18.7	0.8
TC001629	-19.8	-17.0	-18.9	-19.7	-16.2	-16.9	-16.6	-17.3	-18.0	-17.1	-17.5	-17.3	-18.3	-18.7	1.1
TC003466	-18.8	-18.0	-19.1	-19.2	-18.8	-19.0	-17.2	-18.0	-19.7	-17.7	-18.2	-18.6	-18.5	-19.4	0.7
TC004574	-16.3	-15.9	-18.8	-18.3	-16.7	-17.0	-15.4	-16.3	-18.0	-16.9	-16.9	-17.1	-16.9	-17.5	0.9
TC000960	-16.8	-16.0	-18.0	-18.2	-18.6	-18.9	-16.9	-17.5	-17.9	-16.6	-16.8	-17.4	-17.1	-16.8	0.8
TC005191	-18.4	-17.4	-19.1	-19.5	-17.6	-18.2	-18.3	-18.4	-17.8	-17.1	-17.6	-18.1	-19.7	-20.5	1.0
TC011192	-18.6	-17.0	-18.6	-19.0	-18.1	-18.6	-16.8	-17.8	-18.5	-18.2	-18.0	-18.0	-19.2	-18.9	0.7
TC005122	-16.2	-15.8	-18.6	-18.9	-18.2	-18.8	-15.8	-16.1	-16.6	-16.3	-16.3	-16.7	-19.5	-19.4	1.4
TC005123	-19.8	-18.6	-19.4	-20.1	-17.5	-18.4	-17.3	-18.0	-19.8	-18.4	-18.9	-19.4	-19.1	-20.2	0.9
Desaturase															
TC000549	-24.8	-24.6	-24.6	-24.9	-23.2	-23.1	-18.3	-15.4	-27.5	NA	-25.7	-27.6	-22.6	-28.7	3.7
TC003656	-19.4	-16.4	-18.8	-18.6	-18.1	-18.0	-16.1	-17.6	-16.9	-15.8	-16.6	-15.7	-18.1	-17.4	1.2
TC006231	-18.7	-18.1	-19.8	-20.1	-21.7	-22.4	-19.8	-18.5	-18.6	-17.2	-17.5	-18.4	-18.7	-19.2	1.5
TC006232	-18.4	-17.5	-17.5	-17.6	-17.1	-17.8	-18.6	-18.7	-19.2	-16.1	-16.6	-17.3	-16.3	-17.3	0.9
TC011471	-19.9	-16.5	-24.0	-23.2	-24.4	-22.3	-13.5	-14.5	-14.9	-14.5	-15.0	-15.0	-16.9	-17.2	3.9
TC014819	-18.9	-16.0	-16.9	-17.0	-16.7	-17.2	-15.6	-16.5	-17.2	-18.6	-18.4	-18.4	-18.3	-17.4	1.0
TC014820	-26.3	-26.2	-23.1	-24.4	-26.2	-25.9	-24.6	-25.2	-26.3	-27.9	-25.8	-25.8	-26.2	-23.5	1.3
TC014821	-22.2	-17.8	-13.5	-13.3	-16.5	-16.8	-17.8	-17.7	-19.6	-20.4	-18.6	-19.0	-20.5	-16.2	2.5

OGS No.	E	L	P_fm	P_m	A0_fm	A0_m	A10_fm	A10_m	s1-ctl	s2-tthr	s3-mthr	s4-fthr	s5-mabd	s6-fabd	RDI-SD
TC015108	-18.2	-25.9	-24.0	-23.9	-22.9	-23.2	-25.2	-25.4	-26.5	-25.8	-24.6	-24.8	-25.0	-25.4	2.0
TC015338	-26.2	-24.1	-24.4	-23.7	-25.7	-23.4	-23.6	-23.9	-26.7	-28.4	NA	NA	-26.0	-27.5	1.7
TC015349	-25.8	-22.7	-19.8	-20.8	-21.2	-21.7	-22.7	-22.3	-24.9	-20.1	-18.7	-19.2	-18.3	-19.7	2.2
TC015382	-24.8	-19.8	-20.2	-20.9	-20.3	-20.4	-22.1	-21.0	-25.0	-18.9	-18.4	-18.6	-17.6	-19.1	2.2
TC015383	-23.3	-25.3	-20.7	-21.9	-23.1	-23.7	-23.1	-21.7	-25.2	-25.6	-23.9	-25.8	-23.3	-24.8	1.5
TC015395	-26.4	-26.9	-25.6	-26.2	-25.3	-27.2	-25.2	-26.4	NA	-28.6	NA	NA	NA	NA	1.1
TC015856	-17.6	-17.2	-17.8	-17.8	-17.6	-17.3	-16.3	-16.9	-18.7	-18.3	-18.5	-18.6	-18.3	-18.4	0.7
TC016399	-18.7	-18.3	-16.2	-15.9	-17.7	-18.4	-17.4	-17.7	-21.1	-22.1	-20.2	-20.8	-18.6	-19.7	1.8
TC016409	-27.5	-27.4	-27.7	-27.7	-27.4	-27.6	-27.3	-26.9	-29.0	-29.1	-29.0	NA	-28.9	-29.2	0.8
TC016414	-21.5	-22.4	-16.1	-17.2	-23.1	-22.4	-18.9	-22.8	-23.6	-23.5	-24.0	-24.8	-26.3	-23.7	2.9
TC016415	-18.3	-15.8	-18.7	-18.6	-18.9	-19.5	-13.5	-15.9	-18.4	-16.6	-16.9	-16.7	-18.2	-18.1	1.6
Elongase															
TC002898	-22.1	-19.3	-15.4	-15.3	-21.3	-20.7	-19.4	-19.8	-22.3	-18.7	-18.0	-18.3	-19.8	-21.5	2.2
TC002899	-20.1	-18.9	-20.0	-20.1	-20.8	-21.4	-18.5	-19.4	-21.9	-28.3	-26.6	NA	-20.4	-21.0	2.9
TC008803	-22.6	-18.0	-23.7	-22.7	-21.6	-22.3	-15.8	-16.6	-20.0	-26.0	-26.2	-25.3	-17.8	-18.5	3.5
TC010977	-17.1	-17.1	-16.2	-16.5	-17.8	-18.2	-16.6	-17.7	-19.7	-19.7	-19.4	-19.8	-20.3	-20.2	1.5
TC010980	-23.4	-24.9	-23.0	-23.6	-23.6	-25.1	-24.8	-25.4	-24.7	-27.6	-23.7	-26.0	NA	-26.1	1.3
TC010987	-17.7	-17.9	-16.1	-15.9	-15.5	-16.1	-17.4	-18.4	-20.4	-20.8	-21.6	-21.8	-21.8	-21.3	2.4
TC010988	-17.5	-17.8	-16.4	-16.3	-15.5	-16.1	-17.2	-18.5	-20.4	-20.5	-21.3	-21.5	-21.2	-20.8	2.2
TC011121	-20.8	-22.4	-18.9	-19.3	-15.7	-16.4	-18.9	-22.6	-19.2	-27.5	-27.4	NA	-25.5	NA	3.9
TC011937	-15.9	-14.7	-13.5	-13.7	-14.3	-14.7	-14.5	-15.7	-18.5	-17.1	-17.8	-18.4	-17.1	-18.2	1.8
TC011938	-16.4	-16.1	-16.6	-16.9	-16.6	-16.9	-15.5	-18.0	-19.6	-20.0	-19.5	-19.5	-19.2	-19.9	1.6
TC013861	-18.4	-15.8	-16.4	-16.3	-17.5	-16.8	-15.0	-16.8	-19.4	-18.6	-17.3	-17.2	-18.1	-17.9	1.2
TC015657	-24.0	-23.7	-23.2	-23.8	-19.5	-20.5	-22.3	-24.0	-23.2	-25.4	-22.4	-22.1	-22.6	-23.1	1.5
TC015658	-20.7	-18.2	-18.5	-19.7	-14.7	-15.7	-17.5	-18.2	-20.3	-18.9	-19.1	-19.5	-19.1	-18.9	1.6
TC016278	-15.9	-18.9	-14.8	-14.7	-13.3	-13.9	-18.3	-15.8	-17.5	-18.8	-17.9	-17.9	-16.8	-16.4	1.8

OGS No.	E	L	P_fm	P_m	A0_fm	A0_m	A10_fm	A10_m	s1-ctl	s2-tthr	s3-mthr	s4-fthr	s5-mabd	s6-fabd	RDI-SD
TC016279	-20.6	-18.4	-16.7	-16.8	-19.4	-20.1	-17.9	-18.1	-21.5	-17.2	-17.2	-17.1	-17.1	-18.9	1.5
TC016280	-23.9	-23.2	-18.0	-19.2	-20.6	-21.3	-17.3	-21.2	-26.8	-17.5	-16.5	-16.8	-16.3	-18.4	3.2

The numbers in the table are the relative depth indices (RDI).The other abbreviations: E: 0-72h embryo stage; L: larva L5-L7 stage; P_fm: female pupae stage (a mixture of early-, mid- and late-pupa); P_m: male pupae stage (also a mixture), A0_fm: A0 female adult stage; A0_m: A0 male adult stage; A10_fm: A10 female adult; A10_m: A10 male adult; s1_ctl: sample 1 in the transcriptome sequencing in Part 3.2, anterior abdomen control; s2_tthr: sample 2, *tar* prothoracic glands; s3_mthr: sample 3, male prothoracic glands; s4_fthr: sample 4, female prothoracic glands; s5_mabd: sample 5, male abdominal glands; s6_fabd: sample 6, female abdominal glands; SD: standard deviations of all the RDIs.

3.14 Characterization of four desaturase candidates

Based on the conserved domain, two desaturase (TC006231 and TC006232) were chosen because of their similarities to cytochrome b5 like heme/ steroid binding domain and delta5 FA desaturase. Delta5 desaturase is a critical enzyme in the pathways for the biosynthesis of the polyunsaturated fatty acids (Hastings et al., 2001), and remains to be well explored in insects. The other two (TC015382, GT64; TC015349) had much higher reads in all wild-type gland samples than in the anterior abdomen control (TC015382, more than 64 times; TC015349, more than 43 times). Therefore, they were also analyzed. Referring to the candidate numbering in Part 3.6, TC015349 was designated as GT78, TC006231 as GT79, and TC006232 as GT80.

3.14.1 Whole sequence cloning of the four desaturases

The open reading frames (ORFs) of these four desaturases were successfully amplified. However, the RACE confirmation of the ORF was not fruitful in some cases. The sequences we got are presented in **Dataset 13**.

3.14.2 Functional analyses based on RNAi and GC-MS

RNAi and GC-MS of these four desaturases did not show any significant differences. Double injection were also performed, neither GT64+GT78 nor GT79+GT80 presented any missing of volatile components in the gland secretions.

3.14.3 Enzyme activity tests of the desaturases

The desaturase activity was tested in a desaturase mutated yeast strain. GT79 (TC006231) and GT80 (TC006232) showed no measurable activities (data not presented). However, in the yeast transformed with GT64 (TC015382) or GT78 (TC015349) expression constructs, two additional unsaturated FAs (where the purple arrows indicated in **Figure 22**) were found compared to the empty vector. And the positions of the double bonds were at position 5 in 16:1 at least, which is relatively rare in nature. (The yeast based enzyme activity tests were mainly done by Dr. Ellen Hornung from Department of Biochemistry, GZMB, Georg-August-University of Göttingen)

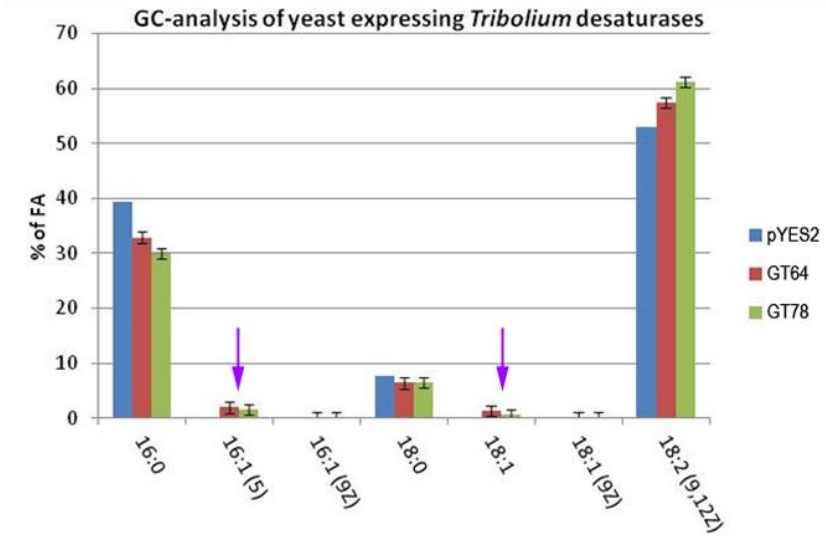

Figure 22 Fatty acid patterns of the yeast expressing *Tribolium* desaturases. X-axis: different fatty acids. Y-axis: the percentage of the fatty acid. The purple arrows indicate the two extra FAs detected in GT64 / GT78 expressing yeast strains. The error bars stand for the standard deviations at N=3-4. (From Dr. Ellen Hornung)

3.15 Characterization of an *alkene-less* gene

In the functional analysis of the most highly and gland-specifically expressed genes in Part 3.6 of this thesis, one novel gene (GT12) showed very strong reduction of

alkenes in both pairs of glands (see **Figure 23**). It was designated as *Tcas-alkene-less P450* (*Tcas-al P450*), referring to its RNAi-phenotype and conserved domain. In order to elucidate the mechanism of alkene biosynthesis, this gene was characterized further.

3.15.1 Whole sequence cloning and quantification of the volatiles in alkene-less knock-down

The whole sequence of *Tcas-al P450* was cloned and presented in **Dataset 13**. In 5'RACE, two clear bands were obtained, therefore this gene might have two transcript variants. The longer one encodes a protein with 492aa, which is named as Tcas-alkene-less P450 variant A (Tcas-al P450A). And the shorter version is 328aa called Tcas-alkene-less P450 variant B (Tcas-al P450B).

After RNAi of this gene, no alkene was detectable in both pairs of odoriferous glands, which was also confirmed by injection of the second non-overlapping dsRNA fragment. The quantification of the gland volatiles in the knock-down and wild-type is presented in **Figure 24**. The statistical comparisons between different groups and sexes are shown in **Figure 25**. All alkenes in *Tcas-al P450* knock-down were significantly reduced compared to wild type either in male or female, whereas the quinones showed no significant differences in most cases (except for EBQ in female abdominal glands).

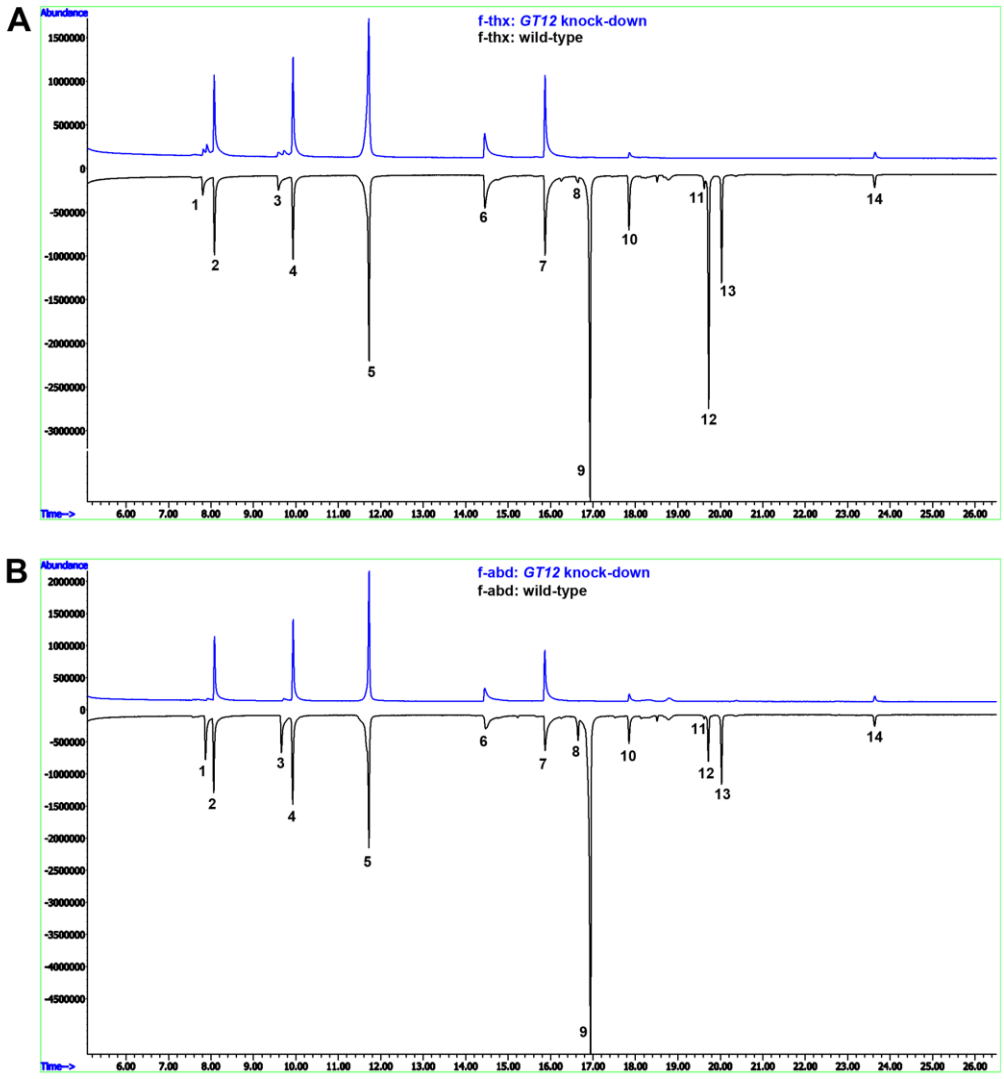

Figure 23 GC-MS chromatograms of wild type and *GT12* knock-down odoriferous glands. GC-MS was performed to check potential chemical alterations in gland volatiles of *GT12* knock-downs that have condensed secretions in both glands. A, prothoracic glands (thx), B, abdominal glands (abd). The upper blue chromatogram is *GT12* knock-down and the lower black one wild-type. Both glands of *GT12* knock-downs presented no detectable alkenes at all. The peaks were: 1 and 2: methyl-1,4-benzoquinone; 3 and 4: ethyl-1,4-benzoquinone; 5: 1-dodecene, artificially added as an internal control; 6: methyl-1,4-hydroquinone; 7: ethyl-1,4-hydroquinone; 8: 1,6-pentadecadiene; 9: 1-pentadecene; 10: 1,2-dimethoxy-4-n-propylbenzene; 11: 1-Hexadecene; 12: 1,8-heptadecadiene; 13: 1-Heptadecene; 14: n-Hexadecanoic acid methyl ester, which also exists in empty control and is believed to be background. PS: the double bond positions in 1,6-pentadecadiene and 1,8-heptadecadiene have not been confirmed; these results are from females, but the males showed the same phenotype and chromatogram.

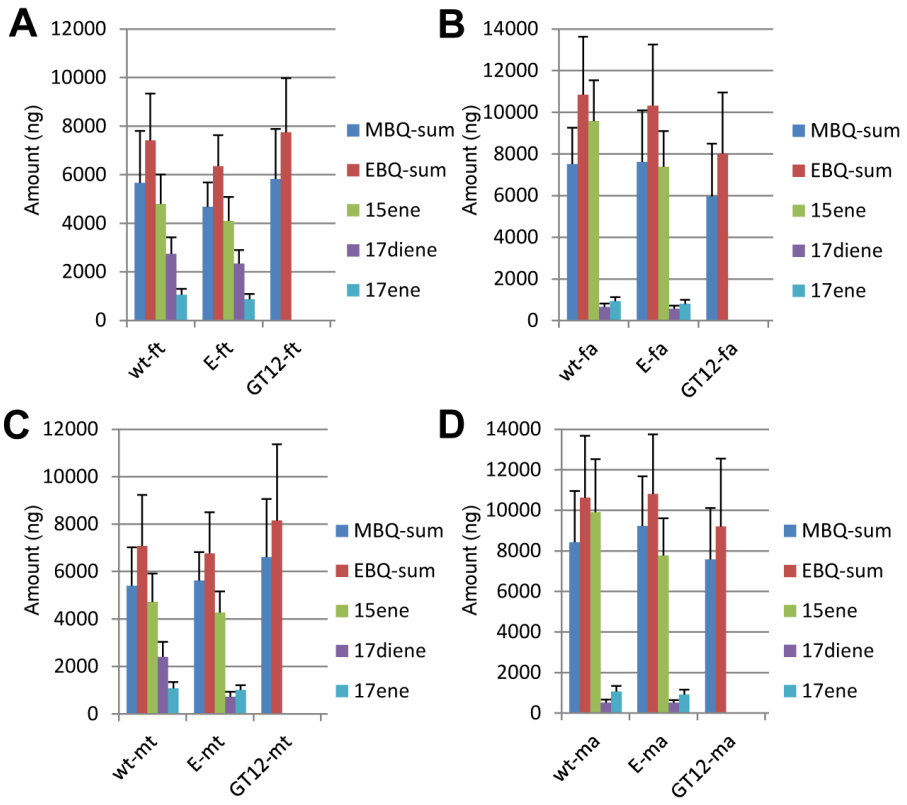

Figure 24 Quantification of main glandular volatiles by GC-MS in wild-type and novel *alkene-less* gene RNAi-knockdowns. Comparisons in female thoracic glands (ft) (A), female abdominal glands (fa) (B), male thoracic glands (mt) (C), and male abdominal glands (ma) (D). Y-axis: amount in nanogram; X-axis: wt and *Tcas-al P450* RNAi-knockdowns. Abbreviations: wt: wild-type; E: dsEGFP-injected control; GT12: *Tcas-al P450*; MBQ-sum: methyl-1,4-benzoquinone; EBQ-sum: ethyl-1,4-benzoquinone; 15ene: 1-pentadecene; 17diene: 1,8-heptadecadiene; 17ene: 1-heptadecene. The error bars indicate standard deviations at N=18-24.

A

Comparison	Sex	Gland type	MBQ (ng)	EBQ (ng)	15ene (ng)	17diene (ng)	17ene (ng)	Quinones (nmol)	Alkenes (nmol)
wt - E	male	thx	no	no	no	***	no	no	***
		abd	no	no	**	no	no	no	*
		both	no	no	*	***	no	no	**
	female	thx	no	no	no	no	*	no	no
		abd	no	no	**	no	no	no	**
		both	no	no	**	no	**	no	**
wt - GT12	male	thx	no	no	***	***	***	no	***
		abd	no	no	***	***	***	no	***
		both	no	no	***	***	***	no	***
	female	thx	no	no	***	***	***	no	***
		abd	no	**	***	***	***	*	***
		both	no	no	***	***	***	no	***

B

Comparison	Treatment	Gland type	MBQ (ng)	EBQ (ng)	15ene (ng)	17diene (ng)	17ene (ng)	Quinones (nmol)	Alkenes (nmol)
male vs. female	wt	thx	no	no	no	no	no	no	no
		abd	no	no	no	**	no	no	no
		both	no	no	no	no	no	no	no
	E	thx	**	no	no	***	no	no	*
		abd	*	no	no	no	no	no	no
		both	**	no	no	***	**	*	no
	GT12	thx	no	no	NA	NA	NA	no	NA
		abd	*	no	NA	NA	NA	no	NA
		both	no	no	NA	NA	NA	no	NA

Figure 25 The statistical comparisons between different groups and sexes after knock-down of the novel *alkene-less* gene. A: Comparisons between controls and *GT12* (*Tcas-al P450*) knock-down. A non-parametric method (Wilcoxon) was used. B: Comparisons between male and female inside one group. Student t-test method was used. Abbreviations: no: P>0.05; *: 0.01<P<0.05; **: 0.001<P<0.01; ***: P<0.001; NA: not available. N=15-30.

3.15.2 Phylogeny of the novel *alkene-less* gene *Tcas-al P450*

After quantification of the gland volatiles in *Tcas-al P450* knockdowns, their phylogeny was explored. In the phylogenetic tree (**Figure 26A**), Tcas-al P450 was grouped together with other five *Tribolium* homologs, and close to four homologs from *Nasonia vitripennis,* and six homologs from *Aedes aegypti.* Then the relative transcriptomic expression levels were explored for all the *Tribolium* homologs. The homologs were linked with corresponding OGS numbers and explored in the

transcriptomic libraries (**Dataset 14**). It was shown (**Figure 26B**) that no other gene was as highly expressed in the gland samples except for the identified *alkene-less* gene, although two genes contained about 32 times (2 to the power of 5, GI:91082229, **Figure 26B**) or 8 times (2 to the power of 3, GI:167234443, **Figure 26B**) higher reads, which were yet classified to another branch. In conclusion, this indicates that Tcas-al P450 most probably has evolved independently and specifically for the chemical defensive system in *Tribolium*.

3.15.3 Expression pattern of the *alkene-less* gene in gland tissue

The expression pattern of *Tcas-al P450* (*GT12*) was explored in dissected odoriferous glands. The gene showed strong expressions only in gland cell type 1 (**Figure 27**, right lower corner of **B1** and **B2**, lower zoomed triangles) but not in cell type 2 (**Figure 27**, right lower corner of **B1** and **B2**, upper zoomed triangles) in both pairs of glands (the name of the cell types can refer to Eisner et al., 1964; Happ, 1968), which confirms its involvement in *Tribolium* defensive secretion and suggests that cell type 1 might play the main role for alkene synthesis.

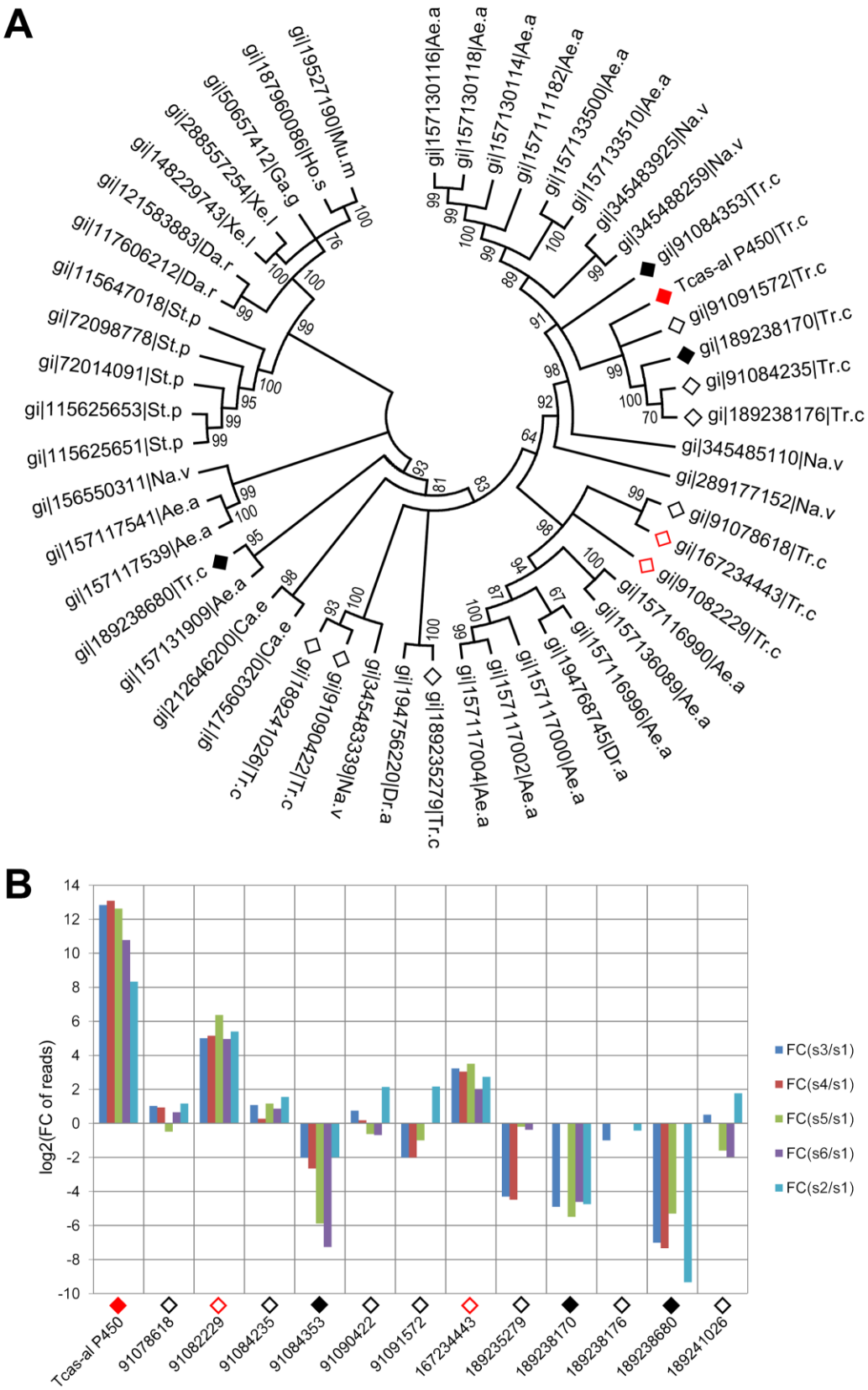

Figure 26 The phylogenetic tree of Tcas-al P450 and the relative transcriptomic gland expression levels of its *Tribolium* homologs.

Figure 26 The phylogenetic tree of Tcas-al P450 and the relative transcriptomic gland expression levels of its *Tribolium* homologs. A: the phylogenetic tree of the novel *alkene-less* gene, all the *Tribolium* homologs were marked based on their relative gland expression levels (B), with the solid red square indicating the alkene-less gene, with open red squares genes relatively high expressed in gland samples, with solid black squares relatively high expressed in the control sample, and with open black squares indicating the other *Tribolium* homologs. The numbers on the branching points are the statistical frequencies; B, the relative expression levels of the *Tribolium* homologs of Tcas-al P450, along the X-axis the different genes are presented (using the same GI numbers and expression level square codes as in Panel A), while Y-axis presents log2[fold change of reads in glands against control]. For abbreviations see Figure 16.

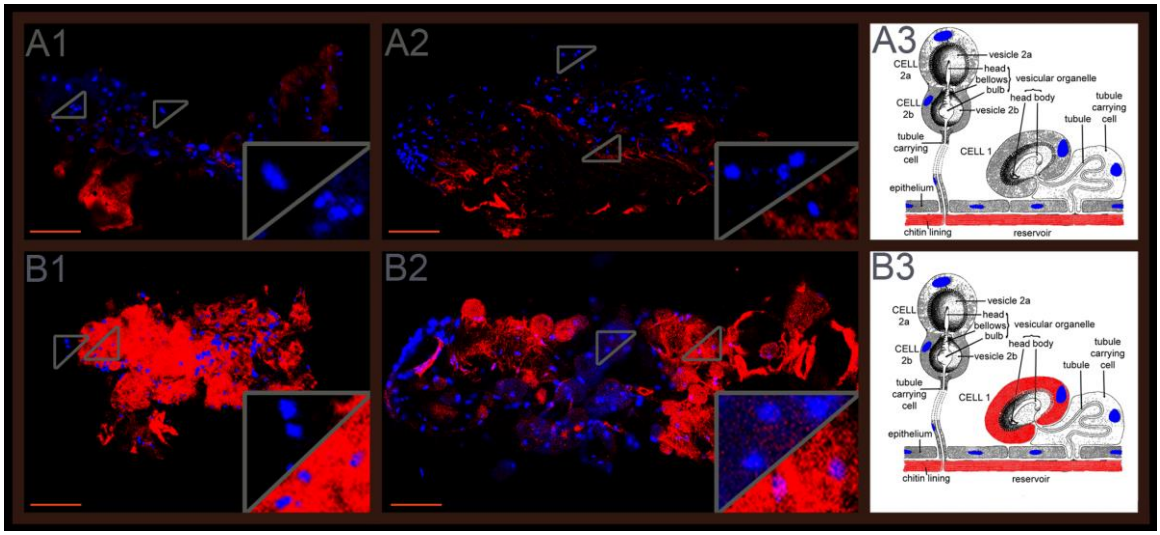

Figure 27 Expression patterns of the novel alkene-less gene *Tcas-al P450*. The first column (A1, B1) shows prothoracic glands, the second (A2, B2) abdominal glands, and the third (A3, B3) gland schemes modified after Happ (Happ, 1968). A1-A3, *Tcas-al P450* (*GT12*) sense probes. B1-B3, *Tcas-al P450* (*GT12*) antisense probes. In the right lower corner of the panels in the first and second column, the expressions were digitally magnified 4 times, with their original positions indicated by triangles within the same panel. Cell type 1 and cell type 2 were separately indicated in both pairs of glands, cell type 1 was zoomed in the lower triangle in the right lower corner of the panel, and cell type 2 in the upper triangle. In both pairs of glands, *Tcas-al P450* (*GT12*) expressed only in cell type 1. Scale bars: 50 µm.

3.15.4 Phenoloxidase activity assay of the *alkene-less* knock-down

As the knock-downs of the three novel *quinone-less* genes in Part 1 showed reduced phenoloxidase activities, similar experiment was also performed in the *alkene-less* knock-down. The phenoloxidase (PO) activities are presented in **Figure 28**. The *Tcas-al P450* knockdown was significant different from wild-type in females, while the buffer- and EGFP-injected control had no differences with wild-type (**Figure 28A)**. However, in the males, the *alkene-less* knock-down showed no significant difference with any of the controls (**Figure 28A)**. These results fit very well with the quantification data (**Figure 25A**), which showed that the quinones in the female *alkene-less* knock-down were significantly different from wild-type, but not in the male. These suggest that the phenoloxidase activity is probably related to quinone

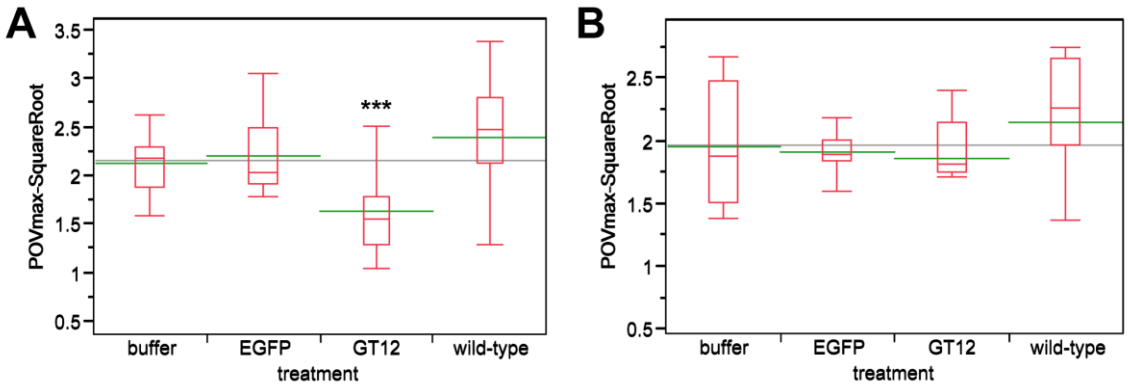

Figure 28 Phenoloxidase activity assays of wild-type and novel *alkene-less* gene RNAi knock-down. The Y-axes indicate the square root of PO Vmax, red boxes are boxplots, green lines represent the mean value, the gray lines represent the grand mean, while the X-axes present wt, control injections, and the RNAi-knockdowns. Buffer: buffer-injection control; EGFP: dsEGFP-injection control; GT12: *Tcas-al P450*. A, females, the asterisks (*) mark the t-test results comparing to wild-type: ***: p<0.001. Buffer- and EGFP-injected controls were not significantly different from wild-type; B, males, *Tcas-al P450* knockdown was not significantly different from any of the others

level in *Tribolium*. (The PO test was performed in collaboration with Dr. Gerrit Joop from Department of Evolutionary Ecology and Genetics, Zoological Institute, Christian-Albrechts-University of Kiel)

3.15.5 Enzyme activity test of the alkene-less gene

P450 enzymes have been reported to possess a novel function of fatty acid decarboxylase, which plays essential roles in 1-alkene (Rude et al., 2011) or cuticular hydrocarbon biosynthesis (Qiu et al., 2012). On account of the alkene-less phenotype after RNAi, we proposed that Tcas-al P450 may also have FA decarboxylase activity. However, the results from the activity test using GC/MS showed no detectable extra signals. Additionally, the *in vitro* purification of enzyme was not successful either. And the incubation of the cell lysates with substrates did not give any extra signal as well. (The activity tests in this section were done by Dr. Florian Brodhun from Department of Biochemistry, GZMB, Georg-August-University of Göttingen).

4. Discussion

4.1 Transcriptome sequencing

Transcriptome sequencing was performed in odoriferous gland samples from *Tribolium castaneum* to identify novel gene functions in defensive quinone and alkene biosyntheses. In a next generation sequencing approach, 27.8-29.7 million reads were obtained, of which only 50 to 61% reads were successfully mapped to the *Tribolium* genome. Part of the low mapping ratio is probably explainable by the strain differences used for genome sequencing (inbred Georgia 2 strain) (Tribolium Genome Sequencing Consortium et al., 2008) and the San Bernardino strain we used for transcriptomics together with the strict mapping parameters. However, this did neither affect the comparison and subtraction between different samples, nor the library subtraction results, since all our wild-type samples have the same strain background and all samples were treated identically. Only the *tar* mutation is in different genetic background derived from *sooty* (Sokoloff, 1966) and *Maxillopedia-Dachs3* strains (mxp^{Dachs3}) (Beeman et al., 1992). However, the mapping ratio for this sample was similar to the others. Another reason for the low mapping ratio might be that the official gene set was from a combination of different automated gene prediction programs and annotation pipelines (Tribolium Genome Sequencing Consortium et al., 2008), which makes it possible that there were still unidentified genes in the *Tribolium* genome.

4.2 Transcriptome library subtractions and GO annotation

The comparisons I performed were between different tissues in wild-type and *tar* mutant. During the library subtractions, I chose a general cut-off of fold change at 64 times, which is much higher compared to many microarray analyses (mostly two times), but the number of the genes I got was reasonably high and seemed suitable to start to work with. Only subtraction Group 7 (male abdominal glands specific genes), with 299 genes (**Figure 10**), showed an unusual high number, which might, however be explained by the fact that the male accessory glands are hard to dissect away from the abdominal glands and many of the genes in Group 7 might actually be male accessory gland-specifically expressed genes. As these were not a topic of this study, these potentially interesting genes remain for future analysis.

GO annotations revealed that the glands have quite active metabolisms with many catalytic and binding related genes being highly expressed. The GO annotation rate of the genes, that had coverage of more than 50 in all the glands, was 70.1%, while the control had 78.8% (**Dataset 9**). This suggests that there are more orphan genes expressed in *Tribolium* odoriferous glands than in the control. In addition, only 53.6% of all the 511 genes from the subtractions were annotated, and surprisingly, Group 7 (male specific glands genes) had an annotation rate of only 42.5%, suggesting an even higher number of genes with unknown functions. I identified also some glucosidases, phenol oxidases and peroxidases highly transcribed in the glands, that are candidate enzymes to be involved in quinone biosynthesis. In conclusion, our transcriptome data have reliably detected candidate genes involved in quinone biosynthetic mechanisms of chemical defense in the red flour beetle.

4.3 Functional analysis of the most highly and gland-specifically expressed genes

Exploring the functions of a first batch of highly gland-specifically expressed genes by RNAi and GC-MS to potentially identify novel gene functions in quinone biosynthesis, 67 of 77 genes (87%) showed alterations of at least one secreted chemical, which not only confirmed their importance for semiochemical synthesis, but also signified the effectiveness of our transcriptome screening. Surprisingly, some genes with very high reads in the glands showed no big changes at the chemical level. For example, *GT26* (*TC007317*), *GT35* (*TC010551*) and *GT41* (*TC011337*) from Group 1 had more than 441, 514 and 690 times higher reads respectively in all wild-type gland samples than control (**Dataset 8**), however, their knock-downs showed less than 75% reductions, or even neglectable changes (**Dataset 2**). I suggest that these genes might be involved in other biological processes indirectly related to chemical secretion. Additionally, in Group 10, the *GT23* gene (*TC006131*) that had more than 126 times enriched reads in s2-tthr (*tar* prothoracic gland sample) compared to s3-mthr and s4-fthr (male and female prothoracic gland samples; **Dataset 8**), showed no changes in prothoracic glands, but slightly increased amounts of quinones and reduced amounts of alkenes in abdominal glands. Encoding the odorant binding protein 21 (OBP21, GI:270012767), GT23 might be involved in olfaction system. It is possible that the mutated *tar* somehow caused the mis-expression of this gene in a different type of tissue, or OBP21 belongs to the ubiquitous OBP type, such as encapsulin (Leal, 2005), which is probably involved in diverse physiological functions

(Pelletier and Leal, 2009). Moreover, *GT23* showed about 10 times more reads in wild-type prothoracic glands than in the control sample. In addition, another OBP (*GT76*) and two chemosensory protein (*GT30*, *GT77*) encoding genes showed remarkable expression changes in the prothoracic glands of wild-type compared to *tar* mutants in the opposite direction. *GT30*, *GT76*, and *GT77* are expressed at high levels in wild-type prothoracic glands, but their expression is strongly reduced in *tar* mutants. None of these four genes is expressed at significant levels in the abdominal glands, indicating a specific function for the anterior glands. However, no significant changes in volatile gland contents could be detected after RNAi knock-down of those genes.

During the morphological analyses, many abnormal glands were observed (**Figure 13**). Their phenotypes could be explained as the knock-downs triggered the inhibition of chemical syntheses or the blocking of their transportation, or in some cases, the accumulation of intermediate substrates or unknown polymers (of black or brown color). It was proposed for previously identified *msg* mutants that the black material is of high-molecular-weight and polymeric consisting of polymerized prematurely formed quinones due to the absence of the inhibitor in oxidation of hydroquinone (Roth and Eisner, 1962; Engelhardt et al., 1965).

4.4 Quantification of volatile gland contents

In the quantification part, the main glandular contents were quantified separately in both pairs of glands for the first time. Assuming that stage A10 at 32.5°C is equal to

A12 at 30°C, which was predicted based on the *Tribolium* life parameter table (Sokoloff, 1974), the MBQ and EBQ amounts we got (**Dataset 11**) in wild-type were 20-30% (females) and 40-70% (males) higher than the amounts detected by Unruh *et al.* (Unruh et al., 1998). This indicates that the dissection based extraction is much more accurate than the homogenization based method, since the latter may cause the loss of unstable chemicals during the crude preparation. Moreover, in our experiments, the males and females were not separated before harvesting, which is much closer to the natural conditions compared to the method Unruh *et al.* used (Unruh et al., 1998). In addition, more EBQ was detected in our tests (molar ratio of MBQ/EBQ: 0.81 in female, 0.87 in male), while the previously reported ratio was in the range of 0.59-0.61 (Markarian et al., 1978; Pappas and Wardrop, 1996). However, the weight ratio of quinones in the whole beetle (61.5%) was only a bit higher than 58.3% reported previously (Markarian et al., 1978). Interestingly, different hydrocarbon compositions were observed between the prothoracic and abdominal glands, which might reflect the dissimilar usage of their precursors, fatty acids (Cavill, 1971), in distinct body parts and sexes. Furthermore, except for heptadecadiene in abdominal glands, all other components presented no significant differences between male and female at stage A10. Therefore, I propose that both sexes possess similar secretion levels in normal environment, and the higher level of benzoquinones in female observed before (Unruh et al., 1998) was due to a different energy allocation when they produce no or less eggs as virgins, since reproduction (mating and egg production) could change the energy allocation and fitness in several other species (Fowler and Partridge, 1989; Chapman et al., 1995; Kemp and Rutowski, 2004; Gilg and Kruse, 2003; Rönn et al., 2006).

4.5 Characterization of three novel quinone-less genes and their functions

After the first functional analyses of the complete set of highly gland-specifically expressed genes, three genes causing a quinone-less phenotype at knock-down were characterized further in our work. The quantitative data clearly showed the loss of quinones and the reduction of alkenes in both pairs of glands. Surprisingly, all the alkenes in *Tcas-ql MRP* (*GT63*) knock-downs showed no significant differences to wild-type in prothoracic glands but were significantly different in abdominal glands, while *Tcas-ql VTGl* (*GT39*) knock-downs caused significant differences to wild-type in almost all the comparisons except the three alkenes in the male abdominal glands. *Tcas-ql ARSB* (*GT62*) knock-downs showed significant changes to wild-type in all comparisons (**Dataset 11**). This implies that *Tcas-ql MRP* (*GT63*) has distinct functions in different glands, while *Tcas-ql VTGl* (*GT39*) and *Tcas-ql ARSB* (*GT62*) function diversely in both glands of the distinct sexes.

Potential molecular functions of these three genes in quinone synthesis are predicted on account of the homology and conserved domain analyses. Possessing a pancreatic lipase-like enzyme domain, Tcas-ql VTGl (GT39) is a vitellogenin like protein (31% identity). Vitellogenin is classified as a glycolipoprotein, having properties of a sugar, fat and protein, and belongs to a lipid transport protein family (Tufail and Takeda, 2009). Some data in mealworm showed that a vitellogenin like protein (19.6% identity) could enhance the melanin synthetic process (Lee et al., 2000), in which o-quinones were produced in an intermediate step right before

synthesizing eumelanin (Hearing, 2011; Eisenman and Casadevall, 2012). Possibly, the benzoquinone production in odoriferous glands has similar pathways, in which Tcas-ql VTGl (GT39) regulates the related enzyme activity or reactions yet with more important roles, since almost no quinones were detected in its knock-down. Provided that common synthetic steps exist, the black material in *msg* and *tar* mutants might actually be composed of melanin or something alike.

Tcas-ql ARSB (GT62) is an arylsulfatase B (ARSB) protein (45% identity), which has a sulfatase domain responsible to hydrolyze sulfates in the body by breaking down large sugar molecules called glycosaminoglycans (GAGs). ARSB targets two GAGs in particular: dermatan sulfate and chondroitin sulfate. ARSB is located in lysosomes, compartments within cells that digest and recycle different types of molecules (U.S. National Library of Medicine, 2010). The deficiency of ARSB is the cause of mucopolysaccharidosis VI (MPS VI) which occurs in humans and cats, called also Maroteaux-Lamy syndrome. MPS VI is a progressive condition that causes many tissues and organs to enlarge and become inflamed or scarred, skeletal abnormalities are also common in this condition (Litjens and Hopwood, 2001; Neufeld and Muenzer, 2001). Since lysosomes are the waste disposal system in the cell (Saftig and Klumperman, 2009), a few possible functions of Tcas-ql ARSB (GT62) are proposed. Firstly, Tcas-ql ARSB (GT62) may have important roles in the detoxication of toxic substances in gland cells, whose knock-down leads to the initiation of an assumed feedback loop, then to the inhibitions of secretory chemical syntheses. Secondly, since different subcellular localization prediction tools gave distinct results (data not shown), Tcas-ql ARSB (GT62) may not be located in

lysosomes but in the cytoplasm or elsewhere, functioning as an essential transporter for the intermediates involved in both quinone and alkene production, or as a key enzyme responsible for the activation of the newly translated transporters or other vital related proteins, or simply controlling the energy source of transportation, such as the pH gradient, or ion donators.

Tcas-ql MRP (GT63) belongs to ATP-binding cassette transporters, subfamily C (ABCC), which is also known as multidrug resistance-associated protein (MRP). Depending on ATP, the members of the MRP family can transport both hydrophobic uncharged molecules and water-soluble anionic compounds (Glavinas et al., 2004). The latter includes the substrates conjugated with anions, such as glutathione, glucuronate or sulfate (Homolya et al., 2003). Considering our data, Tcas-ql MRP (GT63) might be an important transporter for the quinone precursors in all gland secretory cells, which also transports some alkene precursors in abdominal glands. And the transportations may occur from the hemolymph to glandular cells, or from the secreting cells to the vesicular compartments, where the toxicant-producing reactions are being segregated to (Happ, 1968).

Despite of these predictions on the functions of the three *quinone-less* genes based on homologs, it should be noted that our phylogenic analyses show that they evolved independently and particularly for the chemical defense in the red flour beetle. Moreover, based on the GWMFISH results that confirm their expressions in the secretory units, all three genes play essential roles in producing the defensive quinones in the odoriferous glands of *T. castaneum.*

4.6 Microbe inhibition and phenol oxidase activity assays

In chemical secretion of *Tribolium*, the quinones and the alkenes (hydrocarbons) have their respective roles. Quinones are toxic and quite reactive, therefore mainly responsible for the defense against pathogens, parasitoids, and predators. Alkenes probably work as organic solvents and spreading agents for the quinones, which aid absorption by various enemies and improve the defensive effects (Blum, 1981). Our inhibition assay results confirm these descriptions, since the *quinone-less* knock-downs (*Tcas-ql MRP*, *GT63*) showed no microbe inhibitions at all, whereas the alkene-less knock-down (GT12) presented only reduced inhibition effects.

In insects, innate immune responses include antimicrobial peptides, phagocytosis, nodulation, melanotic encapsulation and wound healing, which endow potential hosts the abilities to defend against pathogens and parasites (Ashida and Brey, 1998; Cerenius and Söderhäll, 2004; Kanost et al., 2004; Mavrouli et al., 2005; Vilcinskas, 2013). The chemical defense system is also responsible for defending the host from infection by other organisms. Therefore, it was interesting to check how innate immunity was affected, when the chemical defense system is knocked-down. An oxidoreductase (PO) activity has been commonly assayed to provide a general index of melanization innate immune responses in invertebrates (Armitage and Siva-Jothy, 2005), since the activation of PO leads to the melanization reactions of invading pathogens, which is a major aspect of the innate immune system (Söderhäll and Cerenius, 1998). Therefore, PO activities were examined in *quinone-less* gene

knock-downs compared to wild-type, buffer injected and EGFP dsRNA injected beetles. The obtained results indicate that the chemical defense may be linked with melanotic encapsulation innate immune responses. Thus the three *quinone-less* genes necessary for quinone biosynthesis in odoriferous glands might also be involved in the melanization cascade. In addition, the genomic annotation and expression analyses of the *Tribolium* POs showed that some POs are highly expressed in all gland samples but low in control, which implies that they might mainly function in the chemical defense system, and their preferred substrates are in the glands. However, whether they are involved in the melanin pathway is so far unknown. In case the POs are multifunctional, a linkage and crosstalk between these two systems would exist.

4.7 Fatty acid metabolism in *Tribolium* development and gland biology

Fatty acid profiling in different developmental stages and the adult glands revealed the FA compositions in this newly emerged genetic insect model, and additionally the fact that the FA profiles are quantitatively various and well adapted to the particular demands in every developmental stage, and even in a specific organ/ tissue. Moreover, the annotation of related genes and the exploration of their relative expression levels provided a platform to further elucidate the mechanisms behind at a molecular level.

4.8 The functions of the desaturase candidates

Four of 19 annotated desaturases were functionally analyzed in this Part. However, RNAi did not cause any tremendous alkene alterations in the glandular defensive secretions, even in the knock-downs of GT64 and GT78, which showed nice delta5 desaturase activities in the yeast activity tests. This reflects the possible existence of a complex compensation system in beetle desaturases, i.e. the function of one or two desaturase(s) can be compensated by another one in case of mutation, knock-down or a low expression level. Or the target desaturases do not play any important roles in the glands, which might be true for GT79 and GT80, since they did not show any measurable activities in the yeast assays. However, for GT64 and GT78, it would be hard to explain why they are much more highly transcribed in the gland samples than in the control. If the compensation system does exist, then the desaturase must be a vital component to sustain the general metabolism, since the living organisms only keep additional backups for the essential pathways.

4.9 The *alkene-less* gene

The *alkene-less* gene presented a very strong RNAi phenotype, and is expressed specifically in glandular secretory cell type 1. In addition, it is also the only P450 homolog highly transcribed in the odoriferous glands, and specially evolved for the chemical defense system in *Tribolium.* Classical P450-enzymes catalyze monooxygenation reactions that are essential for many different steps in drug metabolism (Guengerich, 2008). Last year however, one P450 enzyme was reported

for a novel function as a terminal olefin-forming fatty acid decarboxylase in a group of bacteria *Jeotgalicoccus* spp., and its activity was conferred by heterologous expression in *E.coli* (Rude et al., 2011). Later, another P450 from *Drosophila melanogaster* was identified as decarboxylase involved in cuticular hydrocarbon biosynthesis as well (Qiu et al., 2012). However, our Tcas-al P450 share very less amino acids with the former one (query coverage=38%, max. identities=33%). And the latter one from the fruit fly only has 32% identities under 92% of query coverage. It seems like that Tcas-al P450 might be a different type of decarboxylase with distinct mechanisms.

Possible explanation for no observed activity in *E.coli* is that the *Tribolium* enzyme requires an ion donator to initiate the reaction, or that the substrate is different inside the beetle body. It seems that the prokaryotic expression system is not the right one for our purpose. Based on these and the information on gland contents, we propose to co-express Tcas-al P450 and the desaturases (GT64 and GT78) in an eukaryotic yeast system in order to verify the activity, to see whether the desaturases provide Tcas-al P450 with special substrates, and then to elucidate the biosynthetic mechanism of alkenes in *Tribolium*.

4.10 Potential alkene synthetic pathway related to fatty acid metabolism

To sum up all the data on the fatty acid metabolism and alkene synthesis, we suggest that 1-pentadecene in the gland secretions is produced from the decarboxylation of 16:0. And 1-heptadecene is derived from the decarboxylation of 18:0. In addition,

16:0 and 18:0 can also be desaturated by delta5 desaturase, which were then used as substrates for decarboxylase to possibly form 1,4-pentadecadiene and 1,4-heptadecadiene (**Figure 29**). However, a few more experiments need to be performed for verification.

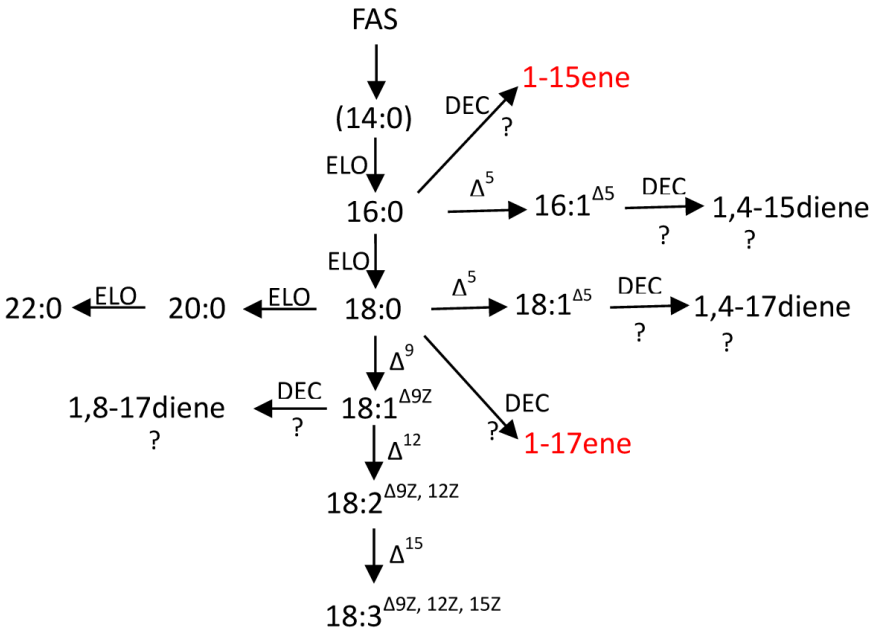

Figure 29 Hypothetic plan for biosynthesis of alkenes in the glands. The steps with question marks are being verified currently. Abbreviations: FAS: fatty acid synthase; ELO: elongase; Δ5: delta5 desaturase; DEC: decarboxylase; 1,4-15diene: 1,4-pentadecadiene. See Figure 24 for the other abbreviations.

5. Outlook

Coleoptera is an order of insects commonly called beetles. The name Coleoptera, derived from the Greek words *"koleos"* meaning sheath and *"ptera"* meaning wings (together "sheathed wing"), refers to the hardened, thickened and sheath-like or shell-like front wings, called elytra, which serve as protective covers for the membranous hind wings and the rear part of the beetle's body.

The order Coleoptera is the largest order in the class Insecta, constituting almost 25% of all known life-forms (Powell, 2009). About 40% of all described insect species are beetles [about 400,000 species (Hammond, 1992)], and new species are discovered frequently. Some estimates put the total number of species, described and undescribed, at as high as 100 million, but a figure of 1 million is more widely accepted (Chapman, 2009).

About 3⁄4 of beetle species are phytophagous in both larval and adult stages, i.e. living in or on plants, wood, fungi, and a variety of stored products, including cereals, tobacco, and dried fruits. Many of these plants are important for agriculture, forestry, and the household, therefore many beetles can be considered pests (Gilliott, 1995). Some species can cause remarkable damage. For example, the Boll weevil (*Anthonomus grandis*) feeds on cotton buds and flowers. Around 1892, this beetle crossed the Rio Grande near Brownsville, Texas to enter the United States from Mexico and had covered the entire state by 1915 (Mississippi State University, 2008). By the mid-1920s it had entered all cotton growing regions in the U.S., traveling 40 to 160 miles (60–260 km) per year. It remains the most destructive cotton pest in

North America. It has been estimated that since the boll weevil entered U.S. it has cost cotton producers about $13 billion, and recently about $300 million per year (Mississippi State University, 2008). Another example is western corn rootworm (*Diabrotica virgifera virgifera*), the larvae can destroy significant percentages of corn if left untreated. In U.S., current estimates show that 30 million acres (120,000 km^2) of corn (out of 80 million grown) are infested with corn rootworms and the affected area is expected to grow over the next 20 years. The United States Department of Agriculture estimates that corn rootworms cause $1 billion in lost revenue each year, which includes $800 million in yield loss and $200 million in cost of treatment for corn growers (The Dow Chemical Company, 2006).

Present pest management methods include conventional insecticides, ecological and biotechnological approaches (Pedigo and Rice, 2005). The conventional insecticides work well most times, but have low species-specificities. Also, the development of insecticide resistance in insects is becoming more and more problematic for insecticide usage. The ecological methods are mostly not very efficient though being environment-friendly. Compared to these two, the biotechnology based approaches are better and more sustainable for pest control. Commercial biotechnology solutions for controlling lepidopteran and coleopteran pests on crops depend on the expression of *Bacillus thuringiensis* (Bt) insecticidal proteins (James, 2003; Vaughn et al., 2005), which permeabilize the membranes of gut epithelial cells of susceptible insects (Rajamohan et al., 1998) and kill them. It was quite successful at the beginning, but later insect resistance to the Bt proteins arose (Tabashnik et al., 2008).

Therefore, new targets or toxins, which are more specific than Bt proteins, are needed for developing novel pest control methods.

Chemical defense is one of the most important traits endowing insects with the ability to live in a wide range of ecological environments (Eisner, 1970). On one hand, breaking or weakening the chemical defense system will put the beetles in a dangerous state, which will then inspire the development of new pest management solutions. On the other hand, the biology of the chemical defense system is a wonder in the nature and extraordinarily interesting itself. For instance, the defensive chemical spray of bombardier beetles (*Brachinus* species) is ejected at 100°C with an audible detonation (Eisner, 1958) from a pair of glands that open at the tip of the abdomen (Aneshansley et al., 1969). And the spray can be aimed in virtually any direction. The beetle can target its individual segments of the legs, and even the sites on its back (Eisner and Aneshansley, 1999). Besides the bombardier beetle, the rove beetle (genus *Stenus* Latreille and genus *Dianous* Leach) is also an eye-opener. Owing to the secretions from a pair of pygidial glands (Schildknecht et al., 1975), the beetle can move over the water surface in a rapid and extraordinary manner (Piffard, 1901), by employing the spreading potential of the secretions without moving its legs (Lang et al., 2012). The velocity of *Stenus comma* can reach 0.75 ms^{-1}, and if the secretion is continuous, a distance up to 15 m can be covered (Linsenmair and Jander, 1963).

Together with the fact that the molecular basis of the controlled synthesis and secretion behind the chemical defense system remain to be explored, it is of great importance to apply new research on this topic at the molecular biological level.

In respect to this purpose, my Ph.D. thesis is presenting the red flour beetle, *Tribolium castaneum*, as a successful research object with highly sophisticated genetic tools (Wang *et al.*, 2007), and a chemical defense system (Roth and Howland, 1941; Roth and Eisner, 1962). The results of my thesis represent a great starting point for the analysis of genes involved in defensive gland function. However, there are plenty of questions that remain to be answered: What genes are involved in the development of the secretory glands in the red flour beetle, *Tribolium castaneum*? How do the genes that involved in the synthesis of chemical defensive components cooperate with each other to contribute to an effective defense? What genes could be used in biotechnological control of coleopteran pests? What genes / enzymes could be applied to produce certain industrially important chemicals?

6. References

Alexander, P., and Barton, D. H. R. (1943). The excretion of ethylquinone by the flour beetle. The Biochemical Journal *37*, 463–465. Available at: http://www.pubmedcentral.nih.gov/articlerender.fcgi?artid=1257939&tool=pmcentrez&rendertype=abstract [Accessed March 26, 2012].

Aneshansley, D. J., Eisner, T., Widom, J. M., and Widom, B. (1969). Biochemistry at 100{degrees}C: Explosive Secretory Discharge of Bombardier Beetles (Brachinus). Science (New York, N.Y.) *165*, 61–63. Available at: http://www.ncbi.nlm.nih.gov/pubmed/17840686.

Armitage, S., and Siva-Jothy, M. (2005). Immune function responds to selection for cuticular colour in Tenebrio molitor. Heredity *94*, 650–656. Available at: http://www.ncbi.nlm.nih.gov/pubmed/15815710 [Accessed March 20, 2012].

Arrese, E. L., and Soulages, J. L. (2010). Insect fat body: energy, metabolism, and regulation. Annual review of entomology *55*, 207–225. Available at: http://www.ncbi.nlm.nih.gov/pmc/articles/PMC3075550/ [Accessed November 2, 2012].

Ashida, M., and Brey, P. (1998). Recent advances on the research of the insect prophenoloxidase cascade. In Molecular mechanisms of immune responses in insects, P. Brey and D. Hultmark, eds. (London, UK: Chapman & Hall), p. 135.

Asp, J., Abramsson, A., and Betsholtz, C. (2006). Nonradioactive in situ hybridization on frozen sections and whole mounts. Methods in molecular biology (Clifton, N.J.) *326*, 89–102. Available at: http://www.ncbi.nlm.nih.gov/pubmed/16780195.

Beeman, R. W., Stuart, J. J., Haas, M. S., and Friesen, K. S. (1992). Chromosome extraction and revision of linkage group 2 in Tribolium castaneum. The Journal of heredity *87*, 224–232. Available at: http://www.ncbi.nlm.nih.gov/pubmed/8683098.

Blum, M. S. (1981). Chemical defenses of arthropods. United Kin. (London: Academic Press) Available at: http://www.cabdirect.org/abstracts/19820594729.html;jsessionid=6D34AB6A23BB5FBEB2313F77658399B7 [Accessed August 9, 2012].

Bucher, G., Scholten, J., and Klingler, M. (2002). Parental RNAi in Tribolium (Coleoptera). Current biology : CB *12*, R85–6. Available at: http://www.ncbi.nlm.nih.gov/pubmed/11839285 [Accessed August 13, 2012].

Campbell, M. K., and Farrell, S. O. (2006). Biochemistry 5th ed. (Cengage Learning).

Cavill, G. W. K. (1971). Chemistry of Some Insect Secretions. Journal and Proceedings of the Royal Society of New South Wales. *103*, 109–118. Available at: http://www.ncbi.nlm.nih.gov/pubmed/10440781.

Cerenius, L., Lee, B. L., and Söderhäll, K. (2008). The proPO-system: pros and cons for its role in invertebrate immunity. Trends in immunology *29*, 263–271. Available at: http://www.ncbi.nlm.nih.gov/pubmed/18457993 [Accessed July 17, 2012].

Cerenius, L., and Söderhäll, K. (2004). The prophenoloxidase-activating system in invertebrates. Immunological reviews *198*, 116–126. Available at: http://www.ncbi.nlm.nih.gov/pubmed/15199959.

Chapman, A. D. (2009). Numbers of living species in Australia and the world Second. (Canberra, Australia: Australian Biological Resources Study (ABRS)) Available at: http://www.environment.gov.au/biodiversity/abrs/publications/other/species-numbers/2009/06-references.html [Accessed August 9, 2012].

Chapman, R. F. (1998). The Insects: Structure and Function 4th ed. (New York: Cambridge University Press).

Chapman, T., Liddle, L. F., Kalb, J. M., Wolfner, M. F., and Partridge, L. (1995). Cost of mating in Drosophila melanogaster females is mediated by male accessory gland products. Nature *373*, 241–244. Available at: http://dx.doi.org/10.1038/373241a0 [Accessed November 6, 2012].

Chittenden, F. H. (1896). Insects Affecting Cereals and Other Dry Vegetable Foods. Bulletin of the United States Department of Agriculture; Division of Entomology (New Series) *4*, 112–130.

Conesa, A., Götz, S., García-Gómez, J. M., Terol, J., Talón, M., and Robles, M. (2005). Blast2GO: a universal tool for annotation, visualization and analysis in functional genomics research. Bioinformatics *21*, 3674–3676. Available at: http://bioinformatics.oxfordjournals.org/cgi/content/abstract/21/18/3674 [Accessed March 9, 2012].

Conn, H. J., and Dimmick, I. (1947). Soil Bacteria Similar in Morphology to Mycobacterium and Corynebacterium. Journal of bacteriology *54*, 291–303. Available at: http://www.pubmedcentral.nih.gov/articlerender.fcgi?artid=526554&tool=pmcentrez&rendertype=abstract [Accessed June 7, 2012].

Dean, R., Collins, J., and Locke, M. (1985). Structure of the fat body. In Comprehensive Insect Physiology, Biochemistry, and Pharmacology., G. Kerkut and L. Gilbert, eds. (New York: Pergamon), pp. 155–210.

Eisenman, H. C., and Casadevall, A. (2012). Synthesis and assembly of fungal melanin. Applied microbiology and biotechnology *93*, 931–940. Available at: http://www.ncbi.nlm.nih.gov/pubmed/22173481 [Accessed October 30, 2012].

Eisner, T. (1966). Beetle's spray discourages predators. Natural History *75*, 42–47.

Eisner, T. (1970). Chemical defense against predation in arthropods. In Chemical Ecology, E. Sondheimer and J. B. Simeone, eds. (New York: Academic Press), pp. 157–217.

Eisner, T. (1958). The protective role of the spray mechanism of the Bombardier Beetle, Brachynus ballustarius. Journal of Insect Physiology *2*, 215–220.

Eisner, T., and Aneshansley, D. J. (1999). Spray aiming in the bombardier beetle: photographic evidence. Proceedings of the National Academy of Sciences of the

United States of America *96*, 9705–9709. Available at: http://www.pubmedcentral.nih.gov/articlerender.fcgi?artid=22274&tool=pmcentrez&rendertype=abstract.

Eisner, T., McHenry, F., and Salpeter, M. M. (1964). Defense mechanisms of arthropods. XV. Morphology of the quinone-producing glands of a tenebrionid beetle (ELEODES longicollis lec.). Journal of morphology *115*, 355–399. Available at: http://onlinelibrary.wiley.com/doi/10.1002/jmor.1051150304/abstract [Accessed June 4, 2012].

Eisner, T., and Meinwald, J. (1966). Defensive secretions of arthropods. Science *153*, 1341–1350. Available at: http://www.sciencemag.org/content/153/3742/1341.short [Accessed June 9, 2012].

Von Endt, D. W., and Wheeler, J. W. (1971). 1-Pentadecene production in Tribolium confusum. Science *172*, 60–61. Available at: http://www.sciencemag.org/content/172/3978/60.short [Accessed March 19, 2012].

Engelhardt, M., Rapoport, H., and Sokoloff, A. (1965). Odorous secretion of normal and mutant Tribolium confusum. Science (New York, N.Y.) *150*, 632–633. Available at: http://www.ncbi.nlm.nih.gov/pubmed/5837106 [Accessed August 13, 2012].

Fast, P. G. (1970). Insect lipids. Progress in the chemistry of fats and other lipids *11*, 181–242.

Faye, I., and Wyatt, G. R. (1980). The synthesis of antibacterial proteins in isolated fat body from Cecropia silkmoth pupae. Experientia *36*, 1325–1326. Available at: http://www.ncbi.nlm.nih.gov/pubmed/7449923 [Accessed October 28, 2012].

Fowler, K., and Partridge, L. (1989). A cost of mating in female fruitflies. Nature *338*, 760–761. Available at: http://dx.doi.org/10.1038/338760a0 [Accessed November 11, 2012].

Friedrich, M., and Benzer, S. (2000). Divergent decapentaplegic expression patterns in compound eye development and the evolution of insect metamorphosis. The Journal of experimental zoology *288*, 39–55. Available at: http://www.ncbi.nlm.nih.gov/pubmed/10750052 [Accessed May 14, 2012].

Gilg, M. R., and Kruse, K. C. (2003). Reproduction Decreases Life Span in the Giant Waterbug (Belostoma flumineum). The American Midland Naturalist *149*, 306–319. Available at: http://dx.doi.org/10.1674/0003-0031(2003)149[0306:RDLSIT]2.0.CO;2 [Accessed November 11, 2012].

Gilliott, C. (1995). Entomology 2nd ed. (Springer-Verlag New York, LLC.).

Glavinas, H., Krajcsi, P., Cserepes, J., and Sarkadi, B. (2004). The role of ABC transporters in drug resistance, metabolism and toxicity. Current drug delivery *1*, 27–42. Available at: http://www.ncbi.nlm.nih.gov/pubmed/16305368 [Accessed August 27, 2012].

Görgen, G., Frößl, C., Boland, W., and Dettner, K. (1990). Biosynthesis of 1-alkenes in the defensive secretions of Tribolium confusum (Tenebrionidae); stereochemical implications. Experientia *46*, 700–704. Available at: http://www.springerlink.com/content/hx288200k15331hr/ [Accessed August 10, 2012].

Götz, S., García-Gómez, J. M., Terol, J., Williams, T. D., Nagaraj, S. H., Nueda, M. J., Robles, M., Talón, M., Dopazo, J., and Conesa, A. (2008). High-throughput functional annotation and data mining with the Blast2GO suite. Nucleic acids research *36*, 3420–3435. Available at: http://nar.oxfordjournals.org/cgi/content/abstract/36/10/3420 [Accessed March 3, 2012].

Guengerich, F. P. (2008). Cytochrome p450 and chemical toxicology. Chemical research in toxicology *21*, 70–83. Available at: http://www.ncbi.nlm.nih.gov/pubmed/18052394.

Hammond, P. M. (1992). Species inventory. In Global Biodiversity: Status of the Earth's Living Resources, B. Groombridge, ed. (London: Chapman and Hall), pp. 17–39.

Hannon, G. (2002). RNA interference. Nature *418*, 24–26. Available at: http://codex.cshl.org/publications/Hannon_2002_12110901.pdf [Accessed June 1, 2012].

Happ, G. M. (1968). Quinone and hydrocarbon production in the defensive glands of Eleodes longicollis and Tribolium castaneum (Coleoptera, Tenebrionidae). Journal of insect physiology *14*, 1821–1837. Available at: http://www.sciencedirect.com/science/article/pii/002219106890214X.

Hastings, N., Agaba, M., Tocher, D. R., Leaver, M. J., Dick, J. R., Sargent, J. R., and Teale, A. J. (2001). A vertebrate fatty acid desaturase with Delta 5 and Delta 6 activities. Proceedings of the National Academy of Sciences of the United States of America *98*, 14304–14309. Available at: http://www.pubmedcentral.nih.gov/articlerender.fcgi?artid=64677&tool=pmcentrez&rendertype=abstract [Accessed December 14, 2012].

Hearing, V. J. (2011). Determination of melanin synthetic pathways. The Journal of investigative dermatology *131*, E8–E11. Available at: http://www.ncbi.nlm.nih.gov/pubmed/22094404 [Accessed October 30, 2012].

Homolya, L., Váradi, A., and Sarkadi, B. (2003). Multidrug resistance-associated proteins: Export pumps for conjugates with glutathione, glucuronate or sulfate. BioFactors (Oxford, England) *17*, 103–114. Available at: http://www.ncbi.nlm.nih.gov/pubmed/12897433 [Accessed August 23, 2012].

Horn, T., and Boutros, M. (2010). E-RNAi: a web application for the multi-species design of RNAi reagents--2010 update. Nucleic acids research *38*, W332–9. Available at: http://nar.oxfordjournals.org/cgi/content/abstract/38/suppl_2/W332 [Accessed March 12, 2012].

IUPAC (1997). Compendium of Chemical Terminology (the "Gold Book") 2nd ed. (Oxford: Blackwell Scientific Publications) Available at: http://goldbook.iupac.org/F02330.html.

James, C. (2003). Global review of commercialized transgenic crops. Current Science *84*, 303–309. Available at: http://faculty.washington.edu/jhannah/geog270aut07/readings/GreenGeneRevolutions/Clive - GlobalreviewTransgeneticCrops.pdf [Accessed December 20, 2012].

Kanost, M. R., Jiang, H., and Yu, X.-Q. (2004). Innate immune responses of a lepidopteran insect, Manduca sexta. Immunological reviews *198*, 97–105. Available at: http://www.ncbi.nlm.nih.gov/pubmed/15199957 [Accessed July 31, 2012].

Katoh, K., Kuma, K., Toh, H., and Miyata, T. (2005). MAFFT version 5: improvement in accuracy of multiple sequence alignment. Nucleic acids research *33*, 511–518. Available at: http://nar.oxfordjournals.org/cgi/content/abstract/33/2/511 [Accessed March 11, 2012].

Kemp, D. J., and Rutowski, R. L. (2004). A survival cost to mating in a polyandrous butterfly, Colias eurytheme. Oikos *105*, 65–70. Available at: http://doi.wiley.com/10.1111/j.0030-1299.2004.12874.x [Accessed November 11, 2012].

Kim, H. S., Murphy, T., Xia, J., Caragea, D., Park, Y., Beeman, R. W., Lorenzen, M. D., Butcher, S., Manak, J. R., and Brown, S. J. (2010). BeetleBase in 2010: revisions to provide comprehensive genomic information for Tribolium castaneum.

Nucleic acids research *38*, D437–42. Available at: http://nar.oxfordjournals.org/cgi/content/abstract/38/suppl_1/D437 [Accessed June 6, 2012].

Ladish, R. K., Ladish, S. K., and Howe, P. M. (1967). Quinoid Secretions in Grain and Flour Beetles. Nature *215*, 939–940. Available at: http://dx.doi.org/10.1038/215939a0 [Accessed August 16, 2012].

Lalitha, S. (2000). Primer Premier 5. Biotech Software & Internet Report *1*, 270–272. Available at: http://online.liebertpub.com/doi/abs/10.1089%2F152791600459894.

Lang, C., Seifert, K., and Dettner, K. (2012). Skimming behaviour and spreading potential of Stenus species and Dianous coerulescens (Coleoptera: Staphylinidae). Die Naturwissenschaften *99*, 937–947. Available at: http://www.ncbi.nlm.nih.gov/pubmed/23086390 [Accessed November 2, 2012].

Lappin, G. R., and Sauer, J. D. (1989). Alpha olefin applications handbook. (New York.: Marcel Dekker Inc.).

Law, J. H., and Wells, M. A. (1989). Insects as biochemical models. The Journal of biological chemistry *264*, 16335–16338. Available at: http://www.ncbi.nlm.nih.gov/pubmed/2674129 [Accessed December 10, 2012].

Leal, W. S. (2005). Pheromone reception. Topics in Current Chemistry *240*, 1–36. Available at: http://www.springerlink.com/index/WV1PY7HYC4861T2D.pdf [Accessed August 22, 2012].

Lee, K. M., Lee, K. Y., Choi, H. W., Cho, M. Y., Kwon, T. H., Kawabata, S., and Lee, B. L. (2000). Activated phenoloxidase from Tenebrio molitor larvae enhances the synthesis of melanin by using a vitellogenin-like protein in the presence of dopamine. European Journal of Biochemistry *267*, 3695–3703. Available at:

http://doi.wiley.com/10.1046/j.1432-1327.2000.01402.x [Accessed May 28, 2012].

Lehninger, A. L., Nelson, D. L., Cox, M. M., and Nelson, D. L. P. D. (2005). Principles of Biochemistry 4th ed. (New York: W. H. Freeman and Company).

Linsenmair, K. E., and Jander, R. (1963). Das entspannungsschwimmen von Velia und Stenus. Naturwissenschaften *50*, 231.

Litjens, T., and Hopwood, J. J. (2001). Mucopolysaccharidosis type VI: Structural and clinical implications of mutations in N-acetylgalactosamine-4-sulfatase. Human mutation *18*, 282–295. Available at: http://www.ncbi.nlm.nih.gov/pubmed/11668612 [Accessed August 26, 2012].

Loconti, J. D., and Roth, L. M. (1953). Composition of the odorous secretion of Tribolium castaneum. Annals of the Entomological Society of America *46*, 281–289. Available at: http://www.ingentaconnect.com/content/esa/aesa/1953/00000046/00000002/art00011 [Accessed August 10, 2012].

Lorenzen, M. D., Doyungan, Z., Savard, J., Snow, K., Crumly, L. R., Shippy, T. D., Stuart, J. J., Brown, S. J., and Beeman, R. W. (2005). Genetic linkage maps of the red flour beetle, Tribolium castaneum, based on bacterial artificial chromosomes and expressed sequence tags. Genetics *170*, 741–747. Available at: http://www.pubmedcentral.nih.gov/articlerender.fcgi?artid=1450394&tool=pmcentrez&rendertype=abstract [Accessed March 8, 2012].

Markarian, H., Florentine, G. J., and Prait Jr., J. J. (1978). Quinone production of some species of Tribolium. Journal of Insect Physiology *24*, 785–790. Available at: http://www.sciencedirect.com/science/article/pii/0022191078900963 [Accessed August 10, 2012].

Mavrouli, M. D., Tsakas, S., Theodorou, G. L., Lampropoulou, M., and Marmaras, V. J. (2005). MAP kinases mediate phagocytosis and melanization via prophenoloxidase activation in medfly hemocytes. Biochimica et biophysica acta *1744*, 145–156. Available at: http://www.ncbi.nlm.nih.gov/pubmed/15921769 [Accessed July 31, 2012].

Mendez-Perez, D., Begemann, M. B., and Pfleger, B. F. (2011). Modular synthase-encoding gene involved in α-olefin biosynthesis in Synechococcus sp. strain PCC 7002. Applied and environmental microbiology *77*, 4264–4267. Available at: http://www.pubmedcentral.nih.gov/articlerender.fcgi?artid=3131656&tool=pmcentrez&rendertype=abstract [Accessed November 3, 2012].

Mississippi State University (2008). History of the Boll Weevil in the United States. Economic impacts of the boll weevil. Available at: http://web.archive.org/web/20080512023346/http://www.bollweevil.ext.msstate.edu/webpage_history.htm.

Neufeld, E., and Muenzer, J. (2001). The mucopolysaccharidoses. In The metabolic and molecular bases of inherited disease., C. Scriver, A. Beaudet, W. Sly, and D. Valle, eds. (New York: McGraw-Hill), pp. 3421–3452.

Ney, P., and Boland, W. (1987). Biosynthesis of 1-alkenes in higher plants. A model study with the composite Carthamus tinctorius L. European Journal of Biochemistry *162*, 203–211.

Osborne, P., and Dearden, P. K. (2005). Non-radioactive in-situ hybridisation to honeybee embryos and ovaries. Apidologie *36*, 113–118.

Pappas, P. W., and Wardrop, S. M. (1996). Quantification of benzoquinones in the flour beetles, Tribolium castaneum and Tribolium confusum. Preparative biochemistry & biotechnology *26*, 53–66. Available at: http://www.ncbi.nlm.nih.gov/pubmed/8744422 [Accessed March 26, 2012].

Payne, N. M. (1925). Some effects of Tribolium on flour. Journal of Economic Entomology *18*, 737–744. Available at: http://www.ingentaconnect.com/content/esa/jee/1925/00000018/00000005/art00020.

Pedigo, L. P., and Rice, M. E. (2005). Entomology and Pest Management 5th ed. D. Yarnell, M. Rego, and A. B. Wolf, eds. (Prentice Hall).

Pelletier, J., and Leal, W. S. (2009). Genome analysis and expression patterns of odorant-binding proteins from the Southern House mosquito Culex pipiens quinquefasciatus. PloS one *4*, e6237. Available at: http://dx.plos.org/10.1371/journal.pone.0006237 [Accessed August 22, 2012].

Piffard, A. (1901). Steni gliding on the surface of water. Entomologists Monthly Magazine *12*, 99.

Posnien, N., Schinko, J., Grossmann, D., Shippy, T. D., Konopova, B., and Bucher, G. (2009). RNAi in the red flour beetle (Tribolium). Cold Spring Harbor protocols *2009*, pdb.prot5256. Available at: http://www.ncbi.nlm.nih.gov/pubmed/20147232 [Accessed May 9, 2012].

Powell, J. A. (2009). Coleoptera. In Encyclopedia of Insects, V. H. Resh and R. T. Cardé, eds. (Academic Press), p. 1132.

Prendeville, H. R., and Stevens, L. (2002). Microbe inhibition by Tribolium flour beetles varies with beetle species, strain, sex, and microbe group. Journal of chemical ecology *28*, 1183–1190. Available at: http://www.ncbi.nlm.nih.gov/pubmed/12184396.

Price, M. N., Dehal, P. S., and Arkin, A. P. (2010). FastTree 2--approximately maximum-likelihood trees for large alignments. PloS one *5*, e9490. Available at: http://dx.plos.org/10.1371/journal.pone.0009490 [Accessed March 12, 2012].

Qiu, Y., Tittiger, C., Wicker-Thomas, C., Le Goff, G., Young, S., Wajnberg, E., Fricaux, T., Taquet, N., Blomquist, G. J., and Feyereisen, R. (2012). An insect-specific

P450 oxidative decarbonylase for cuticular hydrocarbon biosynthesis. Proceedings of the National Academy of Sciences of the United States of America, 1–6. Available at: http://www.ncbi.nlm.nih.gov/pubmed/22927409 [Accessed August 30, 2012].

Rajamohan, F., Lee, M. K., and Dean, D. H. (1998). Bacillus thuringiensis insecticidal proteins: molecular mode of action. Progress in nucleic acid research and molecular biology *60*, 1–27. Available at: http://www.ncbi.nlm.nih.gov/pubmed/9594569 [Accessed December 20, 2012].

Roma, G. C., Bueno, O. C., and Camargo-Mathias, M. I. (2010). Morpho-physiological analysis of the insect fat body: a review. Micron (Oxford, England : 1993) *41*, 395–401. Available at: http://www.ncbi.nlm.nih.gov/pubmed/20206534 [Accessed December 10, 2012].

Rönn, J., Katvala, M., and Arnqvist, G. (2006). The costs of mating and egg production in Callosobruchus seed beetles. Animal Behaviour *72*, 335–342. Available at: http://dx.doi.org/10.1016/j.anbehav.2005.10.024 [Accessed November 11, 2012].

Roth, L. M. (1943). Studies on the gaseous secretion of Tribolium confusum Duval. II. The odoriferous glands of Tribolium confusum. Annals of the Entomological Society of America *36*, 397–424. Available at: http://www.ingentaconnect.com/content/esa/aesa/1943/00000036/00000003/art00011 [Accessed June 6, 2012].

Roth, L. M., and Eisner, T. (1962). Chemical defenses of arthropods. Annual Review of Entomology *7*, 107–136. Available at: http://www.annualreviews.org/doi/abs/10.1146/annurev.en.07.010162.000543? [Accessed August 9, 2012].

Roth, L. M., and Howland, R. B. (1941). Studies on the gaseous secretion of Tribolium confusum Duval, Pt. I. Abnormalities produced in Tribolium confusum Duval by

exposure to a secretion given off by the adults. Annals of the Entomological Society of America *34*, 151–175.

Roth, O., Joop, G., Eggert, H., Hilbert, J., Daniel, J., Schmid-Hempel, P., and Kurtz, J. (2010). Paternally derived immune priming for offspring in the red flour beetle, Tribolium castaneum. The Journal of animal ecology *79*, 403–413. Available at: http://www.ncbi.nlm.nih.gov/pubmed/19840170 [Accessed March 30, 2012].

Rude, M. a, Baron, T. S., Brubaker, S., Alibhai, M., Del Cardayre, S. B., and Schirmer, A. (2011). Terminal olefin (1-alkene) biosynthesis by a novel p450 fatty acid decarboxylase from Jeotgalicoccus species. Applied and environmental microbiology *77*, 1718–1727. Available at: http://www.pubmedcentral.nih.gov/articlerender.fcgi?artid=3067255&tool=pmcentrez&rendertype=abstract [Accessed March 20, 2012].

Saftig, P., and Klumperman, J. (2009). Lysosome biogenesis and lysosomal membrane proteins: trafficking meets function. Nature reviews. Molecular cell biology *10*, 623–635. Available at: http://www.ncbi.nlm.nih.gov/pubmed/19672277 [Accessed October 26, 2012].

Sambrook, J., and Russell, D. W. (2006). Inverse PCR. CSH protocols *2006*, pdb.prot3487–. Available at: http://cshprotocols.cshlp.org/content/2006/1/pdb.prot3487 [Accessed December 21, 2012].

Schildknecht, H., Krauss, D., Connert, J., Essenbreis, H., and Orfanides, N. (1975). The spreading alkaloid stenusine from the staphylinid Stenus comma (Coleoptera: Staphylinidae). Angewandte Chemie (International ed. in English) *14*, 421–422. Available at: http://www.ncbi.nlm.nih.gov/pubmed/808986 [Accessed December 21, 2012].

Schinko, J. B., Hillebrand, K., and Bucher, G. (2012). Heat shock-mediated misexpression of genes in the beetle Tribolium castaneum. Development genes

and evolution *222*, 287–298. Available at: http://www.ncbi.nlm.nih.gov/pubmed/22890852 [Accessed October 27, 2012].

Schinko, J. B., Weber, M., Viktorinova, I., Kiupakis, A., Averof, M., Klingler, M., Wimmer, E. A., and Bucher, G. (2010). Functionality of the GAL4/UAS system in Tribolium requires the use of endogenous core promoters. BMC developmental biology *10*, 53. Available at: http://www.pubmedcentral.nih.gov/articlerender.fcgi?artid=2882914&tool=pmcentrez&rendertype=abstract [Accessed October 27, 2012].

Schinko, J., Posnien, N., Kittelmann, S., Koniszewski, N., and Bucher, G. (2009). Single and double whole-mount in situ hybridization in red flour beetle (Tribolium) embryos. Cold Spring Harbor protocols *2009*, pdb.prot5258. Available at: http://cshprotocols.cshlp.org/cgi/content/abstract/2009/8/pdb.prot5258 [Accessed June 8, 2012].

Söderhäll, K., and Cerenius, L. (1998). Role of the prophenoloxidase-activating system in invertebrate immunity. Current Opinion in Immunology *10*, 23–28. Available at: http://dx.doi.org/10.1016/S0952-7915(98)80026-5 [Accessed July 5, 2012].

Sokoloff, A. (1974). The Biology of Tribolium Vol. 2. (Oxford: Clarendon Press).

Sokoloff, A. (1966). The genetics of Tribolium and related species. Advances in genetics, Supplement 1 (New York: Academic Press).

Stanley-Samuelson, D. W., Jurenka, R. A., Cripps, C., Blomquist, G. J., and De Renobales, M. (1988). Fatty acids in insects: Composition, metabolism, and biological significance. Archives of Insect Biochemistry and Physiology *9*, 1–33. Available at: http://doi.wiley.com/10.1002/arch.940090102 [Accessed December 14, 2012].

Suzuki, T., Huynh, V., and Muto, T. (1975). Hydrocarbon repellents isolated from Tribolium castaneum and T. confusum (Coleoptera: Tenebrionidae). Agricultural

and Biological Chemistry *39*, 2207 – 2211. Available at: http://agris.fao.org/agris-search/search/display.do?f=1976/JP/JP76004.xml;JP7601784.

Suzuki, Y., Squires, D. C., and Riddiford, L. M. (2009). Larval leg integrity is maintained by Distal-less and is required for proper timing of metamorphosis in the flour beetle, Tribolium castaneum. Developmental biology *326*, 60–67. Available at: http://www.pubmedcentral.nih.gov/articlerender.fcgi?artid=2762819&tool=pmcentrez&rendertype=abstract [Accessed June 7, 2012].

Tabashnik, B. E., Gassmann, A. J., Crowder, D. W., and Carriére, Y. (2008). Insect resistance to Bt crops: evidence versus theory. Nature biotechnology *26*, 199–202. Available at: http://www.ncbi.nlm.nih.gov/pubmed/18259177 [Accessed November 1, 2012].

Tamura, K., Peterson, D., Peterson, N., Stecher, G., Nei, M., and Kumar, S. (2011). MEGA5: molecular evolutionary genetics analysis using maximum likelihood, evolutionary distance, and maximum parsimony methods. Molecular biology and evolution *28*, 2731–2739. Available at: http://www.pubmedcentral.nih.gov/articlerender.fcgi?artid=3203626&tool=pmcentrez&rendertype=abstract [Accessed February 29, 2012].

Templiera, J., Largeaua, C., and Casadevalla, E. (1991a). Biosynthesis of n-alkatrienes in Botryococcus braunii. Phytochemistry *30*, 2209–2215.

Templiera, J., Largeaua, C., and Casadevalla, E. (1991b). Non-specific elongation-decarboxylation in biosynthesis of cis- and trans-alkadienes by Botryococcus braunii. Phytochemistry *30*, 175–183.

The Dow Chemical Company (2006). Product Safety Assessment (PSA): Herculex RW Rootworm Protection. Available at: http://www.dow.com/productsafety/finder/herculex.htm.

The Gene Ontology Consortium, Ashburner, M., Ball, C. A., Blake, J. A., Botstein, D., Butler, H., Cherry, J. M., Davis, A. P., Dolinski, K., Dwight, S. S., et al. (2000). Gene Ontology: tool for the unification of biology. Nature genetics *25*, 25–29. Available at: http://www.pubmedcentral.nih.gov/articlerender.fcgi?artid=3037419&tool=pmcentrez&rendertype=abstract [Accessed March 8, 2012].

Thompson, S. N. (1973). A review and comparative characterization of the fatty acid composition of seven insect orders. Comparative Biochemistry and Physiology *45*, 467–482.

Tomoyasu, Y., and Denell, R. E. (2004). Larval RNAi in Tribolium (Coleoptera) for analyzing adult development. Development genes and evolution *214*, 575–578. Available at: http://www.ncbi.nlm.nih.gov/pubmed/15365833 [Accessed April 2, 2012].

Tomoyasu, Y., Miller, S. C., Tomita, S., Schoppmeier, M., Grossmann, D., and Bucher, G. (2008). Exploring systemic RNA interference in insects: a genome-wide survey for RNAi genes in Tribolium. Genome Biology *9*, R10. Available at: http://www.pubmedcentral.nih.gov/articlerender.fcgi?artid=2395250&tool=pmcentrez&rendertype=abstract.

Trauner, J., Schinko, J., Lorenzen, M. D., Shippy, T. D., Wimmer, E. A., Beeman, R. W., Klingler, M., Bucher, G., and Brown, S. J. (2009). Large-scale insertional mutagenesis of a coleopteran stored grain pest, the red flour beetle Tribolium castaneum, identifies embryonic lethal mutations and enhancer traps. BMC biology *7*, 73. Available at: http://www.biomedcentral.com/1741-7007/7/73 [Accessed March 5, 2012].

Tribolium Genome Sequencing Consortium, Richards, S., Gibbs, R. A., Weinstock, G. M., Brown, S. J., Denell, R., Beeman, R. W., Gibbs, R., Bucher, G., Friedrich, M., et al. (2008). The genome of the model beetle and pest Tribolium castaneum. Nature *452*, 949–955. Available at: http://dx.doi.org/10.1038/nature06784 [Accessed March 1, 2012].

Tufail, M., and Takeda, M. (2009). Insect vitellogenin/lipophorin receptors: molecular structures, role in oogenesis, and regulatory mechanisms. Journal of insect physiology *55*, 87–103. Available at: http://www.ncbi.nlm.nih.gov/pubmed/19071131 [Accessed October 14, 2012].

U.S. National Library of Medicine (2010). ARSB. Genetics Home Reference. Available at: http://ghr.nlm.nih.gov/gene/ARSB.

Unruh, L. M., Xu, R., and Kramer, K. J. (1998). Benzoquinone levels as a function of age and gender of the red flour beetle, Tribolium castaneum. Insect Biochemistry and Molecular Biology *28*, 969–977. Available at: http://linkinghub.elsevier.com/retrieve/pii/S096517489800085X [Accessed March 19, 2012].

Vaughn, T., Cavato, T., Brar, G., Coombe, T., DeGooyer, T., Ford, S., Groth, M., Howe, A., Johnson, S., Kolacz, K., et al. (2005). A Method of Controlling Corn Rootworm Feeding Using a Protein Expressed in Transgenic Maize. Crop Science *45*, 931. Available at: https://www.agronomy.org/publications/cs/articles/45/3/0931 [Accessed October 29, 2012].

Vilcinskas, A. (2013). Evolutionary plasticity of insect immunity. Journal of insect physiology *59*, 123–129. Available at: http://www.ncbi.nlm.nih.gov/pubmed/22985862 [Accessed March 11, 2013].

Villaverde, M. L., Juárez, M. P., and Mijailovsky, S. (2007). Detection of Tribolium castaneum (Herbst) volatile defensive secretions by solid phase microextraction–capillary gas chromatography (SPME-CGC). Journal of Stored Products Research *43*, 540–545. Available at: http://dx.doi.org/10.1016/j.jspr.2007.03.003 [Accessed April 3, 2012].

Wang, L., Wang, S., Li, Y., Paradesi, M. S. R., and Brown, S. J. (2007). BeetleBase: the model organism database for Tribolium castaneum. Nucleic acids research *35*, D476–9. Available at:

http://www.pubmedcentral.nih.gov/articlerender.fcgi?artid=1669707&tool=pmcentrez&rendertype=abstract [Accessed May 9, 2012].

Weatherston, J. (1967). The chemistry of arthropod defensive substances. Quarterly Reviews, Chemical Society *21*, 287. Available at: http://pubs.rsc.org/en/content/articlehtml/1967/qr/qr9672100287 [Accessed August 9, 2012].

Wilson, E. O. (2006). Threats to Global Diversity Available at: http://www.globalchange.umich.edu/globalchange2/current/lectures/biodiversity/biodiversity.html [Accessed August 9, 2012].

Wirtz, R. A., Taylor, S. L., and Semey, H. G. (1978). Concentrations of substituted p-benzoquinones and 1-pentadecene in the flour beetles Tribolium madens (Charp.) and Tribolium Brevicornis (Lec.) (Coleoptera, Tenebrionidae). Comparative biochemistry and physiology. *61*, 287–290. Available at: http://www.sciencedirect.com/science/article/pii/0306449278900564.

Yezerski, A., Ciccone, C., Rozitski, J., and Volingavage, B. (2007). The effects of a naturally produced benzoquinone on microbes common to flour. Journal of chemical ecology *33*, 1217–1225. Available at: http://www.ncbi.nlm.nih.gov/pubmed/17473960 [Accessed March 26, 2012].

Yezerski, A., Gilmor, T. P., and Stevens, L. (2004). Genetic analysis of benzoquinone production in Tribolium confusum. Journal of chemical ecology *30*, 1035–1044. Available at: http://www.ncbi.nlm.nih.gov/pubmed/15274446.

GEORG-AUGUST-UNIVERSITÄT GÖTTINGEN

Curriculum Vitae

Name:	**Jianwei Li**
Last Degree:	M.Sc.
Mailing Address:	Department of Developmental Biology Johann-Friedrich-Blumenbach-Institute of Zoology and Anthropology, Georg-August-University Göttingen, Justus-von-Liebig-Weg 11 37077, Göttingen, Germany
E-mail Address:	jianwlee@gmail.com, jli@gwdg.de

Education

2008 – present:

Doctoral study, at Department of Developmental Biology, Johann-Friedrich-Blumenbach–Institute of Zoology and Anthropology, Göttingen Center for Molecular Biosciences (GZMB), Ernst-Caspari-Haus, Georg-August-University Göttingen, Germany, with DAAD-CSC and institute scholarship.

Major: Molecular Developmental Biology.

Advisor: Prof. Dr. Ernst A. Wimmer.

Title of Thesis:

Fundamental Efforts to Develop Novel Biotechnological Approaches in Pest Management Applications against Coleoptera: Transcriptomic Exploration of the Chemical Defense Mechanism in the Red Flour Beetle, *Tribolium castaneum*

2008 – 2008:

German study in Tongji University (Shanghai, China) and Carl Duisberg Center (Dortmund, Germany) as a DAAD-CSC scholarship holder.

2007 – 2008:

Research assistant, in the Key Laboratory for Experimental Teratology of the Ministry of Education, Institute of Medical Genetics, School of Medicine, Shangdong University (Supervisor: Prof. Dr. Yaoqin Gong)

2004 – 2007:

Masters study, in Institute of Developmental Biology, the Development Mechanisms and Gene Regulation Key lab of Shandong Province, College of Life Science, Shandong University.

Major: Molecular and Developmental Biology.

Advisor: Prof. Dr. Hongwei Zhang.

Title of Thesis: Studies on the amphioxus development correlated gene: *Smad*, *Tmp21* and comparative researches on the homologous *Rab23* gene in amphioxus and zebrafish.

2000 – 2004:

Bachelors study, in School of Life Science, Lanzhou University.

Major: Biotechnology.

Title of Thesis: Effects of Salinity and pH on Spermatozoal Mobility and Lifespan in *Buffo raddei* Strauch.

Research interests

Pest management, insect development, chemical defense and related biotechnological applications.

Awards and grants

DAAD-CSC PhD research scholarship (2008 - 2012)

Publications

Li, Jianwei, Sabrina Lehmann, Bernhard Weißbecker, Irene Ojeda Naharros, Stefan Schütz, Gerrit Joop, Ernst A. Wimmer. 2013 "Odoriferous defensive stink gland transcriptome to identify novel genes necessary for quinone synthesis in the red flour beetle, *Tribolium castaneum*." (submitted and under review)

Yu, Xuesong*, **Jianwei Li***, Hui Liu, Xiaodan Li, Shangwu Chen, Hongwei Zhang, and Anlong Xu. 2011. "Identification and expression of amphioxus AmphiSmad1/5/8 and AmphiSmad4." *Science China. Life sciences* 54(3): 220–6. [Link]. (*equal contributors)

Li, Jian-Wei*, Yu-Shuang Lin*, Dong-Yan Chen, and Hong-Wei Zhang. 2009. "Isolation, phylogenetic analysis and developmental expression pattern of AmphiRab23b in amphioxus." *Yi chuan = Hereditas / Zhongguo yi chuan xue hui bian ji* 31(12): 1233–40.[Link] (*equal contributors) (Article in Chinese)

Lin, Pengfei*, **Jianwei Li***, Qiji Liu, Fei Mao, Jisheng Li, Rongfang Qiu, Huili Hu, Yang Song, Yang Yang, Guimin Gao, Chuanzhu Yan, Wanling Yang, Changshun Shao, and Yaoqin Gong. 2008. "A missense mutation in SLC33A1, which encodes the acetyl-CoA transporter, causes autosomal-dominant spastic paraplegia (SPG42)." *American journal of human genetics* 83(6): 752–9. [Link] (*equal contributors)

Zhang, Y., L. Wang, M. Shao, **J. Li**, B. Li, and H. Zhang. 2008. "A comparative study on the developmental expression of hadh2 in amphioxus and zebrafish." *Journal of Fish Biology* 72(5): 1215–1222. [Link]

Wang, Lifeng, Dongyan Chen, Ying Zhang, Yushuang Lin, **Jianwei Li**, and Hongwei Zhang. 2008. "Characterization of AGAT, GAMT and CT1 in amphioxus: implications for the evolutionary conservation of creatine metabolism related molecules at the invertebrate-to-vertebrate transition." *Development genes and evolution* 218(11-12): 681–9. [Link]